UNIVERSITY OF CAPE TOWN
IYUNIVESITHI YASEKAPA • UNIVERSITEIT VAN KAAPSTAD

DEPARTMENT OF CIVIL ENGINEERING

FACULTY OF ENGINEERING AND BUILT ENVIRONMENT

TENSILE RELAXATION OF BONDED CONCRETE OVERLAYS

Submitted in partial fulfilment of the requirements for the degree of

MASTER OF SCIENCE IN CIVIL ENGINEERING

by

CRISPEN MASUKU

Supervisors: Dr. H. Beushausen
A/Prof. P. Moyo

February 2009

PLAGIARISM DECLARATION

I know the meaning of plagiarism and I declare that all of the work in this document, save for that which is properly acknowledged, is my own. I also affirm that this work has not been submitted in this, or any other university for examination, or for any other purposes.

Signature……. Date……

DEDICATIONS

This study is dedicated to my family: Unathi, Lisa, Mamthie, Lot, Funa, Ellen, Spa, Mdala and Mama, for their sacrifice and moral support.

ACKNOWLEDGEMENTS

The author wishes to express sincere gratitude to the following;
His supervisors Dr Hans-D. Beushausen and A/Prof. Pilate Moyo, for their invaluable guidance, assistance, friendship and mentorship throughout the study. The author is also grateful to Prof. Alexander for challenging my ideas through constructive criticism and enlightening me. Thank you Elly Yelverton for tolerating my incessant pestering. Warmest gratitude goes to my colleagues Bongani, Jakob, Malumbela, Noor, Charles, Mike, Rachel, Nick and Kungu for their input. The author is profoundly indebted to Ludo for her faith, encouragement, support and most of all love.

The author would also like to acknowledge, Department of Civil Engineering, University of Cape Town, for the opportunity and financial assistance throughout the study.

1 Chronicles 16:34: *Oh give thanks to the LORD, for he is good; for his steadfast love endures forever!*

ABSTRACT

The bonded concrete overlay technique is one of the main techniques used for repair of deteriorated concrete structures. This technique involves removal of a distressed surface layer on a concrete base (substrate) and replacement with a fresh layer of concrete i.e. overlay. Due to thermal and hygral differences in the two composites, differential shrinkage occurs. This leads to overlay shrinkage restraint by the relatively mature substrate.

Restrained shrinkage in bonded concrete overlays can cause stress build up, cracking and even debonding. Tensile relaxation is the main mechanism of stress relief in concrete overlays. This results in less possibility of cracking and debonding. The research described in this study presents an analytical method of analysis. This method is based on tests performed to assess tensile relaxation in concretes subjected to restraint. Although this study is limited in scope, it serves as an introduction to the topic and contributes a valuable bank of results obtained.

In this study, commercial repair mortar (Sika® Rep LW), 0.45 and 0.65 w/c ratio custom-made mixes were investigated. Uniaxial tensile strength, tensile elastic modulus, shrinkage and tensile relaxation tests were done on dog-bone concrete mortar specimens. Test specimens were subjected to constant strain in a Zwick Roell Universal Testing machine. Restraint was achieved by imposing stress equal to 80% of specimen failure stress. Stress curves were plotted, statistically evaluated and modelled.

An analytical model describing tensile stress relaxation and its variation with shrinkage strains and effects of material composition and maturity was developed. The model was based on a parametric study of the main factors contributing to relaxation in bonded concrete overlays. The model was used for predicting the likelihood of failure in bonded concrete overlays made from the above-mentioned mixes. It was found that tensile relaxation is sensitive to w/c ratio, mix composition and maturity. Through modelling results presented in this study, cracking and debonding in bonded concrete overlays can be mitigated in the design phase.

TABLE OF CONTENTS

LIST OF FIGURES

LIST OF TABLES

CHAPTER ONE: INTRODUCTION

1.1 Background and problem statement

Presently, most concrete structures in service are either approaching the end of their design lives or are in need of repair (Emmanuel, Lev & Leslie, 1998). This problem has necessitated the need for effective repair methods as opposed to reconstruction which may be more costly and time consuming. Usually, the selection of effective repair techniques involves striking a balance between costs, suitability to the level of deterioration of the structure and efficiency of repair after it has been implemented (Schrader, 1992).

In structures subjected to moderate and heavy traffic such as highway bridge decks, pavements and airfields, the most prevalent rehabilitation method is to place an overlay on an existing surface (Jun & Victor, 2002). Overlays are applied over concrete substrates to increase service-life, for surface protection and to improve aesthetic appearance. Overlays are placed as a levelling and high-quality riding surface. They are primarily used in rehabilitation and retrofitting projects after removal of distressed surface layer (Indrajit, 2005). The substrate surface is prepared such that whenever a fresh overlay is applied, it adheres to the substrate and a bond is formed. Fig. 1.1 shows the overlay, substrate and the line of contact between the two layers, called the interface.

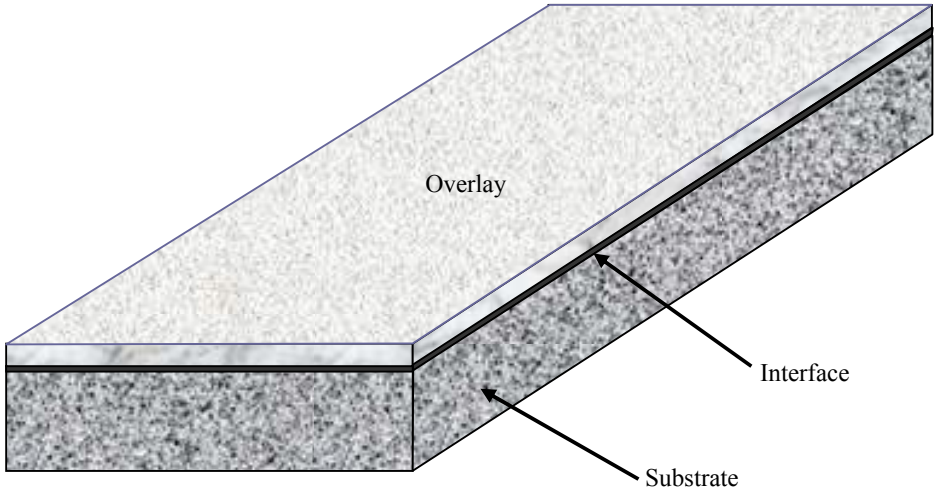

Fig. 1.1: Bonded concrete overlay

The bond formed at the interface creates a boundary condition in the composite section. Provided full bond is assumed, overlay and substrate volume changes at the interface are the same (Beushausen, 2005). Components of this composite system respond differently to different environmental conditions. If the components are analysed individually, it is clear that the overlay, relatively younger than the substrate, undergoes more changes in response to the environment than the substrate.

Environmental and internal effects naturally cause the overlay to undergo shrinkage whilst substrate shrinkage is negligible. Shrinkage mainly involves loss of moisture to the environment as well as due to hydration. This causes gradual volume changes and build-up of interface shear stresses and direct stresses in the composites. These consist mainly of tensile stresses in the overlay which may result in cracking. Failure may occur if the overlay does not have adequate strength to resist tensile stresses. Failure of bonded overlays is thus mainly due to stresses generated due to overlay and substrate interaction.

Relaxation and creep facilitate release of direct stresses in restrained concrete. Creep and relaxation are visco-elastic and time-dependant material properties (Neville, 1981). Creep is the increase in strain under a constant sustained stress whilst relaxation is the reduction in stress under constant strain (Rusch, Jungwirth &

Hilsdorf, 1983). Tensile relaxation in bonded concrete composites has been identified by previous researchers as a major stress relief mechanism (Pigeon & Bissonette, 1999; Beushausen, 2005; Carlswärd, 2006). Through analysis of bonded overlays subjected to restraint, experimental results have shown different values of tensile relaxation. Values in the order of 40% up to 67% have been reported in literature (Pigeon & Bissonette, 1999; Kordina, Schubert & Troitzsch, 2000; Beushausen, 2005).

1.2 Motivation for Research

If sufficient stress relief is achieved, then cracking, debonding and ultimately failure of bonded concrete overlays is avoided. Tensile relaxation is therefore a significant mechanism in the performance of bonded concrete overlays. However, unlike creep mechanisms, very little is known about tensile relaxation. There is currently no direct method of calculating relaxation capacity of overlays in practical situations. For concrete repair works, no reliable design approach, widely accepted guidelines for design specification and their execution is available for the practitioner (Emmons, Vaysburd &. MacDonald, 1995; Granju, 2004). Design codes that are currently in use lack practical input and in-depth guidelines that incorporate tensile relaxation in design of concrete structures.

Tensile relaxation has to be high enough to avoid overlay failure but the degree of relaxation varies with material and environmental factors. Nevertheless, bonded concrete overlay repairs are still carried out without prior attention to these aspects. This may be detrimental to overlay performance. A handful of previous studies simply report on resultant stresses to which overlays may be subjected. However they still lack conclusive evidence in form of experimental work and well-expressed models (Granju, 2004; Beushausen, 2005).

1.3 Aim of research

This research investigates tensile relaxation in different concrete mixes. Main parameters involved are assessed. An analytical model is derived to predict the probable onset of cracking using experimental results. The main aim is to find the actual influence of tensile relaxation in crack mitigation.

1.4 Hypothesis

This research proposes that tensile relaxation is a time dependant material property that is different for specific concretes subjected to shrinkage restraint. Relaxation in specific concretes can be calculated. The possibility of cracking can be modelled analytically based on parameters obtained through analysing experimental data.

1.5 Research objectives

In order to ensure that an overlayed system remains durable and fully functioning during intended service life, it is important to arrest overlay cracking and to prevent delamination (Carlswärd, 2006). Therefore an analytical approach is needed to clearly show the effects of main factors affecting tensile relaxation in bonded concrete overlays. Furthermore, cracking and debonding will be predicted based on development of stresses and other time-dependant factors. In this regard, the objectives of this research are to:

- Identify fundamental relaxation characteristics in relation to influential material factors.
- Validate time-dependency of tensile relaxation.
- Validate mix composition-dependency of tensile relaxation.
- Establish specific degree of relaxation for different conditions.

Although not ultimately the aim of this research, these objectives will also help to clarify mechanical processes occurring during tensile relaxation. For example, studies

by Pigeon & Bissonnette (1995) make mention of publications by Brooks & Neville (1997) and Cook (1972). These point to the viscous shear theory and micro cracking theory as mechanisms occurring during relaxation. However, there is still insufficient experimental and mathematical evidence to support these theories (Rusch, Jungwirth & Hilsdorf, 1983). Evidence can be acquired through experiments that may identify different characteristics responsible for relaxation.

Obtaining sufficient relaxation data requires assessment of the main material and environmental factors affecting tensile relaxation. Such properties as material composition, environmental conditions, maturity, curing period and others will be discussed. These properties may directly influence shrinkage, tensile strength and tensile relaxation in bonded concrete overlays subjected to shrinkage restraint.

CHAPTER TWO: PROPERTIES OF BONDED CONCRETE OVERLAYS

2.1 General

This chapter reviews literature on bonded overlays. Bonded concrete overlays are defined. Their applications are discussed. Factors affecting their performance are also dealt with in detail. A review of past research carried out on bonded concrete overlays is also covered. An introduction of tensile stress relaxation is presented. Tensile relaxation models from previous studies are also discussed and examined. Finally, a summary of all the models is presented. The summary shows how the models can be applied to this study. This may reveal how relevant the previous studies referred to, are to tensile relaxation in bonded concrete overlays.

2.1.1 Definition of bonded concrete overlays

An overlay is a layer of concrete or mortar, seldom thinner than 25 mm. The overlay is placed on and usually bonded onto a worn or cracked concrete surface. Its main use is to either restore or improve the function of the previous surface. It may also be a polymeric concrete usually less than 10 mm thick (ACI, 1999).

2.1.2 Applications of bonded concrete overlays

Overlays also referred to as toppings, are used for a broad range of applications including repair and surface decoration. Common applications of this technique are slabs-on-grade, patch repairs, shotcrete tunnel linings, indoor and outdoor flooring on repair of retaining walls, abutments and bridge decks (Banthia, Yan & Mindess, 1995; Beushausen, 2005). Not only is it implemented on existing structures but also on precast elements which receive an in-situ topping (Beushausen, 2006). A few examples of overlaying are shown in Fig. 2.1, Fig. 2.2 and Fig. 2.3.

Fig. 2.1: Overlay application on slabs-on-grade
www.munic.org

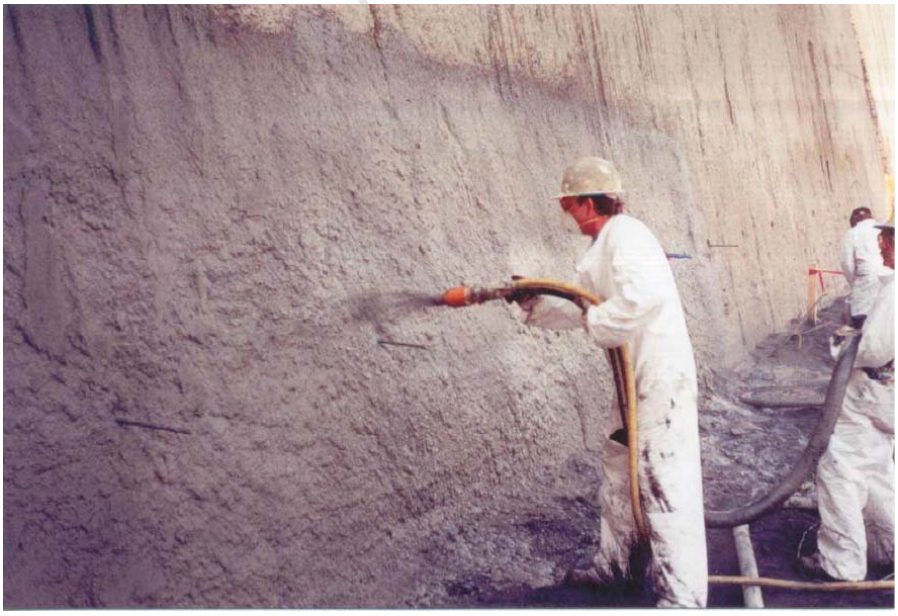

Fig. 2.2: Shotcrete applied on vertical wall
www.mudjacking.com

Fig. 2.3: Overlay repair on concrete footpath
www.gaddis&sonnic.com

A large proportion of highway-bridge decks, pavements and airfields consist of plain or reinforced concrete (Atashi, Lachemi & Kianoush, 2007). However, during their service life, need to repair these concrete structures may arise due to deterioration. The overlay technique has proved to be a reliable tool in concrete repair by providing a new surface to resist exerted loads. Allen and Edwards (1987) state that, if properly applied on concrete pavements, the overlay repair technique can achieve the following properties:

- Restoration of durability.
- Restoring structural integrity i.e. strength, abrasion resistance, etc.
- Increased structural strength of overlayed surface.
- Restoring or improving appearance of the pavement.
- Restoring the structure's fitness for use.

2.1.3 Surface preparation

Bonded concrete overlay repair involves removing the deteriorated concrete layer near the substrate surface and replacing it with a thin concrete layer (Atashi *et al*, 2007). Beushausen (2005), Carlswärd (2006) and Atashi *et al* (2007) state that, for

overlays to perform effectively concrete overlay must be fully bonded to the substrate. They agree that the substrate surface should ideally be treated by shotblasting, water-jetting or sandblasting processes. This creates an interface texture that promotes development of a strong bond between the two composites. In their research spanning over a decade, Morgan (1996), Kim & Nelson (2004) and Meftah *et al* (2006) agree that performance of bonded concrete overlay composites is dependent on quality of the interface bond. They affirm the need for the substrate surface to be clean and free from grit and dust. These elements may create locations within the interface where delamination may occur.

Emmons *et al* (1995) state that proper overlay compaction results in increased bond strength.

Delatte *et al* (1998) propose that formation of interface bond is mainly due to two components. These are interlock and adhesion. Interlock is determined by the roughness of the repaired surface. Adhesion is produced by development of chemical bonds between concrete paste and cured substrate (Atashi *et al*, 2007). Adhesion mechanisms have also been briefly discussed by Beushausen (2005) citing the work of Fiebrich (1994). Fiebrich (1994) detailed that mechanisms are divided basically into mechanical interaction, thermo-dynamic mechanisms and chemical bonding. However, intricate details relating to these individual bonding mechanisms will not be dealt with in this study. For further details, readers are referred to the literature.

2.1.4 Effect of bonding agents

Bonding agents increase bond strength particularly in stiff repair mortars that are unable to fully interact with the substrate. Therefore they cannot undergo full interlock and adhesion. For instance, bonding agents such as Portland cement grout, latex-modified Portland cement grout and epoxy resins, are sometimes used to improve the bond (Beushausen, 2005). Careful surface preparation and use of suitable bonding agents can improve bond strength. However poor workmanship has often resulted in improper application of bonding agents, which has caused subsequent interface failure in bonded overlays (Yuan & Marosszeky, 1994).

2.1.5 Problems relating to bonded concrete overlays

Overlaying is based on bringing into contact two or more concrete layers in order to form a monolithic system. The concept of bringing two or more constituent elements in order to achieve a combination of properties not possessed by each element acting alone has been known since materials were first used (Mumenya, 2007). In bonded concrete overlays, new materials must be successfully integrated with existing materials to form a composite system. This system must be capable of resisting service loads and various environmental factors (Vaysburd *et al* 2000). However environmental factors often lead to cracking of overlay surface and also debonding. Before these can be discussed, it is essential to first mention factors affecting overlay performance.

2.2 Factors influencing overlay performance

The occurrence of overlay failure is governed by 1) composition of overlay concrete, 2) age of concrete, 3) curing procedures, 4) characteristics of bond, and 5) environmental conditions such as temperature, wind and relative humidity. The composition of the overlay concrete determines material parameters such as tensile strength, elastic and visco-elastic properties and shrinkage (Beushausen, 2005). Thus, from this simple review, it is clear that with so many factors impacting bonded overlays, this is a complicated process since all factors have to be taken into account.

2.2.1 Early age cracking and debonding

From results of previous experimental research (Pigeon & Saucier, 1992; Kordina, *et al*, 2000) as well as experience in practice, overlays have often exhibited serious performance problems when improperly applied (Beushausen, 2005). Long-term performance of bonded overlays has often been negatively influenced by early age cracking and debonding of the overlay from the substrate. Debonding is the separation between overlay and substrate characterised by overlay lifting off the substrate. If cracking and debonding are severe, premature failure of bonded overlay composite

occurs. As a consequence, failure modes such as those shown in Fig. 2.4 are common in bonded concrete overlays (Carlswärd, 2006).

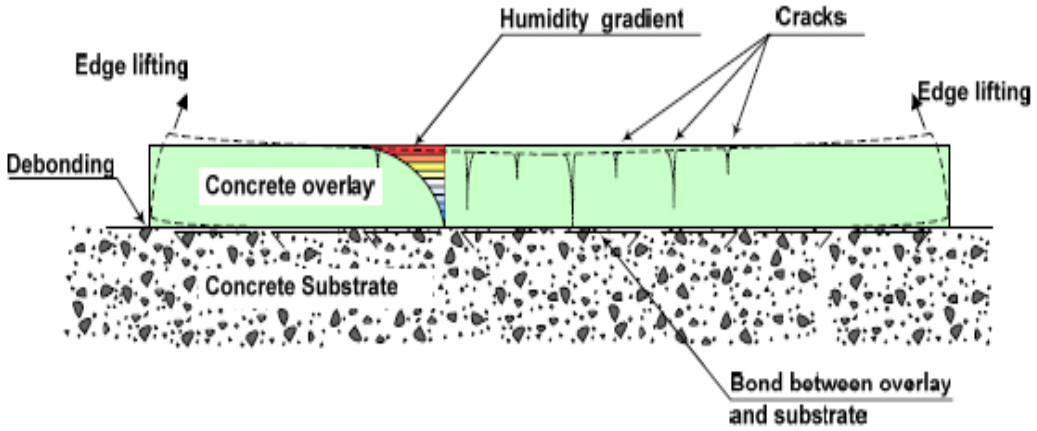

Fig. 2.4: Failure modes in concrete overlays (*Carlswärd, 2006)*.

Moisture loss from overlay may result in cracking and debonding. Firstly the overlay loses moisture to the environment due to drying. Overlays may also lose moisture to the substrate due to absorption. Depending on environmental conditions, a build-up of a humidity gradient as shown in Fig. 2.1 may occur locally within the overlay. Secondly, restrained shrinkage from substrate leads to localised shear stresses at the interface. A stress field near free edges develops. The stress field tends to lift overlay edges vertically. This is shown in Fig. 2.1 by curling or edge lifting. Un-controlled cracking may lead to impaired load capacity or durability, decreased stiffness and increased deformations of the structure (Carlswärd, 2006). Therefore a successful bonded overlay repair procedure has to result in very minimal or no cracking and debonding.

2.2.2 Tensile stress relaxation

Tensile relaxation is the reduction in stress due to imposed strain. Results reported in literature (Pigeon *et al*, 1999, 2000; Beushausen, 2005; Carlswärd, 2006) suggest that tensile relaxation is a major mechanism for stress development of concrete specimens under restrained deformation. However, tensile relaxation is a complicated mechanism to analyse as concrete behaviour in tension is less understood. A number of researchers including Rusch *et al* (1983), Pigeon *et al* (1999), Pigeon *et al* (2000),

Beushausen (2005) and Carlswärd (2006) have studied concrete behaviour in tension. It was concluded that the main mechanical properties affecting performance of bonded concrete overlays are shrinkage, tensile strength, elastic modulus and tensile relaxation.

Mechanical properties influencing the performance of bonded overlays have been mentioned briefly in the preceding paragraph. A schematic of the main factors and their interrelation is shown in Fig. 2.5.

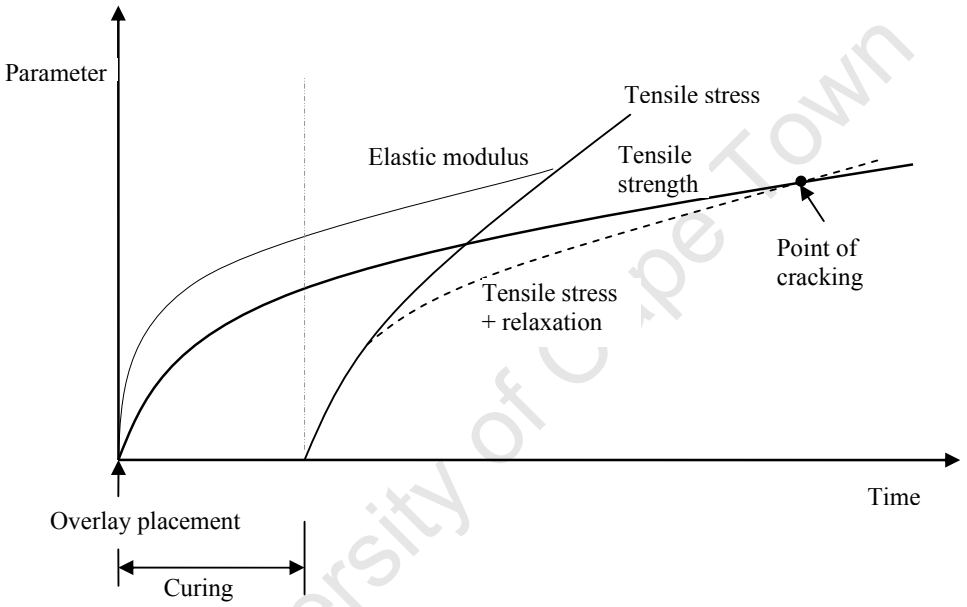

Fig. 2.5: Key properties affecting performance of bonded concrete overlays.

Fig. 2.5 shows the main properties affecting performance of bonded concrete overlays. After the concrete has been cast, elastic modulus and tensile strength start to increase gradually. Ignoring autogenous shrinkage, shrinkage during curing may be assumed to be very low i.e. it is considered as insignificant. As a result, once curing has been completed, drying shrinkage will start to occur. If concrete is allowed to shrink freely without restraint, no stresses develop. However, if concrete is restrained from shrinking, tensile stresses are generated. Tensile stresses increase with an increase in rate of shrinkage. Consequently, if tensile strength of concrete is less than tensile stress, concrete will fail unless stresses are relaxed by tensile relaxation. Therefore tensile relaxation may delay the onset of cracking. Fig. 2.5 shows

relaxation up to a point when cracking starts to develop. A detailed review of parameters affecting performance of bonded concrete overlays is presented in the following sections.

2.3 Shrinkage and Influencing factors

Shrinkage is the time-dependant volume reduction in fresh and hardened concrete. A decrease in volume can be a result of movement of moisture within and out of concrete due to environmental and hydration processes (Alexander, 2001). Major factors influencing shrinkage can be divided into environmental factors and material properties. These include relative humidity, ambient temperature, and material composition such as paste content in the mix.

In case of bonded concrete overlays, excessive moisture loss can also be due to absorption of water by relatively dry substrate. This can result in an increase in overlay shrinkage strain (Beushausen, 2006). At high relative humidities the rate of shrinkage drops as the degree of moisture loss decreases. The converse is true for concrete exposed to lower humidities. If concrete is allowed to shrink freely a curve similar to that shown in Fig. 2.6 is observed. However if concrete is stored in water after being allowed to shrink, the curve would drop as shown (Fig. 2.6). This means that concrete can regain part of its original size but can never recover entirely. The part that cannot be recovered after that is called irreversible shrinkage.

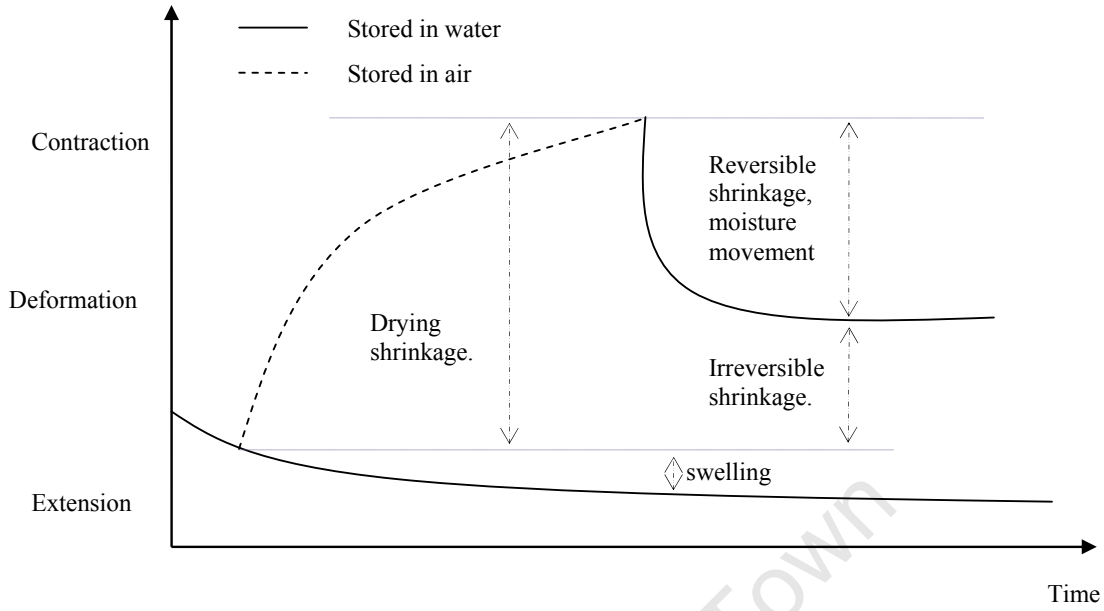

Fig. 2.6: Basic characteristics of shrinkage *(Alexander, 2001)*.

2.3.1 Types of shrinkage

Shrinkage can be classified into four broad categories:

- Plastic shrinkage
- Autogenous shrinkage
- Carbonation shrinkage
- Drying shrinkage

These are discussed in sections that follow.

2.3.1.1 Plastic shrinkage

Plastic shrinkage is the volume reduction of concrete due to rapid removal of water from the concrete surface during early ages. Moisture release may be rapid since the rate of moisture loss often exceeds amount of bleed water. This results in a rapid drawdown in pore water level, which causes an increase in pore water pressure. This tends to bring neighbouring solid particles closer (Sivakumar & Santhanam, 2007). As a result, inner non-shrinking concretes and aggregates versus shrinking of cement

paste at the surface cause restraint. When the resultant stresses equal tensile strength, cracking on the surface of fresh concrete occurs (Kellerman, 2001). Fresh concrete is susceptible to plastic shrinkage cracking especially during hot, windy, and dry weather conditions (Grzybowski & Shah, 1990). Other factors that increase adversity of plastic shrinkage include high concrete temperature and absorption of water from concrete overlay by the substrate. This could be the case if the substrate is not sufficiently saturated and surface dry.

Plastic shrinkage cracks are typically observed in concrete elements with a high surface area to volume ratio e.g. in thin bonded overlays. These cracks are roughly straight but discontinuous and closely spaced depending on dimensions of the specimen (Kellerman, 2001). In overlays with large surface area, crack patterns due to plastic shrinkage are random.

Several researchers (Kellerman, 2001; Banthia & Gupta, 2006; Atashi *et al*, 2007) have recommended that the degree of early age shrinkage can be reduced by good curing practice. This is because curing provides sufficient moisture to prevent the surface from drying out. Consequently this reduces the effects of surface cracking.

Bissonette & Pigeon (1995), Banthia & Gupta (2006) and Carlswärd (2006) showed that the use of fibres reduces occurrence of early age shrinkage cracks. In this case, fibres bridge cracks formed and prevent them from widening. Temperature control, shielding from high winds, reduced use of admixtures that prevent bleeding and the use of shrinkage reducing admixtures is recommended in the construction of overlays (Banthia & Gupta, 2006).

2.3.1.2 Autogenous shrinkage

Similar to plastic shrinkage, autogenous shrinkage occurs during early ages, particularly immediately after setting. Autogenous shrinkage or self-desiccation is due to internal water consumption by hydration reactions. During the hydration process, hydration products have volumes less than their reactants resulting in volume reduction. This is considered as a basic component of shrinkage as volume decrease

occurs without loss of water from the surface of concrete. Autogenous shrinkage is relatively low in normal concretes with w/c ratios above 0.4 compared to concretes having w/c lower than 0.4. This is due to higher consumption of mixing water particularly in high strength concrete. Carlswärd (2006) argued that even though autogenous shrinkage may be lower in normal concrete, its presence could be substantial.

Since it is an internal and chemically initiated shrinkage mechanism, traditional curing methods are ineffective in reducing autogenous shrinkage. Zhutovsky *et al* (2004) used pre-soaked lightweight aggregates in their concrete mix. The aggregates provided additional water for hydration reactions and they concluded that through control of size and porosity of lightweight aggregates, autogenous shrinkage was reduced.

2.3.1.3 Carbonation shrinkage

Carbonation shrinkage is the decrease in concrete volume due to the reaction of hardened cement paste constituents in concrete with atmospheric carbon dioxide. Consequently carbonation may result in lower strength, increase in deflection and cracking (Matsushitaa *et al*, 2004). Carbonation shrinkage takes a long time to occur. Hence laboratory tests for carbonation shrinkage are often accelerated by forcing high concentrations of carbon dioxide through concrete specimens in order to obtain results.

Carbonation is mainly a function of relative humidity and concrete permeability. At intermediate relative humidities between about 50% and 80%, maximum carbonation shrinkage occurs (Sauman, 1971). At a relative humidity greater than 80%, carbon dioxide cannot penetrate the water-filled pore spaces easily and at lower relative humidities, below 40%, the absence of water films reduces the extent of carbonation (Alexander, 2001).

2.3.1.4 Drying shrinkage

Drying shrinkage is caused by loss of moisture from concrete to the environment. Evaporation of free water from capillary pores results in a decrease in the volume of concrete. Development of drying shrinkage is initially rapid and slows down as the material ages. This is due to the slow rate at which moisture is lost from concrete. Hence the strain response is time dependent. According to Asad, Baluch & Al-Ghadib (1997), drying shrinkage of cementitious materials is caused principally by contraction of calcium silicate hydrate (C-S-H) gel in hardened cement paste.

Various shrinkage mechanisms have been proposed. These are capillary tension, surface tension, swelling pressure and movement of interlayer water theories (Section 2.3.2) (Alexander 2001).

2.3.2 Fundamental mechanisms of drying shrinkage in concrete

A number of mechanisms contributing to drying shrinkage of concrete have been detailed in literature (Alexander, 2001; Carlswärd, 2006). The most important factor influencing drying shrinkage is the amount and composition of cement paste. It is within the cement paste that water is lost and volume changes occur. Other factors influencing drying shrinkage are structural geometry and drying conditions (Carlswärd, 2006).

The paste is affected by the w/c ratio. For concrete with w/c ratios between 0.35 and 0.50 it was shown that the extent of shrinkage is directly proportional to the amount of cement paste. In practice, this implies that for a given w/c ratio, shrinkage can be mitigated by reducing the amount of water and increasing the content of aggregates (Carlswärd, 2006).

Shrinkage is controlled by different ways in which water moves within the cement paste as well as its interaction with the environment (Alexander, 2001). Listed below are a number of mechanisms describing the movement of water within the cement paste and their effects on shrinkage. It should be noted that these mechanisms occur at

microscale. As such, it is difficult to verify these mechanisms through conventional methods. Special methods such as spectrometry have been used (Alexander, 2001).

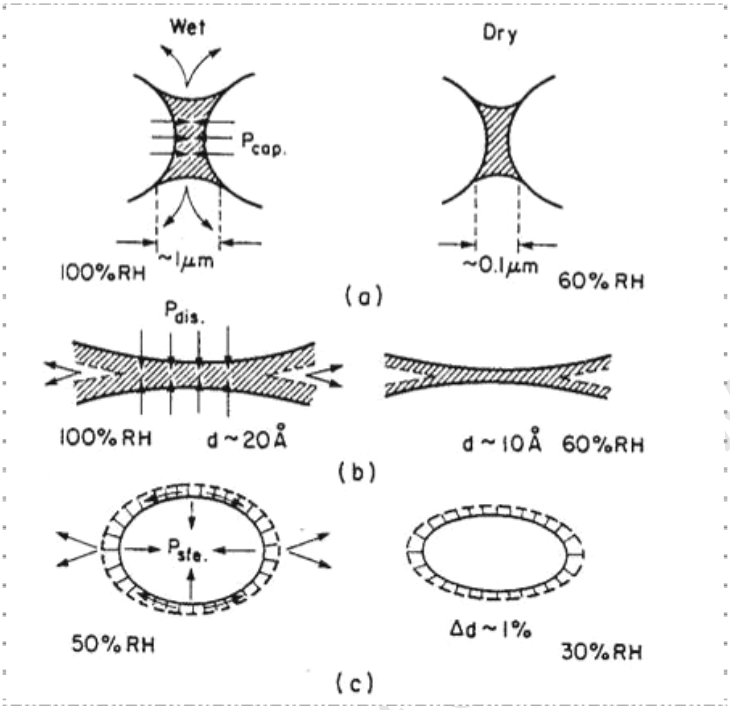

Fig. 2.7: Proposed mechanisms for causes of drying shrinkage of cement paste
(a) Capillary tension; (b) disjoining pressure; (c) surface tension *(Lecture Notes CIV5002Z, 2007)*.

Capillary tension

In capillary tension, water is lost from the paste due to drying. This loss of water occurs in capillary pores of the paste. On drying, menisci are formed. This results in tensile stress build-up in capillary water (Fig. 2.7a). Tensile stresses generated must be balanced by compressive stresses in the surrounding gel causing a volume reduction (Alexander, 2001).

Swelling (disjoining) Pressure

As shown in Fig. 2.7(b), whenever gel particles closely approach one another, adsorbed interlayer water may exert a swelling or disjoining pressure if the free film thickness is greater than interlayer distance. In addition, drying decreases adsorbed film thickness and reduces this pressure causing shrinkage.

Surface tension

Compressive stresses occur inside solid particles due to surface tension. Drying causes surface tension to increase. This results in a corresponding increase in compressive stress in the solids, hence shrinkage (Fig. 2.7c).

2.3.3 Strain due to restrained shrinkage

When concrete is allowed to shrink freely without hindrance, deformations are observed. However when a concrete overlay is bonded to the substrate, differential shrinkage between the overlay and substrate will occur. When a constraint is applied to the concrete overlay such that it cannot shrink freely, stresses are generated.

As shown in Fig. 2.8, before the overlay starts to shrink, the length is denoted '*dx*'. After the overlay shrinks the overall length of reduces due to the strain 'ε'. Since perfect bond is assumed between substrate and overlay i.e. there are no irregularities at the interface causing poor bonding, both substrate and overlay undergo the same linear contraction. Hence imposed strain leads to an induced stress in each section. Strain imposed is linear and so is induced stress. This simplification ignores effects of curvature, interface slip and strain gradients across both overlay and substrate. This simplification is suitable for very thin sections since strain gradients of very thin composites may be considered negligible.

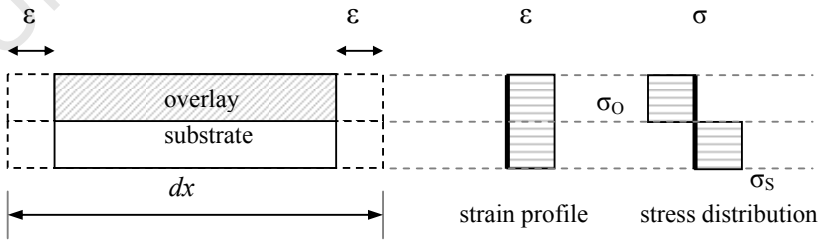

ε – strain.
σ – stress.
σ_O – overlay stress.
σ_S – substrate stress.

Fig. 2.8: Schematics of strains and stresses in a thin composite section *(Beushausen, 2005).*

In Fig. 2.8, the effects of curvature are ignored. For concrete repairs of common dimensions, i.e. thin overlays on stiff substrates, effect of bending moments initiated by differential shrinkage can usually be neglected. Conversely, in members with relatively low substrate stiffness, e.g. structural overlays on concrete slabs, bending moments due to differential shrinkage might cause considerable curvature, resulting in compressive strain in the overlay and hence in partial relief of tensile overlay stress (Beushausen, 2006).

Beushausen (2005) conducted experiments on overlays of different thicknesses. His findings were that for any given composites, degree of restraint to shrinkage was never entirely 100%. This was in agreement with an investigation by Haardt (1991) on the degree of substrate restraint. In his study, Haardt (1991) used FEM analysis. It was found that even if the substrate section is relatively large, overlay shrinkage is not entirely restrained. Furthermore, simulations of overlays as thin as 20 mm attached to substrates of infinite thicknesses showed considerable strain. Strain due to thin overlays was higher than in thicker overlays (Beushausen, 2005).

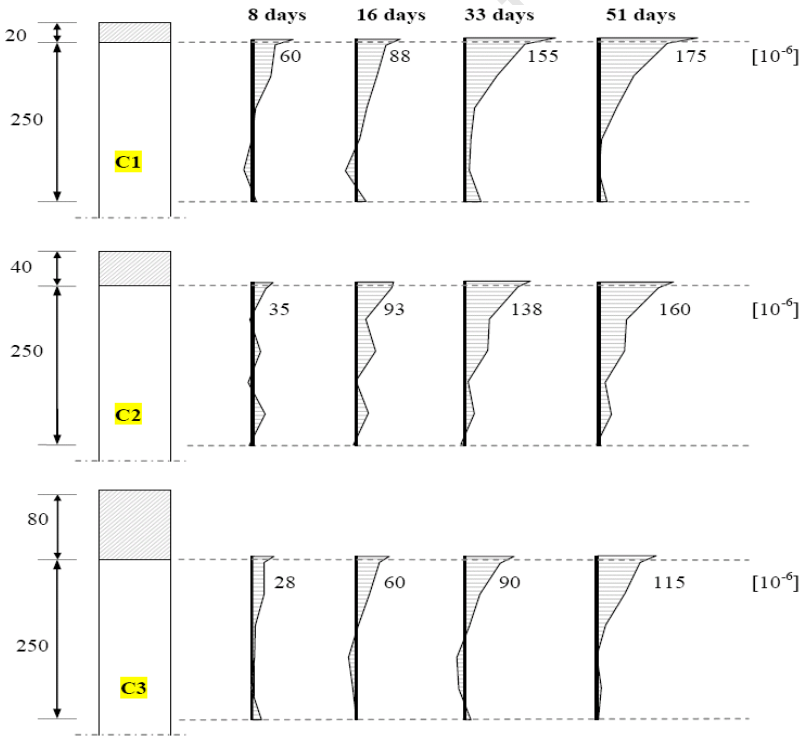

Fig. 2.9: Schematics of strain development across the substrate.
(Beushausen, 2005).

Fig. 2.9 shows strain development on a composite section in relation to different overlay thicknesses. Fig. 2.9 shows results for days 8, 16, 33 and 51. Members denoted C1, C2 and C3 were not allowed to curve. Hence strain values are due to differential shrinkage disregarding effects of curvature. Firstly, it is interesting to note that maximum strain observed was due to shrinkage of the thin overlay, i.e., 20 mm thick. Secondly, the strain profile observed in Fig. 2.9 shows a non-linear and rather uneven outline in the substrate section. This is in direct contrast to the simplified strain gradients observed in Fig. 2.8.

Results of the simulation showed that substrate strain is constant throughout the length of the interface. This is an indication that overlay shrinkage restraint remains constant over the whole overlay surface area. Another observation is the dependency of resultant strains on relative member dimensions (overlay and substrate). Beushausen (2005) found shrinkage strains to be independent of the overlay depth.

2.3.4 Stress due to restrained shrinkage

It is not simple to predict stresses resulting from shrinkage restraint in bonded concrete overlays. This is due to the influence of many factors. These factors include the increase in rate of overlay shrinkage coupled with shrinkage restraint, increase in elastic modulus, substrate creep etc. Shrinkage restraint is affected by substrate creep. On the other hand, substrate creep is affected by compresssive stress imposed by the overlay. Another concern is that creep is dependant upon stress sustained over a period of time. Furthermore direct stresses and bending stresses that are functions of overlay restraint and substrate stiffness are involved.

As a point of departure, it is simpler to look at the effects of direct stresses alone before considering influences of other stress mechanisms. In this case for a fully bonded overlay with consistent restraint along the interface, it can be shown that instantaneous elastic strain of the overlay [2.1] and substrate strain [2.2] at the interface is as follows (Beushausen, 2005).

$$\varepsilon_{restr.O,I} = \varepsilon_{FSS} - \frac{\varepsilon_{FSS}}{1 + \frac{E_s}{E_o}.C_\varepsilon} \quad [2.1]$$

$$\varepsilon_{S,I} = \frac{\varepsilon_{FSS}}{1 + \frac{E_s}{E_o}.C_\varepsilon} \quad [2.2]$$

Where $\varepsilon_{restr.O,I}$ = restrained overlay strain at the interface

ε_{FSS} = overlay free shrinkage strain

E_s = modulus of elasticity of substrate

E_o = modulus of elasticity of overlay

C_ε = constant accounting for combined influences of relative member dimensions and strain profile characteristics

$\varepsilon_{S,I}$ = substrate strain at the interface. $\varepsilon_{S,I} = \varepsilon_{O,I} = \varepsilon_I$

($\varepsilon_{O,I}$ = overlay interface strain, ε_I = interface strain)

In general the stress profile is determined by strain. In bonded concrete overlays the top part of the overlay has more freedom to shrink compared to the interface. Similarly the substrate has higher strains at the interface since it is bonded to the shrinking overlay. This is shown in Fig. 2.10.

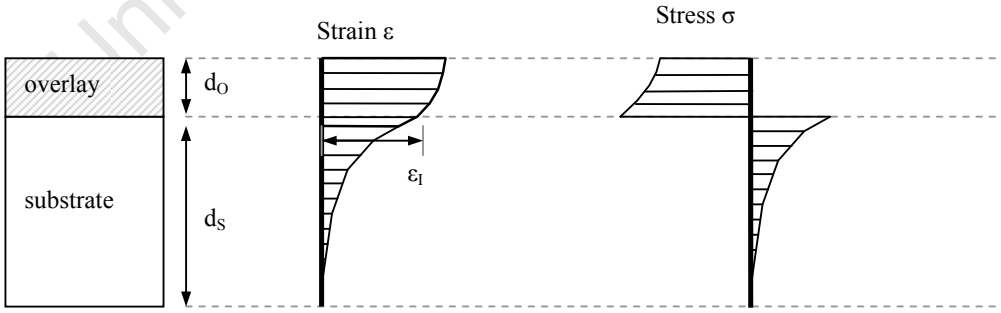

ε_I = Interface strain

d_O = depth of overlay

d_S = depth of substrate

Fig. 2.10: Schematics of strain development in bonded concrete overlays subjected to direct stresses. *(Beushausen, 2005).*

Another influence is that of elastic strain. This complies with linear elastic theory i.e. restrained shrinkage at any given time is proportional to overlay stress. Hence direct elastic stresses due to overlay and substrate strain are represented by [2.3] and [2.4] respectively (Beushausen, 2005).

$$\sigma_{O,I} = \left(\varepsilon_{FSS} - \frac{\varepsilon_{FSS}}{1 + \frac{E_s}{E_o}.C_\varepsilon} \right).E_o \qquad \text{(Tension)} \qquad [2.3]$$

$$\sigma_{S,I} = \left(\frac{\varepsilon_{FSS}}{1 + \frac{E_s}{E_o}.C_\varepsilon} \right).E_s \qquad \text{(Compression)} \qquad [2.4]$$

Where $\sigma_{O,I}$ = direct elastic stress in overlay

$\sigma_{S,I}$ = direct elastic stress in substrate

The rest of the parameters have been defined above

The stresses in equations [2.3] and [2.4] exclude the effects of overlay relaxation. In bonded concrete overlays, direct elastic stresses do not remain constant. They are subject to overlay relaxation and substrate creep. Substrate creep contributes to stress relaxation by increasing the overlay strain. This leads to a reduction in restrained shrinkage. Therefore resultant overlay stress is due to stress relaxed by substrate creep plus stress relaxed due to tensile relaxation. These mechanisms are interdependent. Hence they cannot be dealt with separately.

Interdependence between various mechanisms is shown in Fig. 2.11.

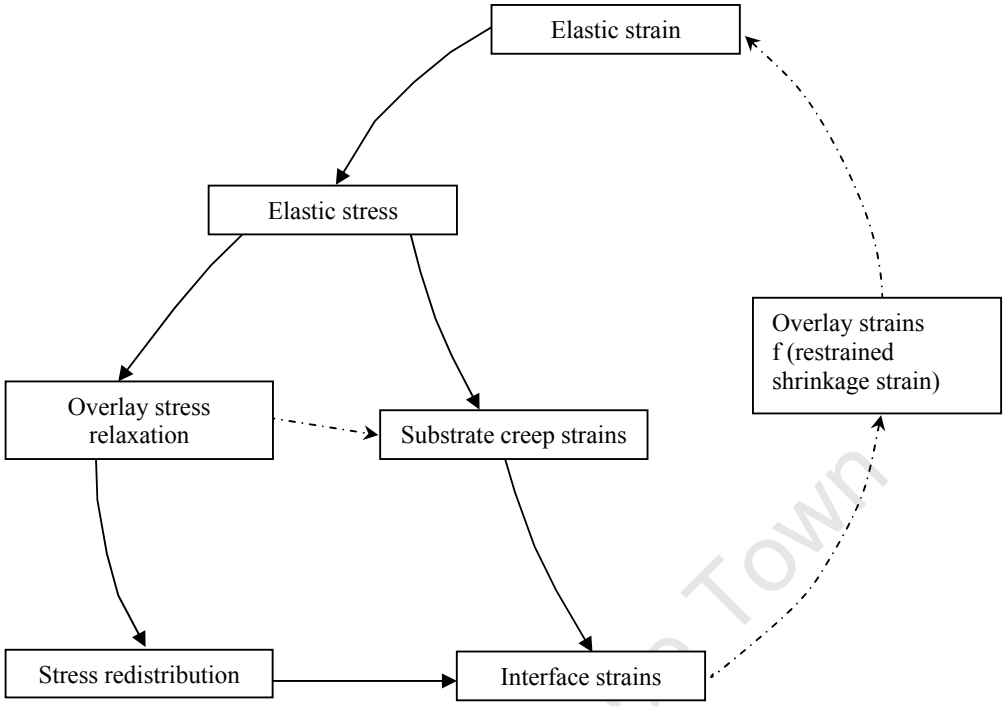

Fig. 2.11: Schematic of related stress and strain mechanisms in bonded overlays

Other stress release mechanisms in concrete overlays can be attributed to curvature and interface slip. However these effects will not be considered in this study as they normally pertain to overlays that are either bonded to relatively flexible substrates or are poorly bonded. In general, overlay stress is directly related to restrained shrinkage.

Therefore including the contribution of creep and relaxation, overlay and substrate stresses can be represented as shown in equations [2.5] and [2.6]. It is worth noting that variables in equations [2.5] and [2.6] are time dependant (Beushausen, 2005).

$$\sigma_{S,I}(t) = \varepsilon_I(t) \cdot E_S = \frac{\psi_O(t,t_o) \cdot \varepsilon_{FSS}(t)}{1 + \frac{E_S}{E_O(t)} \cdot C_\varepsilon} \cdot E_S \qquad \text{(compression)} \qquad [2.5]$$

$$\sigma_{O,I}(t) = (\psi_O(t,t_0)\cdot\varepsilon_{FSS}(t) - \varepsilon_I(t))\cdot E_O(t)$$

$$= \left(\psi_O(t,t_0)\cdot\varepsilon_{FSS}(t) - \frac{\psi_O(t,t_0)\cdot\varepsilon_{FSS}(t)}{1+\frac{E_S}{E_O(t)}\cdot C_\varepsilon} \right)\cdot E_O(t) \qquad [2.6]$$

$$= \psi_O(t,t_0)\cdot\left(\varepsilon_{FSS}(t) - \frac{\varepsilon_{FSS}(t)}{1+\frac{E_S}{E_O(t)}\cdot C_\varepsilon} \right)\cdot E_O(t) \qquad (tension)$$

Where $\sigma_{S,I}(t)$ = direct stress in substrate at age *t*

$\sigma_{O,I}(t)$ = direct stress in overlay at age *t*

t = age at the time of testing

t_0 = age at loading

$\psi_O(t,t_0)$ = relaxation function within the period $(t-t_0)$

$\varepsilon_{FSS}(t)$ = free shrinkage strain of overlay at age *t*

$E_O(t)$ = modulus of elasticity of overlay at age *t*

The rest of the parameters have been described earlier

Stress caused by restrained shrinkage, if not resisted, can result in cracking and debonding of the overlay. Stress can also partly be reduced by curvature and substrate creep (The rest is dealt with in equation [2.6]).

2.4 Tensile creep and tensile relaxation

Tensile creep is defined as the increase in strain due to an imposed constant tensile stress. On the other hand tensile relaxation is the reduction in stress due to a constant imposed strain.

2.4.1 Introduction

This section discusses previous models proposed as a solution to tensile relaxation. Most studies on tensile relaxation have generally used creep properties for determination of relaxation in composite systems. This may be due to lack of

sufficient data accumulated on stress relaxation and in particular tensile stress relaxation (Morimoto & Koyanagi, 1994). It has been stated by Bissonnette & Pigeon (1995) that tensile properties of concrete are generally disregarded in the design of new concrete structures. As a result, difficulties related to accurate measurement of concrete tensile properties probably explain why little attention has been given to tensile stress relaxation.

When subjected to constant tensile or compressive load, for a period of time, concrete will naturally deform in the direction of the load. The resulting strain increases with time. However the increase decays gradually as the loading period is prolonged. Whenever a specimen is loaded in tension, this is called tensile creep. If it is loaded in compression, it is termed compressive creep or more commonly, creep. This is shown diagrammatically in Fig. 2.12 (a) & (b).

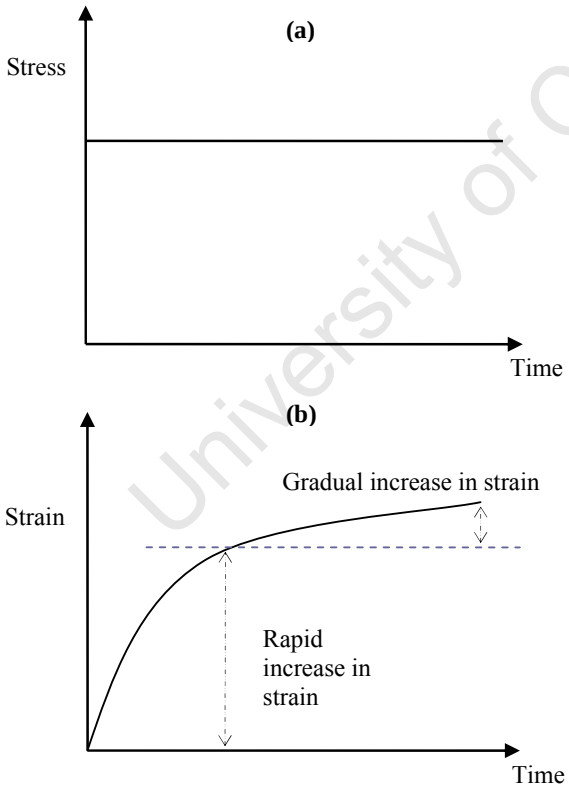

Fig. 2.12: (a) Stress-time curve **(b)** Strain-time curve as a result of creep

When a concrete specimen is subjected to a sustained strain it undergoes relaxation. Relaxation is the general decrease in stress on a body when subjected to sustained

strain. Therefore, stresses due to sustained strain are generated within the member but they decrease gradually with time. Through this research, the stress curve shall be assessed for different concrete mixes. Whenever a specimen is loaded at constant strain in tension, stress decay is termed tensile relaxation. This phenomenon is shown diagrammatically in Fig. 2.13 (a) & (b).

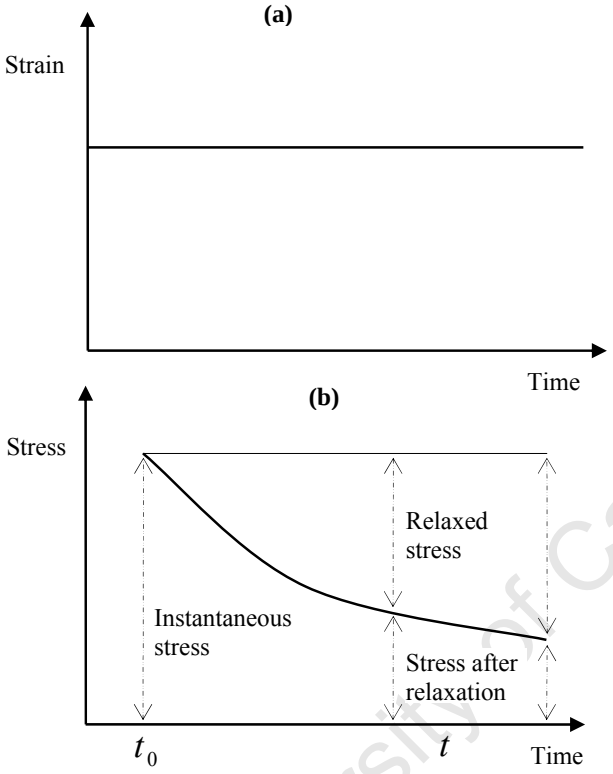

Fig. 2.13: (a) Strain-time curve **(b)** Stress-time curve as a result of relaxation

As perceived by Morimoto & Koyanagi (1994), it seems more appropriate to use the relaxation function to express stress relaxation rather than using creep function.

2.4.2 Mechanisms of creep and relaxation

Contrary to creep in compression, which has been subject to large number of studies, little is known of the viscoelastic behaviour of concrete in tension (Pigeon & Bissonnette, 1999). On the other hand, the subject of concrete in tension has been viewed as rather less important when compared to creep in compression. This is owing to the fact that concrete is mainly used structurally in compression. This has often led to a general treatment of tensile relaxation as a similar process to creep in

compression. This section attempts to outline various mechanisms involved in creep as well as relaxation of concrete.

Various authors attribute creep and relaxation to different processes. Powers (1968) explains that when concrete is subjected to sustained loading, load bearing water within cement paste moves through diffusion mechanisms. On the other hand Feldman and Sereda (1968) used a different approach to investigate mechanisms involved during creep. They proposed a structure of cement paste shown in Fig. 2.14. Their conclusions were that creep is caused by movement of water i.e. interlayer water between gel layers. Furthermore, movement of water causes gel layers to slide over each other causing microstructural changes. With cement paste consisting of numerous such layers sliding over each other, global deformation is imminent.

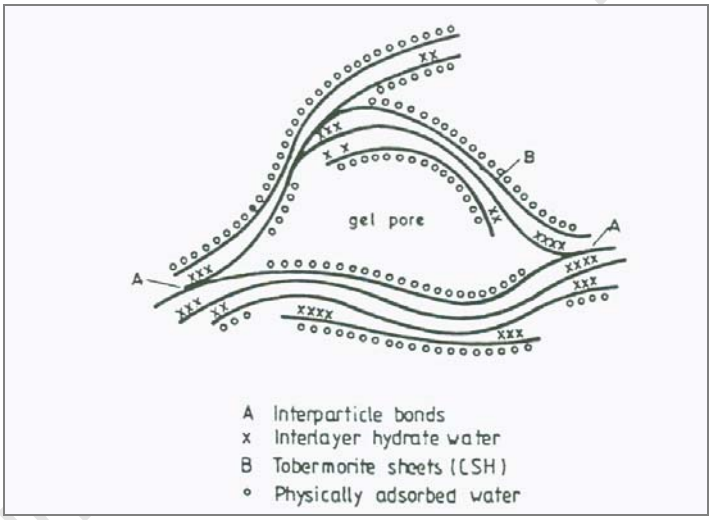

Fig. 2.14: Schematic of cement paste microstructure *(Feldman and Sereda, 1968)*.

When external loads are sustained, changes may occur in the gel structure. Such changes may be reduction in interparticle spacings, reduction of layer thicknesses and displacement of gel layers. This results in formation of new bonds. The external loads mentioned in this case refer to compressive stresses not exceeding 40% of ultimate strength of concrete under consideration. At stresses higher than 40% of ultimate strength of concrete, microcracking occurs. This causes strains much larger than those induced by movement of moisture.

Some changes in the gel structure are reversible whilst others are permanent. Reversible changes constitute elastic strains or delayed elastic strains whilst permanent strain represents creep.

When subjected to tensile stresses, the behaviour of concrete is different because concrete has low tensile strength. A small number of authors attribute this behaviour to microcracking within the concrete matrix. A specific example is the work of Cook (1972) on the theory of microcracking. Moreover results obtained by Pigeon & Bissonnette (1999) indicate that sustained tensile stresses are more likely to cause the formation and opening of microcracks. This is more likely to occur at interfacial transition zones perpendicular to the loading axis. In addition, Pigeon & Bissonnette (1999) use the viscous shear theory to explain mechanisms occurring in concrete under tensile loading. In this particular study, references to the work of Brooks & Neville (1997) are made.

Gutsch & Rostásy (1994) analysed stress-strain relationship of concrete undergoing tensile relaxation. They observed that microcracking within the cement paste caused a loss of stiffness in concrete. Microcracking was detected at a stresses above 730% of tensile strength in the member.

Pigeon & Bissonnette (1999) concluded that the dominant mechanism in relaxation was viscous shear and also the presence of microcracking. This was because their samples showed a small loss of rigidity. Even though there is evidence to show that the dominant mechanism is viscous shear, contribution of other relaxation mechanisms such as microcracking could not be ruled out completely.

2.4.3 Existing models on creep and relaxation

A number of models on creep and relaxation have been proposed by researchers in the past. Models have been derived in order to estimate tensile relaxation of concrete subjected to different degrees of mechanical restraint, varying temperature and humidity gradients. In this study only a few case studies were selected. Emphasis was placed on studies that presented analytical models for tensile relaxation. Studies based

on numerical models were disregarded. This is because analytical models can be applied to a broader range of problems compared to numerical models.

2.4.3.1 CEB-FIP Model Code for relaxation

In the CEB-FIP Model Code 1990 (1993) the relaxation function is given in terms of the creep compliance function (Equation [2.7]). This function is termed a semi-empirical function.

$$\psi(t,t_0) = \frac{1-0.008}{J(t,t_0)} - \frac{0.115}{J(t,t-1)}\left[\frac{J(t-\Delta,t_0)}{J(t,t_0+\Delta)} - 1\right] \quad [2.7]$$

$\psi(t,t_0)$ = relaxation function at time, t due to constant imposed unit strain at time t_0

t = age after loading at which any given parameter is calculated

t_0 = age of member during loading.

$J(t,t_0)$ = creep compliance function representing the total stress dependant strain per unit stress given by equation [2.8].

$$\Delta = \frac{t-t_0}{2}$$

The rest are empirically determined constants

$$J(t,t_0) = \left[\frac{1}{E_c(t_0)} + \frac{\phi(t,t_0)}{E_{ci}}\right] \quad [2.8]$$

$E_c(t_0)$ = modulus of elasticity at the time of loading

$\phi(t,t_0)$ = creep coefficient determined from equation [2.9]

E_{ci} = modulus of elasticity at the end of loading

$$\phi(t,t_0) = \phi_0 \beta_c(t-t_0) \quad [2.9]$$

$\phi(t,t_0)$ = creep coefficient

ϕ_0 = notional creep coefficient [2.10]

β_c = coefficient to describe the development of creep with time after loading [2.15]

t = age of concrete (days) at the moment considered

t_0 = age of concrete at loading (days)

$$\phi_0 = \phi_{RH}\beta(f_{cm})\beta(t_0) \quad [2.10]$$

With

$$\phi_{RH} = 1 + \frac{1 - RH/RH_0}{0.46\left(h/h_0\right)^{1/3}} \quad [2.11]$$

$$\beta(f_{cm}) = \frac{5.3}{\left(f_{cm}/f_{cmo}\right)^{0.5}} \quad [2.12]$$

$$\beta(t_0) = \frac{1}{0.1 + \left(t_0/t_1\right)^{0.2}} \quad [2.13]$$

Where

RH = relative humidity of ambient environment (%)

RH_0 = 100%

$$h = \frac{2A_c}{u} \quad [2.14]$$

h = notational size of member (mm)

h_0 = 100 mm

f_{cm} = mean compressive strength of concrete at 28 days.

f_{cmo} = 10MPa

A_c = cross sectional area of concrete.

u = perimeter of concrete member in contact with atmosphere.

t_1 = 1 day

The development of creep with time is represented by

$$\beta_c(t-t_0)=\left[\frac{(t-t_0)/t_1}{\beta_H+(t-t_0)/t_1}\right]^{0.3} \quad [2.15]$$

With

$$\beta_H=150\left\{1+\left(1.2\frac{RH}{RH_0}\right)^{18}\right\}\frac{h}{h_0}+250\leq 1500 \quad [2.16]$$

All variables have been described above. The exact values are empirical and no detail of their derivation is available in the code.

Equation [2.7] may have been obtained through experimental modelling. However CEB-FIP Model Code 1990 (1993) does not disclose in detail how Equation [2.7] is derived. There is no rationalization how empirical values have been determined. Furthermore the code does not state the type of concrete specimens, concrete mixes, test set-up and test conditions used in developing this model.

CEB-FIP Model Code 1990 (1993) is based on the EC2-91 model (1991) (Ghali and Favre, 1994). The EC 2 model states that the compressive or tensile stress to which the specimen is subjected should not exceed 45% of its ultimate strength. Considering that testing conditions may exceed the prescribed criteria, it is unsafe to assume that this model can be applied to relaxation in bonded concrete overlays.

In summary, from the CEB-FIP Model Code 1990 (1993), factors affecting relaxation could be identified. These are relative humidity, time (maturity), elastic modulus, specimen dimensions, compressive strength and creep coefficient.

2.4.3.2 Ghali and Favre

Ghali and Favre (1994) presented a mathematical expression for relaxation. The expression was based on instantaneous stress and creep functions. The derivation was not specific to a particular magnitude of stress, sample size and loading conditions. Similar to most models, Ghali and Favre (1994) derived a relaxation model from the basis of creep.

They proposed that if a concrete member is subjected to constant strain 'ε_c', induced stress may be represented by [2.17]. If the concrete length does not change i.e. strain remains constant, induced stress decreases with time.

$$\sigma_c(t) = \varepsilon_c r(t, t_0) \qquad [2.17]$$

$\sigma_c(t)$ = stress in concrete at time t after loading

ε_c = constant imposed strain

$r(t, t_0)$ = relaxation function

The relaxation function is defined as the stress at age *t* due to a unit strain introduced at age t_0 and sustained constant during the period t - t_0. Ghali and Favre (1994) represented this expression graphically in the form of a stress time curve (Fig. 2.13).

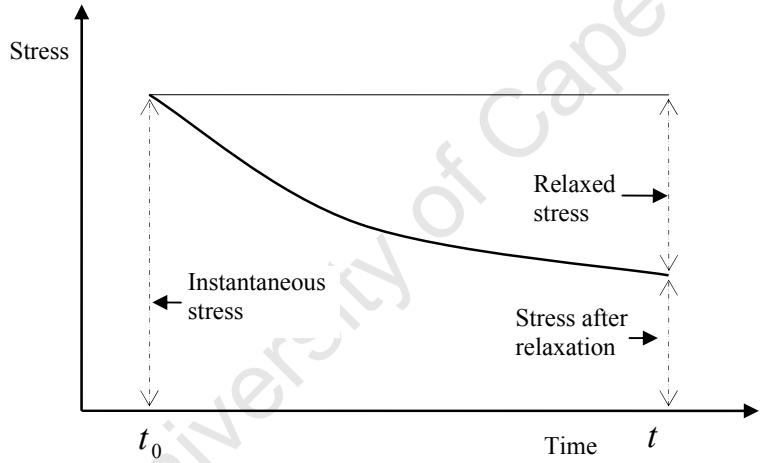

Fig. 2.15: Variation of stress with time due to constant imposed strain *(Ghali & Favre 1994)*.

In order to use Equation 2.17, the Boltzmann principle of superposition was applied. Using superposition, the curve in Fig. 2.15 was divided into a series of small linear stress impulses (Fig. 2.16). Subsequently the relaxation curve is analysed as small subdivisions of stress. The creep expression is then applied.

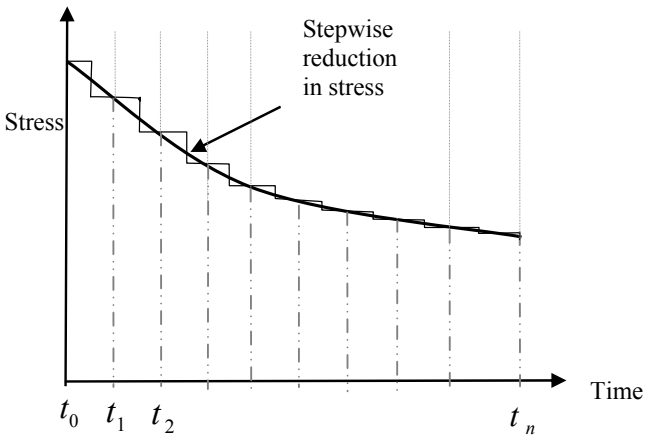

Fig. 2.16: Decomposition of stress history into stress impulses.

A stepwise calculation of the relaxation factor at each stress interval was shown. Time integration approach was used to modify equation [2.17] to form equation [2.18]. This resulted in a time integration model. This model could be fed converted into a simple computer program or spreadsheet. The computer program can be used to determine relaxation at any of loading by simply increasing time. As a result, the expression for relaxation becomes.

$$r\left(t_{i+\frac{1}{2}}, t_0\right) = \frac{1}{\varepsilon_c}\sum_{j=1}^{i}\left(\sigma_c\right)_j \qquad [2.18]$$

$r\left(t_{i+\frac{1}{2}}, t_0\right)$ = relaxation time step

$t_{i+\frac{1}{2}}$ = age at the end of interval i

t_0 = age at loading

The rest of the variables remain the same

σ_c can be calculated directly from the creep equation using time integration to [2.19]. Values of modulus of elasticity, creep coefficients, and shrinkage are assumed to be known at all intervals.

$$\left(\Delta\sigma_c\right)_i = \frac{E_c\left(t_i\right)}{1+\varphi\left(t_{i+\frac{1}{2}}, t_i\right)}\left[\varepsilon_c\left(t_{i+\frac{1}{2}}\right) - \varepsilon_{cs}\left(t_{i+\frac{1}{2}}, t_0\right) - \sum_{j=1}^{i-1}\left(\left(\Delta\sigma_c\right)_j \frac{1+\varphi\left(t_{i+\frac{1}{2}}, t_j\right)}{E_c\left(t_j\right)}\right)\right] \quad [2.19]$$

$\left(\Delta\sigma_c\right)_i$ = stress increment at interval i.

$\varphi\left(t_{i+\frac{1}{2}}, t_i\right)$ = creep coefficient from initial time t_0 up to the time step $t_{i+\frac{1}{2}}$

$\varepsilon_{cs}\left(t_{i+\frac{1}{2}}, t_0\right)$ = shrinkage strain from initial time t_0 up to the time step $t_{i+\frac{1}{2}}$

All variables in this expression have been described in previous equations

Iteration intervals, *i*, and *j* for time and stress, respectively can be varied from 1 up to *n* in order to find the total relaxation at each interval.

The relaxation function in equation [2.18] determined from equation [2.19]. In this case shrinkage strain increment may be assumed to be zero and imposed strain kept constant.

Through experiments, Gutsch & Rostásy (1994), Morimoto & Koyanagi (1994) and Beushausen & Alexander (2006) made further investigations. Their studies focussed mainly on identifying influential parameters. As such, Equation [2.18] can be expanded to represent the relaxation function in terms of material properties and other empirical terms as detailed in Section 2.4.3.3, 2.4.3.4 and 2.4.3.5.

2.4.3.3 Gutsch & Rostásy method

The main objective of the study by Gutsch & Rostásy (1994) was to estimate thermal cracking behaviour of concrete subjected to high tensile stresses at early ages. Furthermore, analysis was aimed at determining restraint stresses generated in large concrete structures during the hydration process. Consequently their study had to deal with crack development as well as to account for viscoelastic behaviour under tensile stress. Gutsch & Rostásy (1994) focused on the effects of mechanical properties such

as tensile strength, compressive strength, and elastic modulus. Crack development, influence of creep and relaxation of stresses was also monitored.

Experimental data was used in developing their model. Three concrete mixes were prepared for testing. Mixes were made of rapid hardening cement (PZ 35 F), slow hardening blend (HOZ 35 L) 65% GGBS to 35% OPC and OPC (PC 45). In all mixes, quartz aggregate of maximum size 16 mm was used (Table 2.1).

Table 2.1: Composition of Concrete mixes *[kg/m^3]* (Gutsch & Rostásy, 1994)

Connstituent	*1*	*2*	*3*
Cement type	PZ 35 F	HOZ 35 L	PC 45
Cement Content	270	390	320
w/c	0.65	0.47	0.42
C/A/FA/SF	1/6.85/0.22/0	1/4.58/0/0	1/5.71/0.13/0.07

C: Calcium, A: Aluminate, FA: Fly ash, SF: Silica Fume.

Tests were carried out in uniaxial tension, creep and relaxation. All specimens were cast, sealed and stored at 20 ^{o}C to prevent moisture loss. In order to model the short-term stress strain behaviour axial tensile test specimens were tested to failure. Tests were done at ages 1, 2, 3, 7 and 28 days. Dimensions and geometry of uniaxial tensile test specimens as well as the testing method were not disclosed.

Specimens measuring 1200 mm x 160 mm x 160 mm were prepared from the concrete mixes in Table 2.1 and loaded in a test frame. The frame was designed for testing creep and relaxation under high tensile stresses. However details regarding the test frame and test set up were not disclosed.

Creep and relaxation tests were performed at 1, 2, 3 and 7 days. Gutsch & Rostásy (1994) derived a formulation for relaxation in both compression and tension. Citing Breitenbucher (1989), Emborg (1989) and Laube (1990), they adopted the theory that development of material properties depends on the hydration process. Material properties such as tensile strength, compressive strength, and elastic modulus at any age could be determined. These parameters are important in relaxation modelling.

Gutsch & Rostásy (1994) first expressed the creep function in terms of hydration parameters. This expression is shown in equation [2.20].

$$\varphi\left(t-t_1,\alpha_1\right)=\frac{\varepsilon_c\left(t,t_1\right)}{\varepsilon_{el}\left(t_1\right)}=P_1\left(\alpha_1\right)\left(\frac{\left(t-t_1\right)}{t_k}\right)^{P_2(\alpha_1)} \quad [2.20]$$

$\varphi\left(t-t_1,\alpha_1\right)$ = creep function

t = age at the end of loading

t_1 = age at loading

α_1 = degree of hydration

$\varepsilon_c\left(t,t_1\right)$ = creep strain

$\varepsilon_{el}\left(t_1\right)$ = elastic strain

$P_1\left(\alpha_1\right)$, $P_2\left(\alpha_1\right)$ = empirical functions of the degree of hydration

$\left(t-t_1\right)$ = duration of loading

t_k = 1 hour

Citing Wittmann (1974) who used empirical methods, Gutsch & Rostásy (1994) transformed the creep function into the relaxation function (Equation [2.21]). Equation [2.21] expresses the relaxation function. The relaxation function is a ratio of stress at any time after loading ($\sigma\left(t,t_1\right)$) to the initial stress at the beginning of loading ($\sigma\left(t_1\right)$).

$$\psi\left(t-t_1,\alpha_1\right)=\frac{\sigma\left(t,t_1\right)}{\sigma\left(t_1\right)}=\exp\left(-P_1\left(\alpha_1\right)\left(\frac{\left(t-t_1\right)}{t_k}\right)^{P_2(\alpha_1)}\right) \quad [2.21]$$

$\psi\left(t-t_1,\alpha_1\right)$ = relaxation function

The rest of the parameters are the same as described above

This model demonstrates that relaxation is dependent on age of loading and degree of hydration. It was observed that relaxation decreases with the degree of hydration and also decreases with age. This agrees with findings obtained by Morimoto & Koyanagi (1994), Bissonnette & Pigeon (1995). Therefore the age at loading and magnitude of

stress were fundamental input parameters in this particular study. Moreover it was shown that the initial stress-strength ratio had less influence on relaxation compared to the degree of hydration and age at loading. This also agrees with findings by Morimoto & Koyanagi (1994). The study by Morimoto & Koyanagi (1994) is discussed in detail in the following section.

2.4.3.4 Morimoto & Koyanagi

Morimoto & Koyanagi (1994) conducted a study aimed at determining stress relaxation in concrete subjected to thermal stresses. Thermal stress was as a result of restrained thermal strain. They focused mainly on the influence of initial stress levels and loading age on tensile relaxation. In compressive relaxation, the influence of testing temperature was investigated.

Morimoto & Koyanagi (1994) developed a model based on experimental data. Data was gathered by preparing and testing 2 concrete samples. These were made of different mix proportions and similar constituents (Table 2.2). Ordinary Portland cement (OPC), river sand and crushed gravel of 25 mm maximum size were used.

Table 2.2: Composition of Concrete mixes *[kg/m^3]* (Morimoto & Koyanagi, 1994)

Constituent	*A*	*B*
Water Content	173	166
Cement Content	346	280
w/c	0.5	0.59
River Sand	793	0
Crushed Gravel	996	1040

400 mm x 100 mm x 100 mm and 860 mm x 100 mm x 100 mm specimens were tested for compression and tensile relaxation respectively. The samples were sealed after curing to prevent moisture losses. Testing was done using a universal testing machine. In the case of compression tests, the universal testing machine was capable of controlling strain. For tensile relaxation tests, a high rigidity loading frame was used (Fig. 2.12). The strain applied to the specimens was indirectly determined by the initial stress level. The initial stress levels in terms of stress-to-strength ratios were 30, 60 and 80%. Compressive and tensile relaxation testing was done at ages 1, 2, 3, 7, 14

and 21 days. Testing temperatures were 20 °C, 40 °C, and 60 °C. Fig. 2.17 (a) and 2.17 (b) show the measured compressive and tensile relaxation.

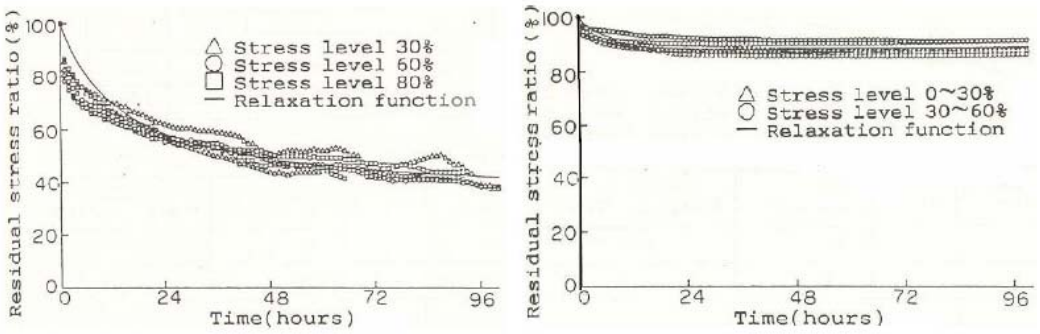

Fig. 2.17(a): Compressive and **(b)** tensile relaxation curve with loading age of 3 days *(Morimoto & Koyanagi, 1994)*

Fig. 2.17 (b) shows small values of tensile relaxation. In general less than 20% relaxation was observed after 96 hours. In contrast, Beushausen (2005) reported 40% to 50% tensile relaxation. Pigeon *et al* (2000) measured relaxation in fully restrained specimens in the order of 67%.

Empirical methods were used for modelling the relaxation function. The empirical formula derived is presented in equation [2.20]. This represents stress relaxation in the form of a ratio of residual stress to initial stress. Experimental constants termed A and C were deduced from experimental data (Fig. 2.17) using the least squares method (Fig. 2.18 & Fig. 2.19).

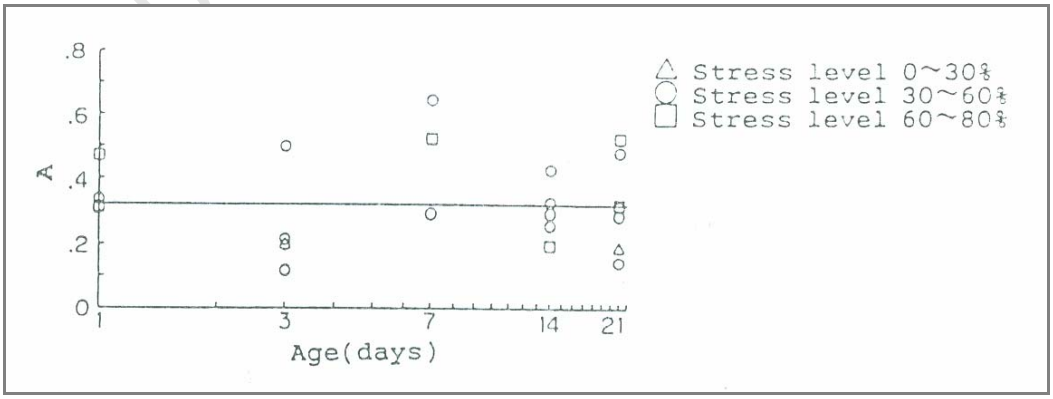

Fig. 2.18: Plot for determining empirical constant A (tensile relaxation test)

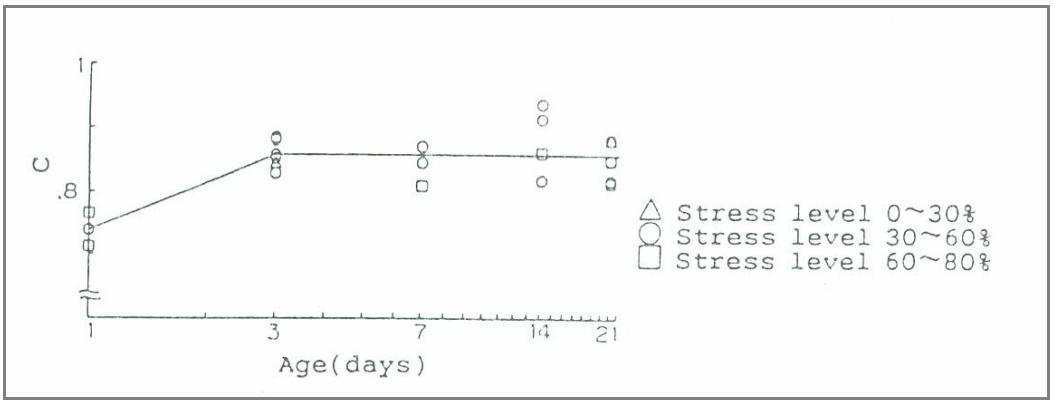

Fig. 2.19: Plot for determining empirical constant C (tensile relaxation test)

The least squares method is a statistical approach for finding a line of best fit from a set of data points. In this case data was obtained by varying stress levels to find constant A and C. Fig. 2.18 and Fig. 2.19 show a very large scatter of results.

Relaxation was expressed in form of equation [2.22].

$$\frac{\sigma_t}{\sigma} = \frac{A + Ct}{A + t} \qquad [2.22]$$

σ_t and σ are residual stresses at a certain time t after loading and initial stress respectively. The equation was then modified for tensile relaxation to equation [2.23].

$$\frac{\sigma_t}{\sigma} = \frac{0.32 + 0.85t}{0.32 + t} \qquad [2.23]$$

This expression is simple to use since it requires only time as an input parameter. However, empirical constants A and C are only valid for specific experiments and test parameters investigated. Nonetheless, fundamental information on relaxation can be identified, e.g. influence of age of loading and development of relaxation with respect to time.

The findings of Morimoto & Koyanagi (1994) were that the rate of relaxation proceeds rapidly during the first hour of loading and decreases with time. This is similar to findings of Gutsch & Rostásy (1994). It was observed that the amount of stress relaxation was proportional to the initial stress. This concurs with findings of

Gutsch & Rostásy (1994). However they observed that the proportionality was only the case for initial stress ranges under 80% of strength. Similar observations have been reported by Neville (1981). Concrete mortar may exhibit linear proportionality up to 80%-85% of its ultimate strength (Neville, 1981).

It was observed that tensile relaxation is smaller and terminates in even shorter periods than compressive relaxation. They also stated that stress relaxation is dependant on the loading age.

Morimoto & Koyanagi (1994) stated that the effects of temperature on stress relaxation were marginal. This finding was contrary to that of Letsch (1991). However, Letsch (1991) tested polymer and polymer modified mortars. These are more susceptible to temperature effects than normal concrete. Nevertheless effects of temperature could be more than just marginal particularly in cases where, apart from mechanical restraint, additional restraint of thermal strains is present. Considering bonded overlays subjected to varying temperature conditions, tensile stresses may be higher due to thermal changes. In this case relaxation is likely to be higher since it is related to imposed stresses.

2.4.3.5 Beushausen and Alexander

Beushausen and Alexander (2006) presented a simplified method for estimating tensile relaxation in bonded concrete overlays at the moment of cracking. Parallel tensile strength tests were done. These were performed in order to find overlay tensile strength during testing period.

Bonded concrete overlays of realistic dimensions were cast and strain targets attached (Fig. 2.20). Based on strain measurements along the interface at both the overlay and the substrate, the composite behaviour could be identified through the strain response. Through strain measurements, Beushausen and Alexander (2006) observed that in the case of bonded concrete overlays, strain measured was proportional to 60% of free shrinkage strain (ε_{FSS}).

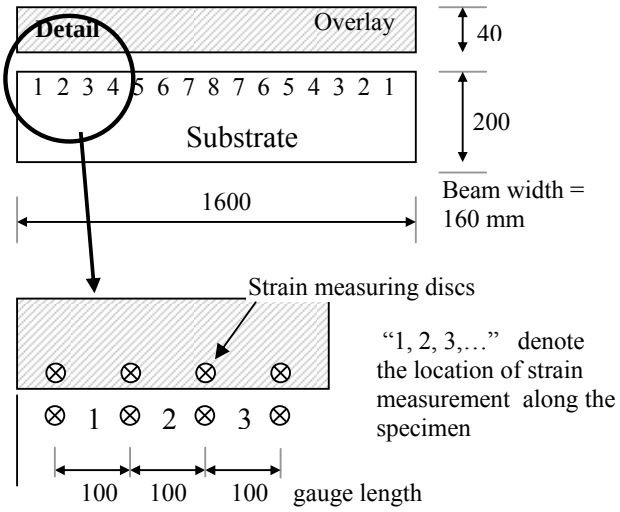

Fig. 2.20: Member dimensions and measuring set up**.**

The expression for the estimation of the magnitude of relaxation used the elastic modulus at the time just before the onset of cracking coupled with the relationship between free shrinkage strain and actual overlay strain. These were used to calculate the actual restraint to which the concrete overlay was subjected. The expression is presented in equation [2.24].

$$\psi_0 = \frac{f_{t,O}}{\left(\varepsilon_{FSS} - \varepsilon_O\right) E_O} \qquad [2.24]$$

ψ_0 = the overlay relaxation factor

$f_{t,O}$ = tensile overlay strength.

$\left(\varepsilon_{FSS} - \varepsilon_O\right)$ = difference between the free shrinkage strain and the measured overlay strain representing the restrained shrinkage.

E_O = modulus of elasticity of the overlay at time of cracking.

Equation [2.24] is a practical approach in attempting to capture relaxation at the moment of cracking. However, the relaxation at any other time cannot be estimated by using equation [2.24]. Moreover if the overlay does not crack, it may be impossible to determine the relaxation.

With respect to fundamental relaxation characteristics, Beushausen and Alexander (2006) concluded that tensile relaxation in bonded concrete overlays occurs shortly after stress initiation and therefore much faster than the rate of stress increase resulting from continuous overlay shrinkage. This is in agreement with findings from

Gutsch & Rostásy (1994) and Morimoto & Koyanagi (1994) who observed that relaxation is rapid at early ages. Therefore to facilitate the prediction of overlay stresses, relaxation can therefore assumed to occur simultaneously with stress initiation. It was recommended that for practical analysis, full relaxation can be assumed to occur simultaneously with stress initiation. Therefore in estimating tensile overlay stresses, the stress-producing shrinkage strain can thus be adjusted $\varepsilon_{\sigma(FSS)}$ by the time dependant overlay relaxation factor $\psi_O(t, t_0)$.

$$\varepsilon_{\sigma(FSS)} = \psi_O(t, t_0) \cdot \varepsilon_{FSS} \qquad [2.25]$$

Beushausen and Alexander (2006) found relaxation in bonded concrete overlays in the range of 40-50%. This is in the order of magnitude as that reported in literature (Gutsch & Rostásy, 1994; Morimoto & Koyanagi, 1994 and Kordina *et al*, 2000). However Pigeon *et al* (2000) measured relaxation in fully restrained specimens in the order of 67%. It is noteworthy that a general comparison of relaxation values obtained using different concrete mixes and test equipments is problematic.

2.4.4 Summary

A gap still remains in modelling tensile relaxation. Several aspects were not addressed in models presented herewith. These aspects are discussed in this summary.

Tensile relaxation values of 20%, 40-50% and 67% have been reported in literature (Gutsch & Rostásy, 1994; Morimoto & Koyanagi, 1994; Kordina *et al*, 2000 and Pigeon *et al*, 2000; Beushausen & Alexander, 2006). It should be noted that tensile relaxation varies with material properties and hence with different concretes.

Gutsch & Rostásy (1994) expressed relaxation using mathematical and empirical formulations. These formulations were based on the relationship between the degree of hydration as well as material properties. It is noteworthy that material properties are expressed in terms of temperature generated. As a result, it is impractical to apply equation [2.9] to overlay relaxation. Gutsch & Rostásy relaxation and creep testing

procedure is not sufficiently clear. Nevertheless it still remains one of the few expressions for describing of stress relaxation in restrained concrete.

The model from CEB-FIP Model Code 1990 (1993) is complicated to use for determining relaxation. A number of creep related mathematical equations are presented in the code. These equations are interrelated. As such that they form a long trail of calculations which must be followed before the solution is reached. In addition, some of the parameters are complex and difficult to determine. With such a 'chain' of equations, it is not simple to apply the CEB-FIP model for relaxation. Owing to these disadvantages, a less complicated model is required.

Morimoto & Koyanagi presented a simplified model for tensile relaxation. Similarly to Gutsch & Rostásy, it can not be applied to the case of bonded overlays. This because the expression is only specific to their test case i.e. mixes, testing conditions etc Their proposed loading frame test set-up can be applied to tensile relaxation testing of specimens to be done in this research.

Equation [2.21] presented by Ghali and Favre is valid and for the case of bonded concrete overlays since the sustained strain 'ε_c' is similar to restrained shrinkage strain The formula presented by Ghali and Favre (1994) is also supported by experimental background. However there is no mention of the magnitude of stress, sample size and loading conditions specific to the model. Hence it seems to be a more theoretical than a practical tool if applied to bonded concrete overlays.

The method given by Beushausen and Alexander gives an indication of the magnitude of relaxation at the onset of cracking. Beushausen and Alexander concluded that, to facilitate prediction of overlay stresses, relaxation can be assumed to occur simultaneously with stress initiation. Following this assumption, tensile overlay stress decreases proportionally with increasing overlay relaxation. Further, relaxation was found to release approximately 40-50% of tensile overlay stress, indicating its major importance for the serviceability of bonded concrete overlays.

CHAPTER THREE: METHODOLOGY OF RESEARCH

3.1 Introduction

This Chapter discusses the research plan for this study. A detailed outline of experimental approach is documented. Fig. 3.1 shows the structure of research methodology.

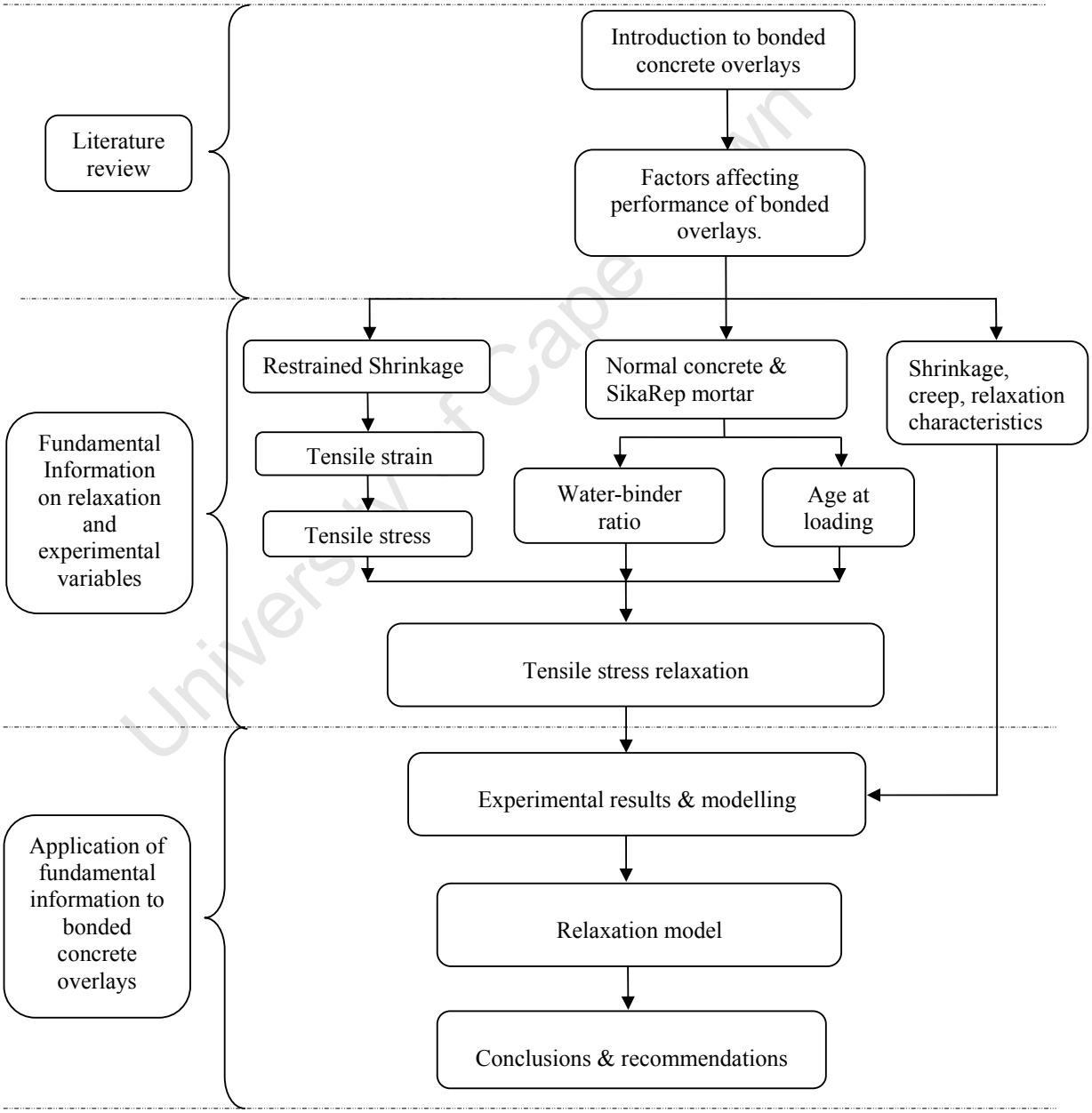

Fig. 3.1: Schematic of thesis structure and research methodology

The introduction and general concepts relating to bonded concrete overlays are covered in Chapter 1. Details pertaining to bonded concrete overlays and their applications including the build up and effects of differential shrinkage are detailed in Chapter 2. In addition, a review of existing models regarding tensile relaxation is also presented. The experimental approach is described in Chapter 4. Experiments to be carried out including influential factors were highlighted in Fig. 3.1. A synopsis of the experimental approach is presented in the following section.

3.2 Experimental approach

A detailed flow chart of the experimental process is presented in Fig. 3.2.

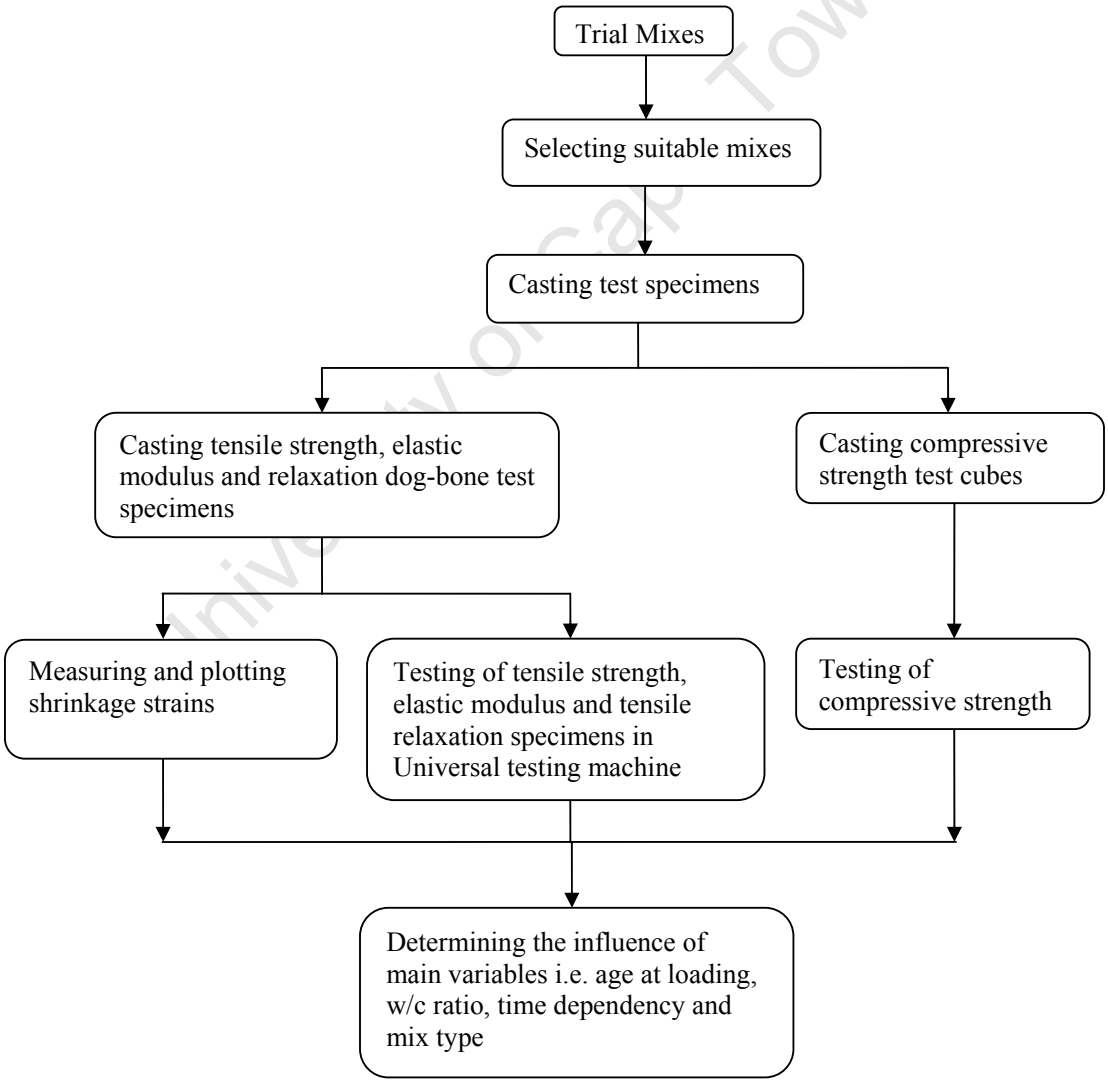

Fig. 3.2: Structure of experimental research.

The experimental procedure starts from designing mixes. Three mixes were selected based on different water-binder ratios and mix composition. 0.45 and 0.60 w/c ratio and a commercial repair mortar were selected. Strength and workability criteria were used in selecting appropriate mix designs. The mix constituents and proportions are detailed in Chapter 4.

After the mix selection, dog-bone specimens were cast. These were for free shrinkage, tensile relaxation, tensile elastic modulus and tensile strength tests. Furthermore, compressive strength test cubes were cast to monitor strength gain of the mix at ages of 2, 3, 4, 7, 14 & 28 days. Free shrinkage specimens were monitored over a period of 12 weeks. Beushausen (2005) measured shrinkage values in bonded concrete overlays and found that restraint was roughly equivalent to 60% of free shrinkage. It was initially planned to adopt this relation in relaxation tests. However strain control was difficult.

Overlays often crack in practice as they experience stress close to their tensile strength. Therefore, in order to model overlay cracking often experienced in practice, 80% stress-strength ratio was chosen as it is more realistic. Tests were carried out using a Zwick universal testing machine. The testing method is shown in Fig. 3.3.

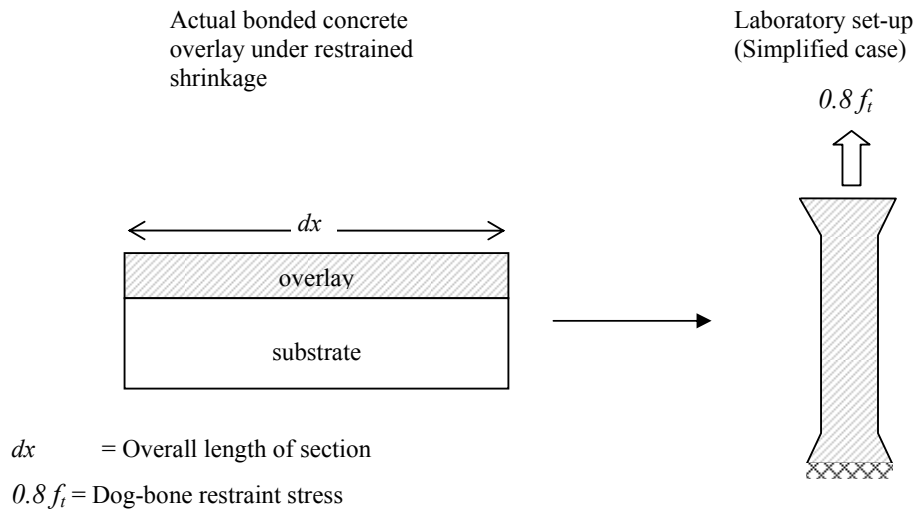

Fig. 3.3: Schematic showing the testing procedure.

Fig. 3.3 illustrates the method of testing. Restraint imposed on an actual bonded concrete overlay may be represented by a dog-bone laboratory specimen subjected to stress or strain. A certain restraint is imposed on dog-bone specimens. This indirectly represents actual bonded concrete overlay strain.

3.3 Summary

Experimental results are presented in Chapter 5. Presentation of analytical models and modelling of the results is done in Chapter 6. The summary, conclusions and suggestions for future research are detailed in Chapter 7. Need for further research would be highlighted in terms of recommendations either for future research or for the optimal design of bonded concrete overlays. This would include reducing the risk of cracking in overlays caused by taking advantage of tensile stress relaxation.

CHAPTER FOUR: EXPERIMENTAL TECHNIQUES

4.1 Introduction

There is limited information in literature on experiments concerning relaxation in bonded concrete overlays. For this reason, this study shall rely on experiments in order to get satisfactory indications or conclusions regarding the development of tensile relaxation in concretes made from different mixes.

Factors that influence overlay stress relaxation can be established in a more organized manner when experimental techniques are used. For example w/c ratio, binder type, elastic modulus, shrinkage, duration of curing and degree of restraint.

For experimental work, several variables were selected for investigation. These variables were identified and classified in terms of test parameters and defined parameters. Test parameters involve variables that can be altered to observe their influence on relaxation. Defined parameters, on the other hand are those variables having a definite magnitude. There is no freedom to change the value of defined parameters during the test. An appropriate example is the value of restrained shrinkage stress which is taken as 80% of specimen tensile strength. This value was selected in order to investigate relaxation under extreme conditions.

Fig. 4.1 shows the main variables to be considered in the testing process.

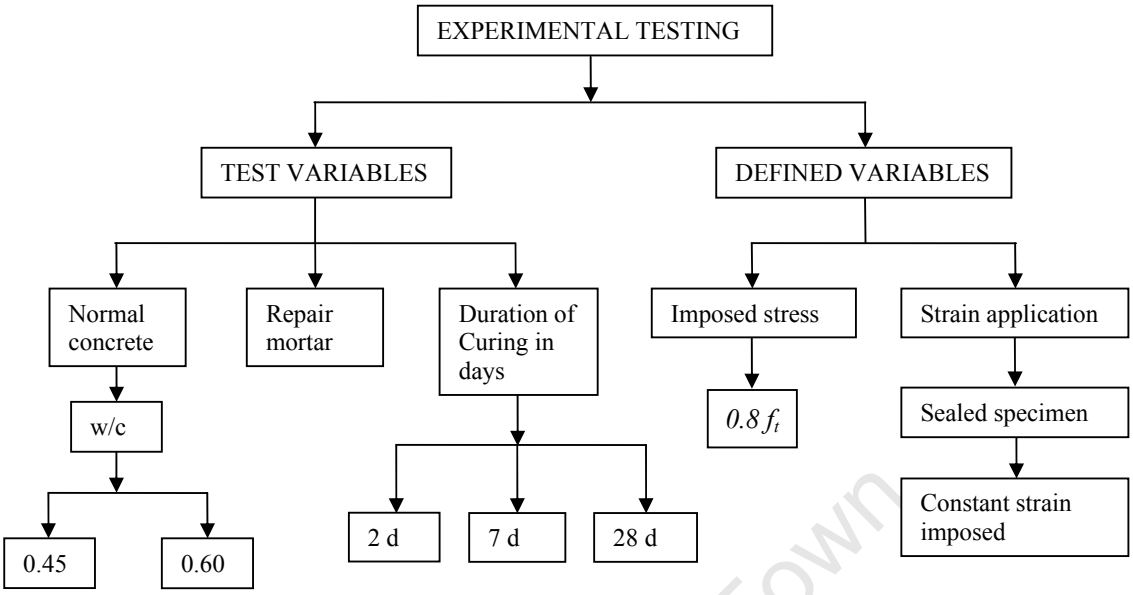

Fig. 4.1: Main parameters considered in experiments.

Fig. 4.1 shows the main parameters considered in experimental testing. However these are not the only influential variables. There are other factors such as temperature conditions and relative humidity that have to be taken into account. Nevertheless the above mentioned factors and their effects on tensile relaxation of overlay stresses shall be discussed further (Section 4.2).

Tensile relaxation tests were performed using a Zwick Universal Testing Machine (UTM). However the UTM is not fully equipped to accommodate any specimen geometry. One of the main requirements was to design appropriate test specimen geometry. This would be done in order to ensure uniform non-eccentric loading. In this regard, the proposed specimen size and geometry and test set up will be described. Other equipment used is also discussed.

Relaxation tests were performed by subjecting test specimens to a defined initial stress-strength ratio. Thereafter strain was kept constant. Reduction in stress with time was then monitored. The specimen was loaded in pure axial tension ensuring that no unforeseen specimen failure occurred. Therefore, an appropriate design for connecting the specimen to UTM will be put forward.

It is important to develop a testing program that is accurate and results in minimum eccentricity and minimum error. The selected test variables are discussed in detail in the following sections.

4.2 Test variables

Test variables relevant to experimental procedure have been highlighted briefly in the introduction to this chapter (Fig. 4.1). A more detailed overview and significance of variables is done in this section.

4.2.1 Concrete mix design and material selection

Three concrete mixes were tested. Tests were performed on normal concrete specimens made of CEM 1 (OPC). Another mix was made from a commercial repair mortar. The mixes eventually chosen had to be robust enough to withstand experimental handling. This is because tensile test specimens are relatively fragile. All mixes did not contain coarse aggregates. This is because coarse aggregates may contribute to dilution and restraint effects (Alexander, 2001).

Klipheuwel sand was used in the normal concrete mixes as it is more well graded compared to Phillipi dune sand. Phillipi dune sand is fine grained whilst Klipheuwel sand has coarse to fine grain size distribution. It should be noted that both Klipheuwel sand and Phillipi dune sand are found in Cape Town. Klipheuwel sand has properties such as good workability hence lower water demand (Alexander, 2001). Superplasticiser was used for low w/c at 0.45 (to improve workability).

4.2.1.1 Water cement ratio

Table 4.1 shows the assumed effects of w/c on compressive and tensile strength, elastic modulus, shrinkage and relaxation. The mixes will comprise of 3 types. Normal concrete mortar was cast with 0.45 and 0.60 w/c ratios. This generally covers the range of normal concretes that may be used in overlays. Both normal concrete paste mixes consisted of similar constituents i.e. fine aggregate, amount of water and

the cement type. Fig. 4.2 shows the effect of w/c as a variable parameter in the mix design.

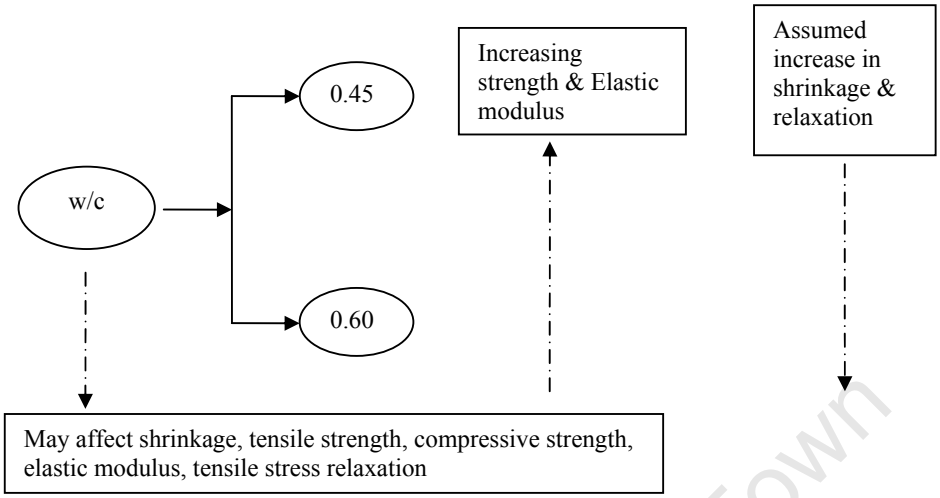

Fig. 4.2: Significance of w/c ratio

Sika® Rep LW repair mortar was used. This is a non-sag, cement based, multi-purpose patching and repair mortar (Sika® Product Manual 2008). A recommended higher level mix proportion was used for Sika® Rep LW repair mortar. The mix was 4 litres of water per 25 kg bag of repair mortar. A slump of 0 mm was obtained.

Table 4.2 shows the mix proportions of all mixes tested. It is noteworthy that the constituents of Sika® Rep LW repair mortar are unknown. Therefore the amount of binder in the mix could not be ascertained. Water content and targeted slump was 330 *l* and 75 mm respectively in normal concrete mixes.

Table 4.1: Mix proportions of all the test samples

Constituent [kg/m³]	*Normal Concrete mortar*		*Sika® Rep LW*
w/c ratio	0.45	0.60	-
Cement	556	417	-
Water	250	250	-
Klipheuwel Sand	1490	1605	-
Superplasticiser [*ml*]	6	-	-

4.2.2 Duration of curing

Due to the fragile nature of tensile relaxation tests, all samples were cured for at least 2 days before loading (Fig. 4.1). This ensured that members did not fall apart during testing. Moreover they gained enough strength to resist stresses due to handling. For example damage may occur when placing specimens in the testing frame.

Apart from tensile relaxation tests, other tests carried out on the UTM were tensile strength and elastic modulus tests. The test schedule was such that tests were run consecutively in the UTM. For example, tensile strength tests were performed first. Immediately after that, relaxation specimens were tested. Finally another tensile strength test would be done after tensile relaxation. The test schedule is presented in detail in Section 4.7.2.

The period of curing was varied between 2 days, 7 days and 28 days. This was done in order to capture the effect of curing at early age up to later age. There is a gradual increase in strength and stiffness of concrete which increases with increasing duration of curing. The curing procedure was such that after samples were demoulded, they were covered in wet burlap and plastic sheets until testing**. "**Long term" tests were also carried out. Specimens were cured for 28 days. Fig. 4.3 shows the assumed influence of curing period on relaxation properties.

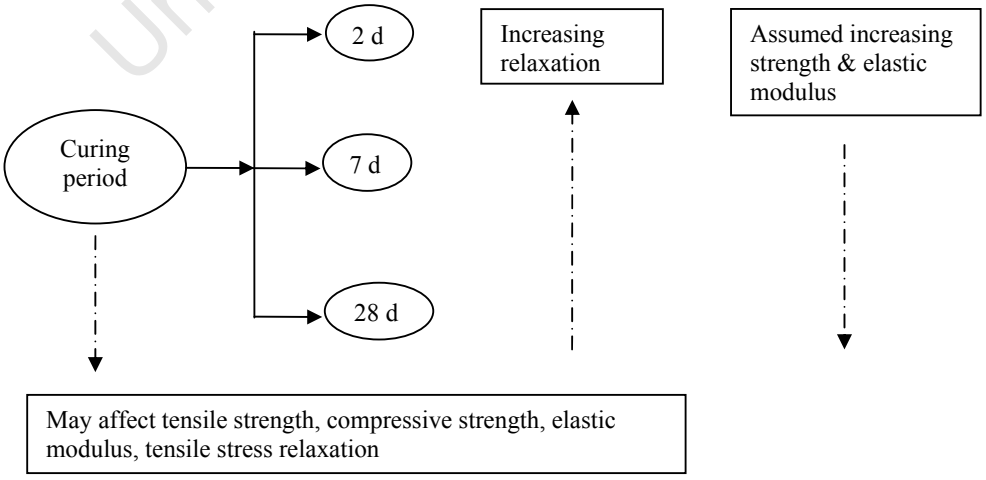

Fig. 4.3: Significance of duration of curing

4.2.3 Laboratory Conditions

It is important that laboratory conditions remain consistent throughout the testing period. Factors such as temperature and relative humidity play an important part on the outcome of relaxation during testing. For example higher temperatures result in a higher degree of relaxation. This is observed in studies focussing on effects of temperature on relaxation presented by Letsch (1991) and Morimoto & Koyanagi (1994). Letsch (1991) measured relaxation in polymer modified mortars arising from thermal restraint.

Relative humidity has a marked influence on the degree of shrinkage attained by concrete. At high values of relative humidity shrinkage is reduced. Likewise, at a lower range of relative humidity, shrinkage increases. Particularly drying shrinkage increases with a decrease in relative humidity whilst carbonation shrinkage may exhibit a more complex response (Alexander, 2001). Hence for consistency, free shrinkage and relaxation specimens were tested in similar environmental conditions.

4.3 Main parameters considered

Reliable test methods are important for predicting performance of bonded concrete overlays. In this regard, main properties in the experimental investigation were identified from literature. These include the ultimate shrinkage, shrinkage rate, restraint conditions, tensile strength, compressive strength, elastic modulus and tensile relaxation influence concrete behaviour under restrained conditions.

In this study, compressive strength tests were done initially to determine the strength of the mixes. Compressive and tensile strength tests were performed at 2, 3, 4, 7, 14 & 28 days. Data obtained from these tests was used to characterise the respective concrete mixes. Fig. 4.4 shows tests carried out.

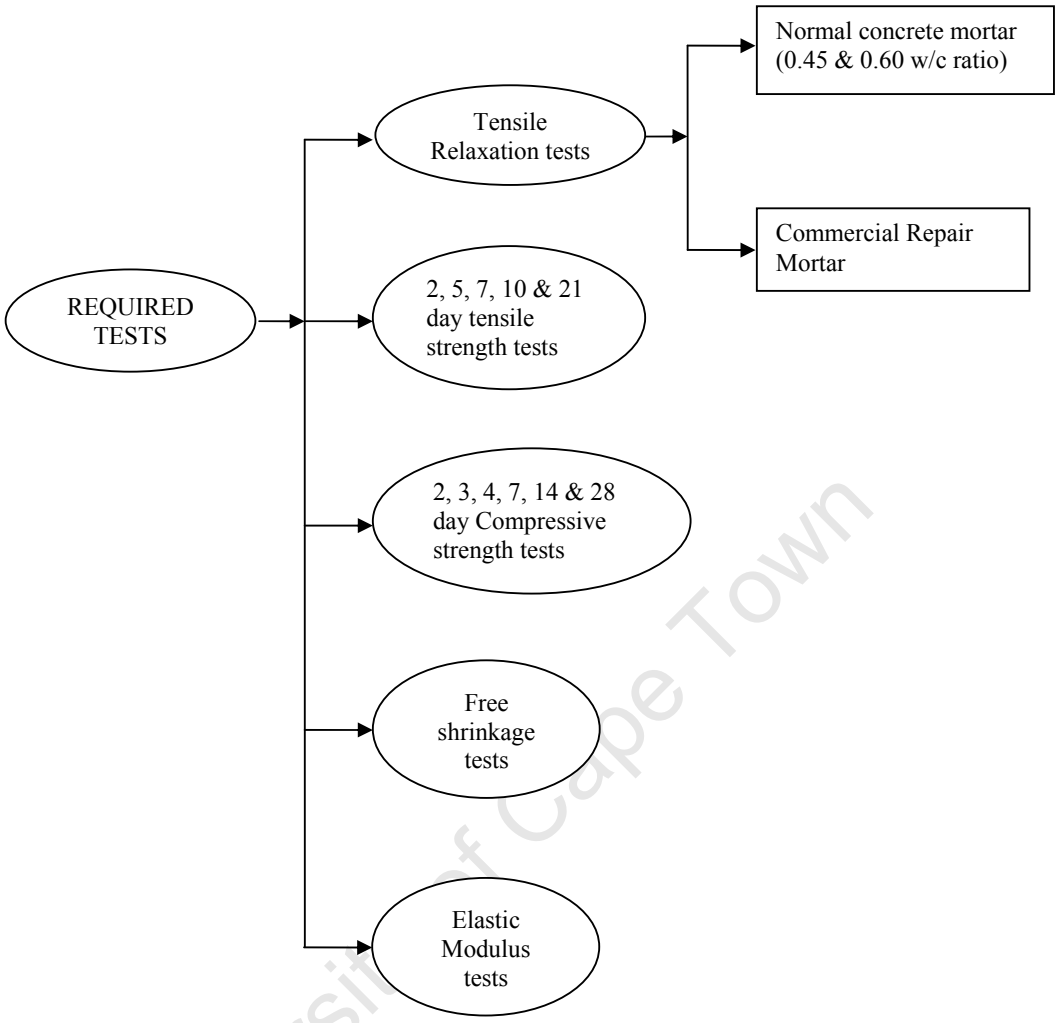

Fig. 4.4: Tests carried out

Short term compression tests were done immediately after curing at 2, 3 and 4 days respectively. 'Short term' in this context refers to the period within which tensile relaxation tests were performed at 2, 3 and 4 days. Four 100 mm x 100 mm concrete compression strength test cubes were cast for each test. One additional cube was reserved in case of any error occurring. Cubes were wet cured before testing. For compressive strength tests, cubes were placed into the compression testing machine and loaded until failure. This was in accordance with the standard compression cube test described in SANS method 863 (1994).

4.3.1 Tensile strength and elastic modulus

For tensile strength tests, specimens of the same geometry as relaxation test specimens, i.e. dog-bone specimens, were subjected to uniaxial tensile force in the UTM until failure. Since relaxation tests were carried out for up to 3 days, tensile tests could only be performed during the first day (day 2 /day 7 /day 28) and in the final day of each relaxation test (day 5 /day 10 /day 31). This is because there was only one UTM. Therefore it was not possible to carry out tensile strength and relaxation at the same time. For the elastic modulus, similarly to tests described by Emberson & Mays (1990) the values were determined from plotted stress-strain curves. Curves were plotted from strain gauge data and stress obtained from UTM.

4.3.2 Free shrinkage strains

Separate dog-bone specimens for free shrinkage strain were cast. Specimens dimensions were 290 mm x 40 mm x 40 mm. Demec points were attached along the specimen length within the prismatic section at 100 mm gauge length. This was in order to measure free shrinkage strains within the prismatic section. Free shrinkage specimens were placed in the laboratory. Strain was measured and recorded for up to 90 days.

Free shrinkage samples were moist-cured (wet burlap and plastic sheets) for 2 days prior to testing. Thereafter they were exposed to laboratory conditions i.e 20-21 ^{0}C and 80% RH and subsequently measured. Specimens were unsealed on all surfaces. This was in agreement with Beushausen and Alexander (2006) who argued that completely unsealed specimens best represent the boundary conditions experienced in actual overlays. Bonded overlays may not only lose moisture through exposed surfaces to the environment. Moisture loss may also occur through the substrate. If the substrate is relatively dry, it tends to absorb water from the overlay.

Asad *et al* (1997) and Vaysburd *et al* (2000) used specimens that were predominantly exposed to one dimensional moisture loss i.e. other faces were sealed to avoid moisture loss in transverse directions. This was disregarding effects of substrate absorption. This may result in underestimating shrinkage strains.

In this study, strains were measured using an extensometer with a gauge length of 100 mm and measuring accuracy of 10 microstrains. Strain data was collected almost daily.

4.3.3 Duration of tensile relaxation tests

In tests done by Morimoto & Koyanagi (1994), tensile relaxation test specimens loaded at ages of 1 day and 3 days showed significant stress relaxation as early as 2-3 hours after loading. It was shown that tensile stress relaxation of approximately 25% and 15% was achieved for the loading age at 1 day and at 3 days respectively.

These researchers (Gutsch & Rostásy, 1994; Morimoto & Koyanagi, 1994; Kordina *et al*, 2000) presented findings pertaining mainly to time taken to reach ultimate tensile relaxation values. In particular, Morimoto & Koyanagi (1994) observed that ultimate relaxation decreases with the age of the concrete. Based on conclusions above and considering time constraints, a testing duration of at least 72 hours was selected for relaxation testing.

4.4 Specimen Geometry for tensile testing

Test specimens were dog bone prisms with extended dovetail ends. Specimens were gripped in specially fabricated jaw assemblies (see Fig. 4.8). The overall dog bone specimen length was 270 mm with the widest section, 90 mm at the gripping area and reducing gradually to 40 mm over a length of 50 mm. The dog bone specimens had a gauge length of 100 mm. Strains were monitored using bonded strain gauges. Fig. 4.5 below shows dimensions of the test specimen.

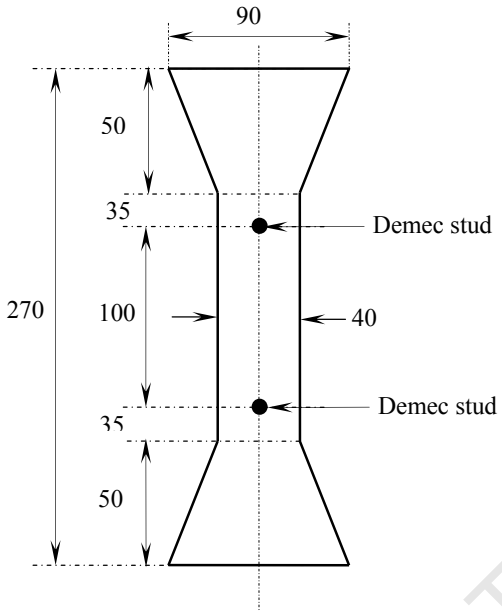

Fig. 4.5: Geometry of test specimen.
(All dimensions are in mm)

The specimen geometry and test apparatus were specifically designed and chosen to eliminate errors in testing. Specimens were designed to avoid effects of shear failure, torsion and bending moments. These effects may arise due to unbalanced specimen alignment (eccentricity). They may also result in non-uniform strain distribution and consequently incorrect results.

At discontinuous edges where the specimen form changes from a prismatic to a truncated "V" section, the specimen was susceptible to intense stress concentrations. This may be due to imposed tensile stresses on the specimen. From a study by Mumenya (2007) a smooth curve connecting the two profiles together was adapted so that the discontinuity was less pronounced. This gradual change in thickness in member geometry would offset local crushing of the specimen. Crushing may be caused by the tip of gripping jaws. Therefore the gradual change in thickness further reduces effects of stress localisation in the specimen.

4.5 Specimen mould

Since there was no existing mould for dog bone specimens, a mould was fabricated in the laboratory. The use of PVC or other plastic material was suitable for dog bone specimen mould. This is because PVC mould is much easier to handle due to its light weight. PVC is waterproof and does no corrode. Hence, absorption of water from concrete during casting is avoided.

Compared to other materials, PVC (Fig. 4.6) could be machined easily into required shape. Relatively smooth inner surfaces could be achieved and it does not to rust. The mould could be put together and dismantled in a simple way.

An image and drawing of the PVC mould used is presented in Fig. 4.6 (a) and Fig. 4.6 (b) respectively.

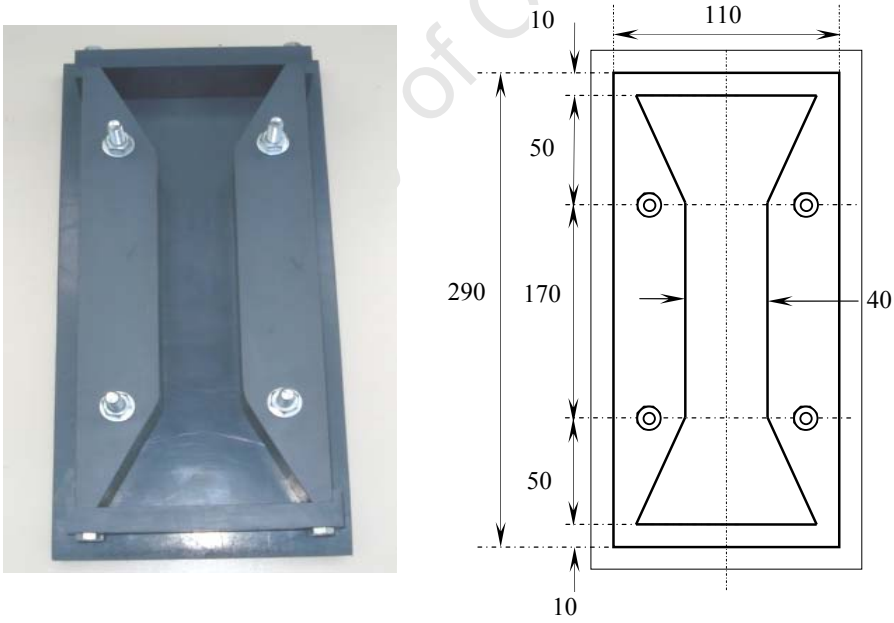

Fig. 4.6 (a): Image of PVC mould used **(b)** Geometry of mould
(All dimensions are in mm)

4.6 Uniaxial tensile testing

4.6.1 Zwick Roell (Z020)

A number of testing methods have been used in the past to test specimens in tension. For this research, the Zwick Roell (Z020) UTM was used. The maximum strength capacity of the Zwick Roell (Z020) UTM is 20 kN.

The testing mechanism was executed in such a way that there was control of imposed stress. Subsequently the resultant induced strain was kept constant. Similar to Morimoto & Koyanagi (1994) and Mumenya (2007), an appropriate loading frame was designed specifically for all tests. The loading frame was fabricated in such a way that it was compatible with standard fixtures of UTM. An example of the Zwick machine (UTM) with a specimen loaded in it is shown in Fig. 4.7.

Fig. 4.7: Zwick Roell Universal Testing Machine.

Direct tensile strength tests were done by loading dog bone specimens in the UTM. The load was applied by the upper crosshead set to a travel of about 0.2 mm per minute until failure. This conforms to loading rates recommended by SANS method 863:5-1994 (1994). This method specifies a time envelope of between three to ten minutes for concrete material tests. Tests performed outside this time envelope address either dynamic or long-term material behaviour (Stander, 2007). This loading rate implied an average stress rate of 1 N/s. Therefore, with an average minimum stress of approximately 2.0 MPa it took about 3 minutes for lower strength specimens to fail. Therefore this was well within the recommended time range.

4.6.2 Aluminium gripping jaws

Gripping jaws were made of aluminium alloy. The aluminium alloy was braced with 10 mm steel plates. This combination was capable of withstanding tensile stresses generated during testing. Jaws were made of a truncated 'V' prism. They were 50 mm wide with 10 mm thick internal plates. Clamps were connected to the UTM crosshead shaft using a swivel bearing. Bearings were fitted to eliminate eccentricity in loading. Bearings allowed for the load to be purely axial since they could pivot and rotate about the contact with the jaws. The gripping jaws are shown in Fig. 4.8.

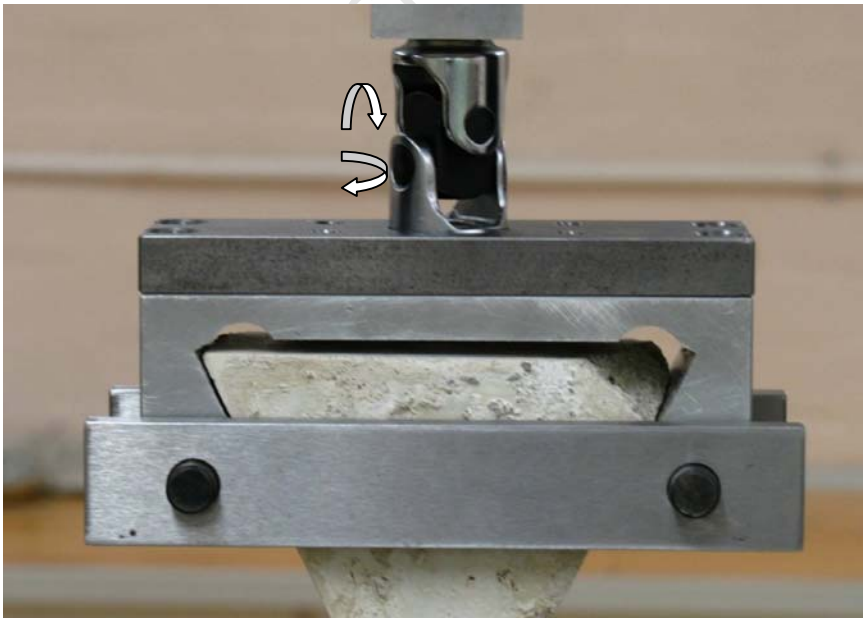

Fig. 4.8: Aluminium grip for tensile relaxation test (connected to bearing).
Arrows indicate rotational degrees of freedom

The dimensions of the gripping jaws were 124 mm x 50 mm x 50 mm. The overall thickness of the plates was 20 mm. The thickness of the aluminium grips was determined from material structural mechanics. Calculations were based on the value of the tensile strength of normal concrete, which is in the range of 5 MPa. This is however an upper limit as tensile strength of relaxation specimens was found to be lower than that. At this value the maximum load that could be subjected on the specimen, assuming ideal conditions, was 10 kN. Therefore the plates were sufficiently stiff to resist bending moments and build-up of extra strain.

Deflection in the clamps was calculated and found to be minor. Deflections may interrupt strain imposed on the specimen during testing. As a result overall strain may be reduced. This may be due to loosening or relaxation of the jaws in response to imposed load.

The tendency of the specimens to be off the line of action of the force is highly likely in such a set up. This results in errors caused by eccentricity. In this case, gripping jaws were equipped with a bearing for free rotation so that any possibility of bending moments was eliminated. Rotation was allowed in the lateral and longitudinal directions. The bearing was in the form of a stiff joint on both crossheads allowing for swivelling once a force is applied on the member. This measure was applied in order to eliminate bending moments and torsional effects in the loading set up.

Eccentricity and bending moments in gripping jaws could result in the specimen failing due to differential forces on either side of member. To ensure that such errors were eliminated, a shaft connecting jaws onto the machine was extended. The shaft was extended to completely fit into the UTM connection unit in order to avoid lateral movement of the upper jaws.

4.7 Tensile relaxation testing procedure

After the specimen had been cast and cured for the required period, it was removed and cleaned thoroughly before testing. Tensile relaxation tests comprised of two types of specimens. These were normal concrete (NC) and commercial repair mortar

specimens as illustrated in Fig. 4.4. All tensile relaxation specimens were tested under sealed conditions. This was done in order to avoid drying shrinkage. Sealing was done by applying a paraffin wax coating. All six exposed surfaces of test samples were sealed to prevent loss of moisture during testing. As a result, there were no additional strains on the specimen due to drying shrinkage. This would enable tensile relaxation to occur at constant strain.

4.7.1 Sealed specimen testing

Specimens were sealed soon after demoulding. They were then kept in sealed condition until testing at a specified age. Sealed tests can be best represented by assuming that shrinkage strain is insignificant. Sealing specimens also represented full-curing. This scenario was impractical because in actual overlays, full curing can never be achieved. From findings of Tao & Weizu (2005), it was shown that in fully cured specimens at early ages, shrinkage continues to occur in a time dependant manner. This is due to thermal dilation and autogenous shrinkage. However all these factors were ignored. As a result shrinkage was slightly underestimated.

Tensile relaxation sealed tests were performed under constant strain. In the absence of an automatic strain monitoring device, tests were performed under a displacement-control mode. This meant that total crosshead travel of the machine was measured. For this reason, the strain output from the UTM was a measure of the distance moved by the crosshead including the strain in the specimen. Hence to measure strain in the specimen, bonded strain gauges were attached. Strain output from bonded strain gauges was measured separately from the data output of the UTM.

It would be more practical to impose a certain value of strain on the first day. This would be increased by a magnitude observed on the free shrinkage and overlay strain data obtained on the second day. The same would be done throughout the duration of the test. This is termed incremental strains since the strains are regularly increased to reproduce gradual increase in overlay restraint. This may be achieved by using unsealed specimens (Fig. 4.9).

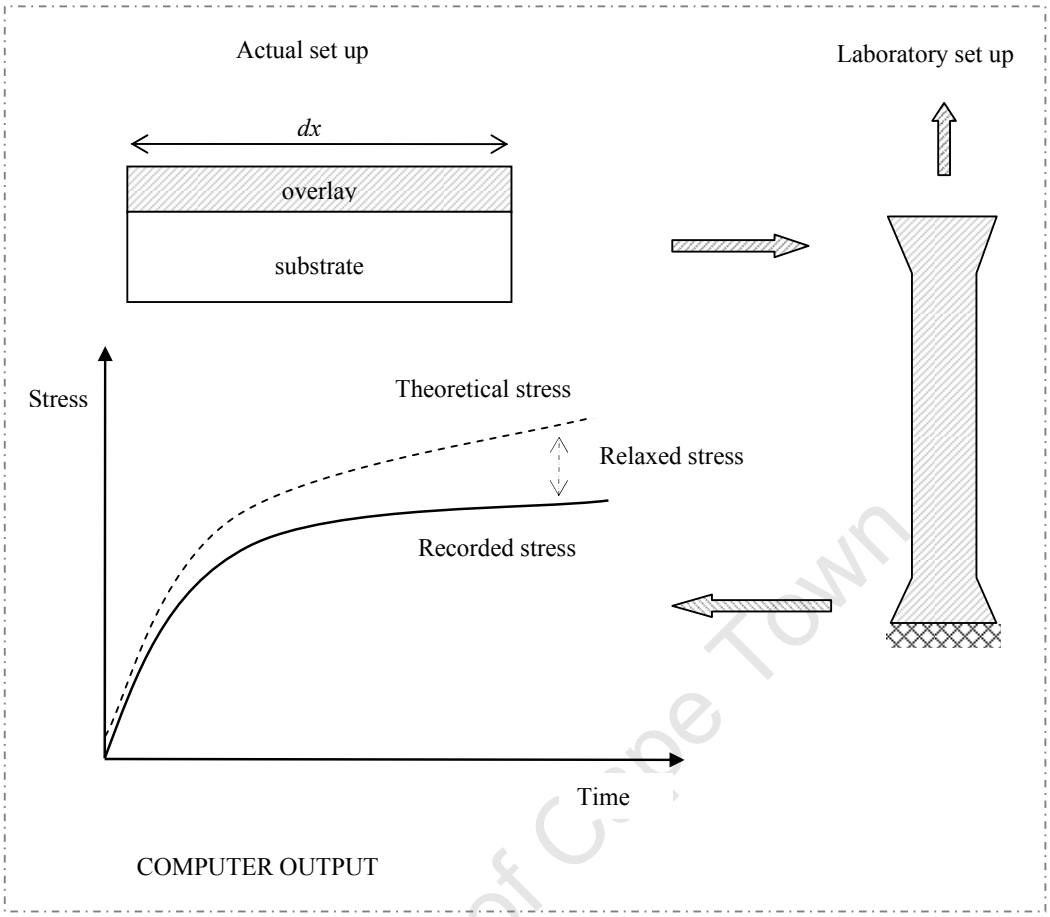

Fig. 4.9: Generalisation of test set up for an unsealed specimen

In principle experiments can be performed on unsealed specimens as well. In this study the author also briefly investigated the relaxation behaviour of unsealed specimens. However very little information was deduced as the results seemed to indicate irregular relaxation curves.

The relaxation capacity may be deduced from theoretical elastic stress values at each point along the curve. Fig. 4.10 shows a schematic of the anticipated stress distribution for sealed and unsealed specimens.

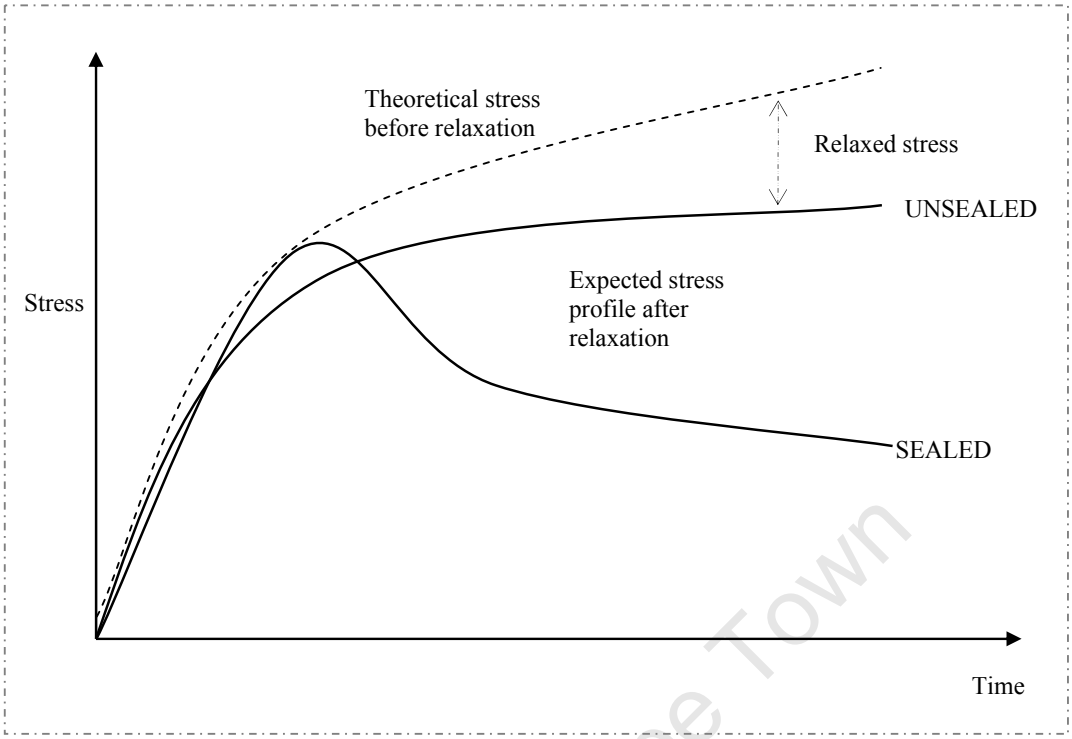

Fig. 4.10: Anticipated stress distribution for sealed and unsealed specimens

Test specimens were inserted into gripping jaws and then held in position within the testing frame. The computer is the main component for data output attached to the UTM. Therefore, as the specimen was loaded, stress within the member would decrease with time. From the computer output, a decreasing stress curve was produced.

The UTM has the software 'testXpert' that enables it to record stress decrease within the specimen under test. This sends signals to the computer attached. The UTM keeps record of stress decay, maintains constant strain and also displays the output on the monitor. Data recorded is readily printed and analysed. Data analysis mainly involves relating initial stresses to stress observed at any time along the curve. This relation includes other parameters which directly affect resultant stresses e.g. the elastic modulus and tensile strength.

4.7.2 Scheduling of tests

Tensile relaxation and tensile strength tests were run continuously throughout the testing period. For the example of 2 days and 7 days specimens, tests were scheduled to run as shown in Fig. 4.11.

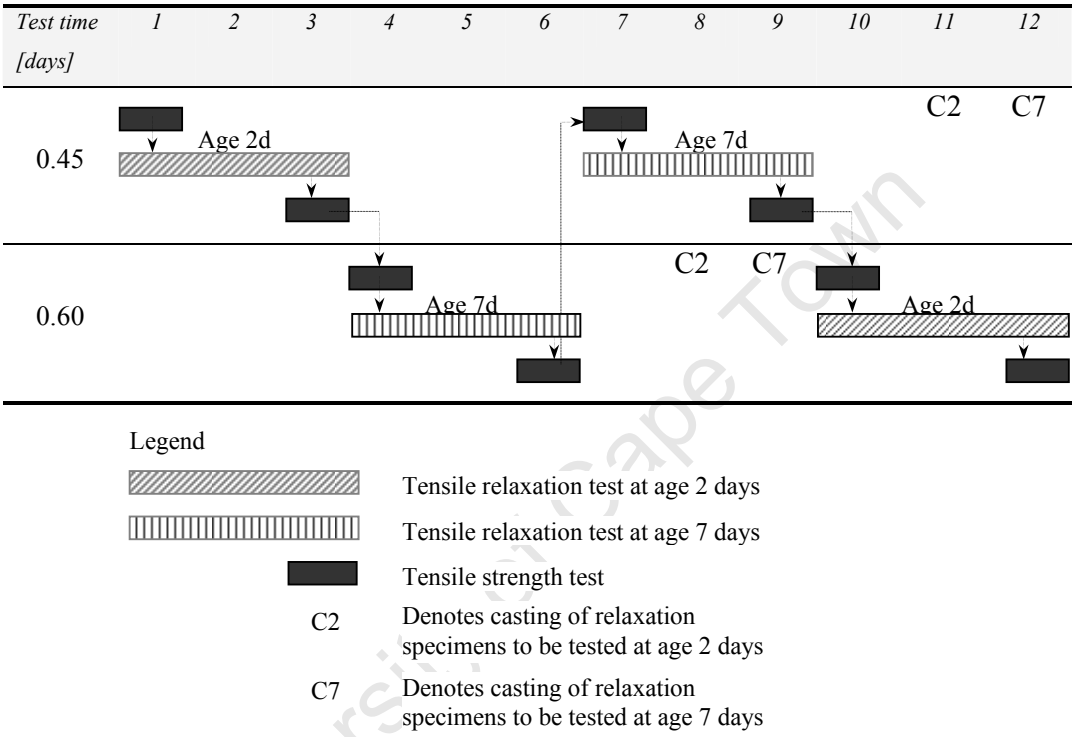

Fig. 4.11: Schematic showing scheduling of tests.

Due to time constraints tests were done continuously. Casting of specimens was done first for 2 day 0.45 w/c ratio specimens and then for 7 day 0.60 w/c ratio specimens. Once 2 day 0.45 w/c ratio specimens were tested, 7 day 0.60 w/c specimens were then tested. The schedule shown in Fig. 4.11 was followed. However, before each tensile relaxation test could be carried out, tensile strength tests were performed. Tensile strength tests were carried out on moist cured specimens. Thereafter, tensile relaxation specimens were tested for at least 72 hours. After a tensile relaxation test, another moist cured dog bone specimen was tested for tensile strength. This was done in order to monitor the strength gain after an additional 72 hours.

Since there were four moulds, four specimens were cast per batch. The first specimen was used for testing tensile relaxation. The second and third specimens were used for testing tensile strength before and after the tensile relaxation test respectively. The fourth specimen was used for testing the tensile strength at either 14, 21 or 28 days.

4.8 Summary

The sections above have discussed the main factors that have been considered in the analysis of tensile relaxation of bonded overlays. Apart from investigating the development of stress within a constrained member, the effects of other parameters such as mix proportions and age at loading also had to be taken into account.

The test set up and information that was deduced from these tests will enable the formulation of a tensile relaxation model. Not all test results were used in the model. Some were used for material characterisation and model assessment. Tests were used in different applications for analysis. For instance elastic modulus was extrapolated from stress-strain curve. This conveniently eliminates the need assigning more test samples in order to find the elastic modulus.

In total, 56 tensile relaxation tests and 143 tensile strength tests were carried out. Experimental tests lasted a period of seven months.

CHAPTER FIVE: EXPERIMENTAL RESULTS AND DISCUSSIONS

5.1 Introduction

This chapter presents and discusses results obtained using experimental techniques detailed in Chapter 4. Results discussed include compressive strength, tensile strength, elastic modulus and shrinkage. Most importantly relaxation is documented. In order to make relaxation test results more accurate, calibration of strains was carried out first. Consequently calibration of strain is discussed.

Tensile relaxation data for normal concrete and commercial repair mortar specimens is obtained. All specimens were sealed. Sealed specimens represent bonded concrete overlays subjected to partial restraint. This is because imposed strain simulates restraint after the overlay has undergone shrinkage. On the other hand, unsealed specimens represent bonded concrete overlays subjected to complete restraint. This latter case is impractical as bonded concrete overlays have been shown to undergo partial shrinkage in service (Beushausen, 2005).

A detailed overview of results is presented in the following sections.

5.2 Strength test results

5.2.1 Compressive strength

Compressive strength tests were carried out on 100 mm x 100 mm concrete mortar cubes. Tests were done for the purpose of material characterisation. Compressive strength cubes were tested at the ages of 2, 3, 4, 7, 14, 21 and 28 days. Data obtained at ages of 2, 3 and 4 days was used to monitor early age strength development. This is the age at which early cracking is likely to occur. Moreover tensile relaxation tests were done at ages 2, 3 and 4 days. For this reason, early age (2, 3 and 4 days) compression tests were carried out to monitor relative strength development within that age. Compressive strength results for 0.45 & 0.60 w/c mixes are presented in Fig. 5.1.

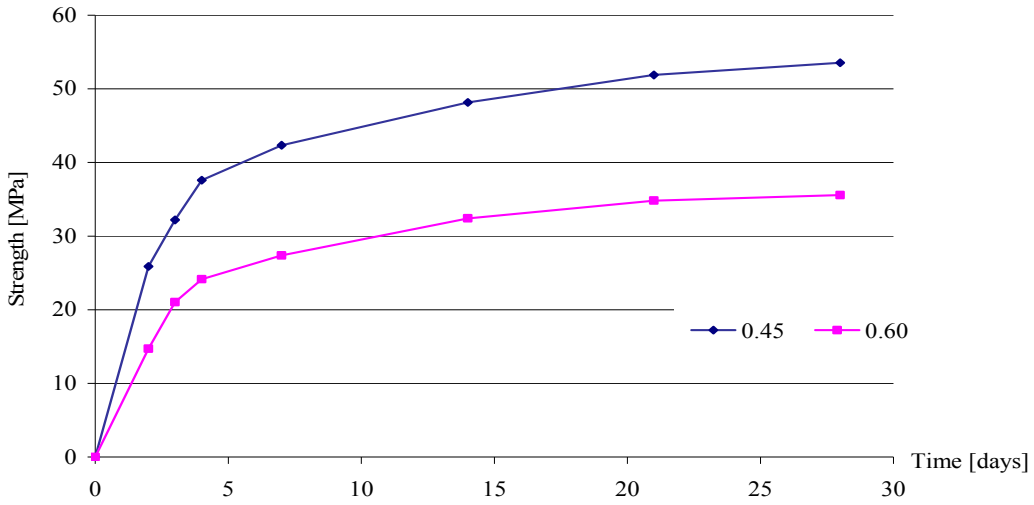

Fig. 5.1: Compressive strength of 0.45 & 0.60 w/c specimens.

As expected 0.45 had higher strength than 0.60 w/c ratio (Fig. 5.1). Due to material constraints, the repair mortar was not tested in compression. In addition the tensile strength of the repair mortar is considered more important in this study.

5.2.2 Tensile strength

Direct uniaxial tensile strength tests were carried out by subjecting dog-bone specimens to increasing tensile stress until failure. This was done using the universal testing machine (UTM). Tests were performed according to SABS method 863:5-1994 (1994). This method specifies a time envelope of between three to ten minutes for concrete material tests.

With regards to the mode of failure, approximately half of all specimens tested failed within the prismatic section. The rest failed due to cracking below the tapered section or within the gripping jaws. As discussed in Chapter 4, this was as a result of high stress concentrations at those points. Fig. 5.2 shows typical dog-bone specimens cracked at prismatic and non-prismatic sections.

Fig. 5.2: Specimens cracked at prismatic (left) and non-prismatic (right) sections respectively.

Tensile strength tests were carried out according to the testing schedule shown in Fig. 4.11. Ultimate tensile strengths were recorded at ages 2, 5, 7, 10 and 14 days. Mean values were calculated and plotted (including standard deviations). Tensile strengths for all mixes are shown in Fig. 5.3.

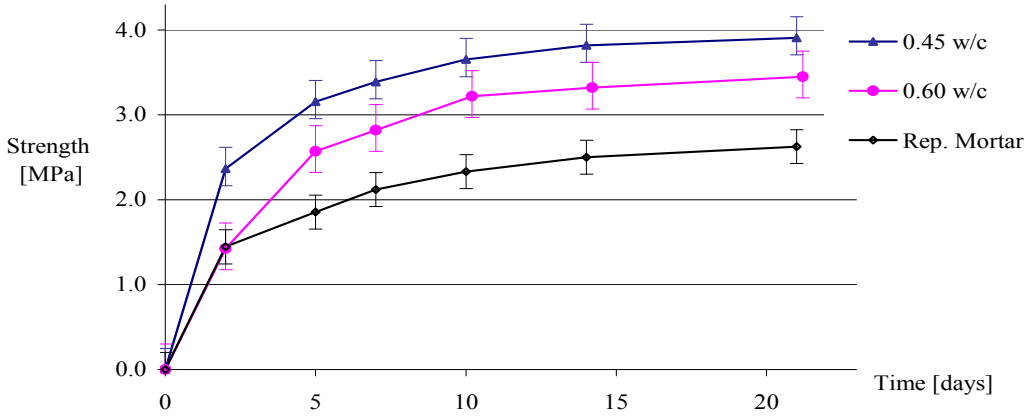

Fig. 5.3: Tensile strength of repair mortar, 0.45 & 0.60 w/c specimens.

5.3 Elastic modulus

The elastic modulus is defined as a slope of the stress-strain curve within the proportional limit of a material. The modulus of elasticity values were calculated from the gradient of secant modulus in the stress-strain curves. Stress-strain curves were obtained from tensile strength tests. Elastic modulus was determined for each mix at the ages at which tensile relaxation testing commenced i.e. at age of 2, 5, 7 and 10 days.

The secant modulus was determined from tensile strength tests. The secant modulus was calculated at a stress-strength ratio of 60%. Mean values of the modulus of elasticity at each age were calculated (Fig. 5.4).

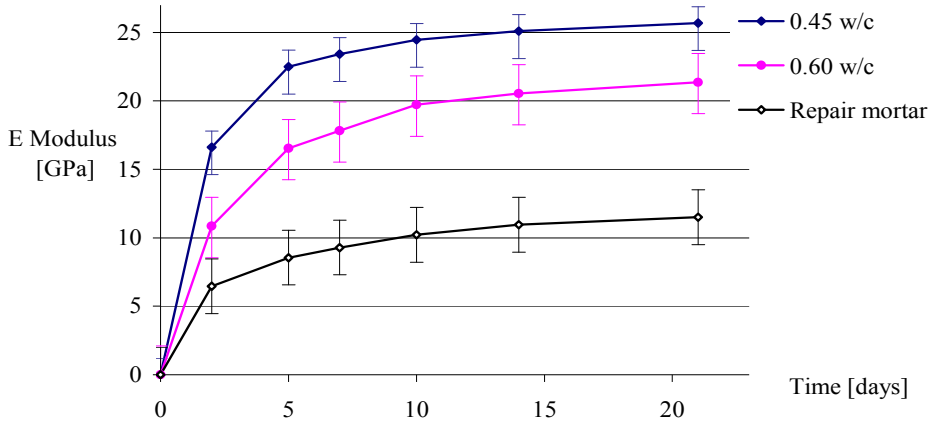

Fig. 5.4: Tensile **e**lastic modulus for repair mortar, 0.45 and 0.60 w/c ratio.

5.4 Shrinkage results

5.4.1 Free shrinkage strain

Free shrinkage strains were monitored for over a period of three months. Specimens were exposed in the testing room as described in Chapter 4. For each w/c ratio, 2 specimens were prepared. As mentioned in Chapter 4, specimens were moist cured for 2 days prior to exposure. Moist curing was done by covering specimens in wet burlap and plastic sheets.

Measurements were taken using a demountable mechanical (Demec) strain gauge with a gauge length of 100 mm. The accuracy of the demec strain gauge was 10 micrometers. A scatter of results was plotted and shrinkage curves were fitted to represent each mix (Fig. 5.5). The best-fit curves were based on nonlinear regression analysis. For the purpose of this study, free shrinkage strain will be presented as positive.

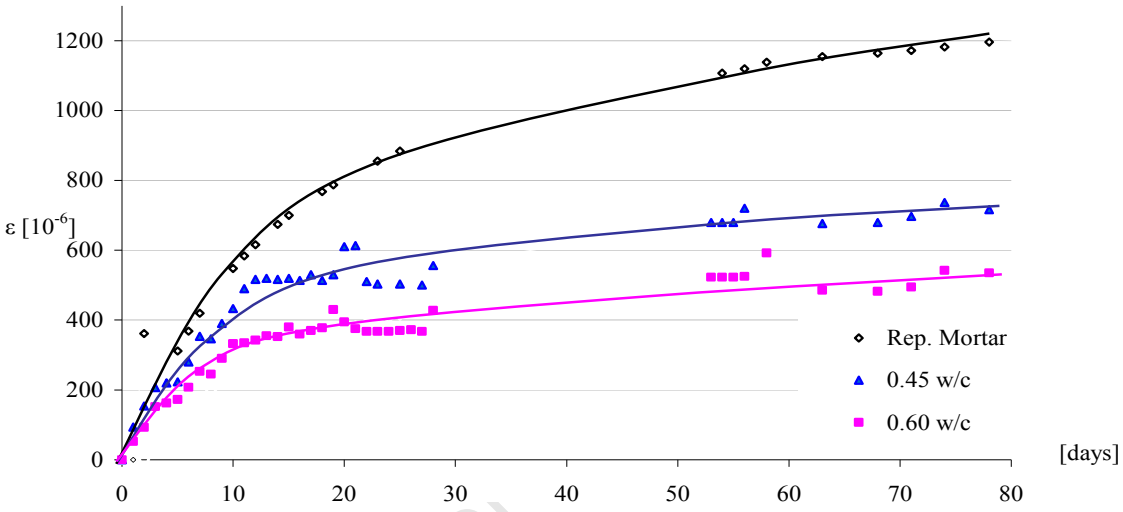

Fig. 5.5: Free shrinkage strain for repair mortar, 0.45 and 0.60 w/c ratio specimens.

A rapid increase in strain during the first two weeks of exposure followed by a generally less rapid increase thereafter was observed. Fluctuations in strain were also observed.

Interestingly, higher shrinkage values were observed in 0.45 w/c ratio specimens. Superficially, this was assumed to result from faulty measurements. However these results were verified by taking readings from another set of specimens exposed to similar conditions. With the exception of drying shrinkage, moisture loss may also have been due to autogenous shrinkage. This may be due to approximately 25% higher volume of cement and about 10% less sand content for 0.45 w/c ratio mix compared to 0.60. Water content was equal in both mixes. Therefore, higher shrinkage in 0.45 water binder mortar may have been due to higher cement and paste content (shrinkage takes place in the paste). The repair mortar showed twice as much shrinkage compared to the 0.45 w/c ratio mix.

5.4.2 Restrained shrinkage

This section gives an indication of stress development vs. strength in the theoretical absence of relaxation. In order to illustrate this scenario, a relation observed by Beushausen (2006) is adopted. Beushausen (2006) reported that restrained shrinkage is directly proportional to free shrinkage. From measurements taken from bonded concrete overlays subjected to restraint, it was shown that shrinkage restraint was roughly 60% of free shrinkage strain. Fig. 5.6 shows the restraint strain values calculated for the first 30 days.

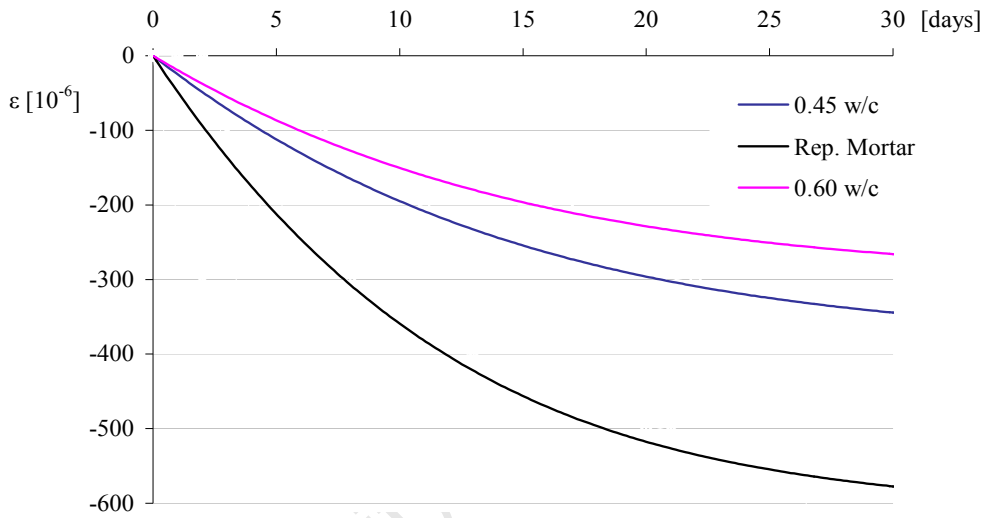

Fig. 5.6: Calculated shrinkage restraint for repair mortar, 0.45 and 0.60 w/c ratio specimens.

Unlike free shrinkage, restraint is represented as negative strain. Free shrinkage causes the specimen to contract and restraint essentially corresponds to a forced-on expansion. Therefore it hinders the specimen from contracting and induces tensile stresses. Stresses due to shrinkage restraint (neglecting relaxation) are shown in Fig. 5.7.

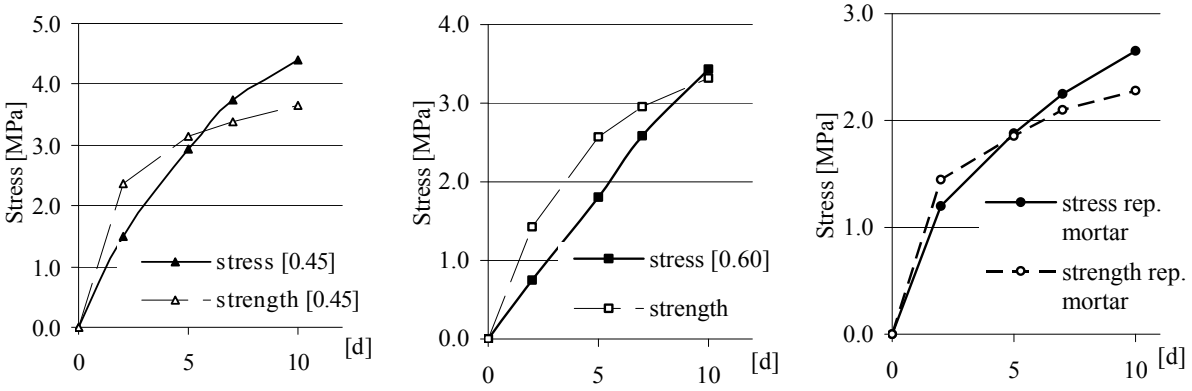

Fig. 5.7: Calculated restraint stress for 0.45 and 0.60 w/c ratio and repair mortar specimens

From Fig. 5.7, stresses generated by restraint after six days are higher than tensile strength of 0.45 w/c ratio specimens. Furthermore, for 0.60 w/c ratio specimen, stress is higher than tensile strength at the age of 9 days. For the repair mortar, the theoretical stresses exceed tensile strength after 5 days. The point at which the stress curve intercepts the strength curve represents the theoretical point of cracking.

As discussed earlier in Chapter 4, there was no control of strain during tests. Tensile relaxation tests could only be performed under displacement-controlled mode. Therefore in order to estimate the imposed strain, calibration was carried out prior to relaxation tests. The calibration method is presented in the following section.

5.5 Calibration of UTM

5.5.1 Introduction

The aim of tensile relaxation testing is to simulate restraint in actual bonded concrete overlays. Subsequently resulting stress decrease is investigated. Restraint was achieved by subjecting specimens to an initial stress. Strain resulting from imposed stress was maintained constant. This was achieved by applying a steady displacement of the UTM crossheads.

However using this method, strain recorded in the UTM was found to be higher than expected in concrete i.e. beyond 200 microstrains. UTM output indicated lack of precision in using displacement control. Consequently, bonded strain gauges were

also used. Bonded strain gauges showed realistic results. Therefore a method of calibrating the UTM in order to achieve required imposed strain was adopted. This section discusses the method used for calibrating UTM strain.

5.5.2 Methodology of strain calibration

It is almost impossible to maintain constant strain in the test specimens throughout a relaxation test. From experiments carried out in this study, additional strain recorded by the UTM was apparently from free play in gripping jaws and from other connection fixtures. Moreover, UTM strain output was found to be the total crosshead travel. Additional strain recorded may possibly have been due to local crushing of small particles of mortar. This may occur between contact surfaces of the jaws and test specimen. Therefore in all tests, inner surfaces of the jaws were cleaned thoroughly to remove loose particles of mortar. This would in theory, ensure an almost perfect surface contact once load was applied.

In order to accurately monitor strains, bonded strain gauges were attached onto test specimens as shown in Fig. 5.8.

Fig. 5.8: Strain calibration test set up.

It was impossible to use bonded strain gauges in all test specimens. This is due to the difficulty to achieve a good bond on moist surfaces of test specimens. As a result some bonded strain gauges would peel off. This resulted in inaccurate strain measurements.

Actual specimen strain was obtained from calibrated UTM output. This was done by using the following procedure (Fig. 5.9).

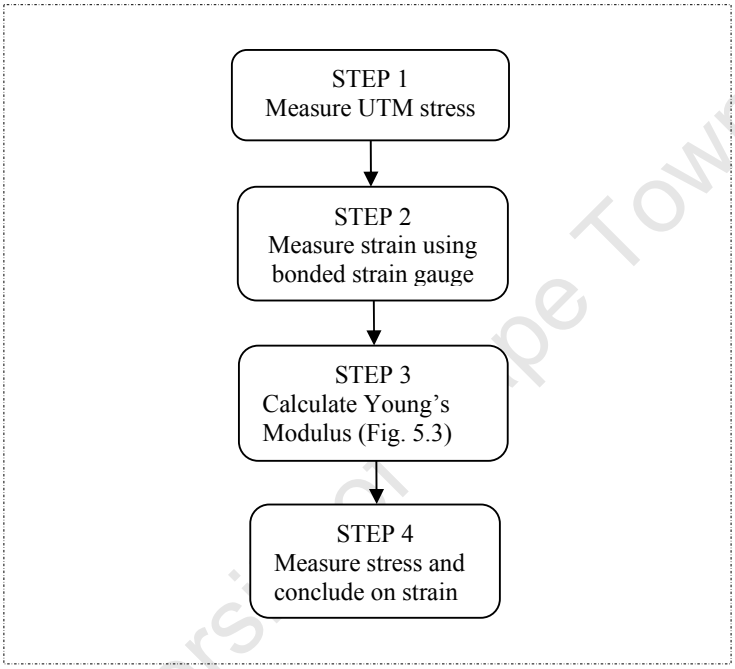

Fig. 5.9: Schematic showing the sequence of calibration

5.5.3 Observations from calibration tests

UTM stress output and bonded strain gauge strains were measured and compared. A direct correlation was identified. Fig. 5.10 shows typical stress and strain outputs from the two sources.

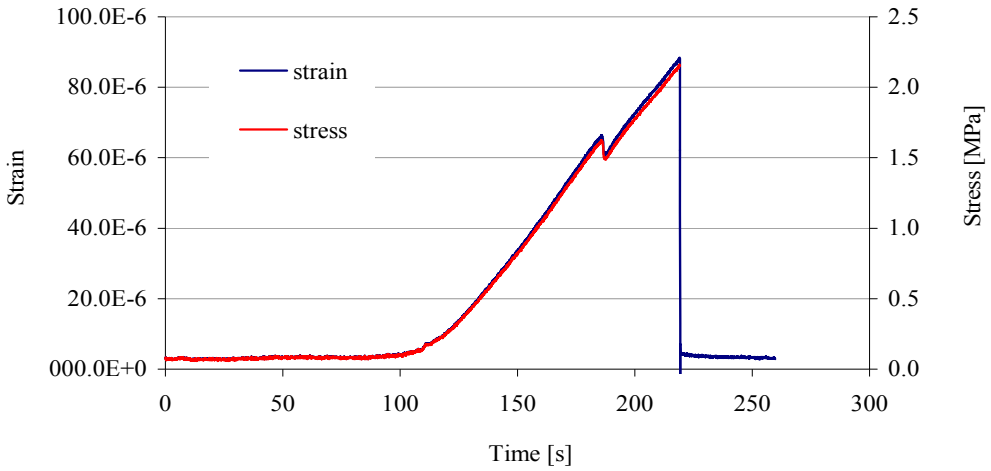

Fig. 5.10: Bonded strain gauge strain (red) and UTM stress (blue) output.

From Fig. 5.10 both curve profiles are clearly superimposed. Preceding full contact between gripping jaws and the specimen, strains recorded on bonded strain gauge and stress on UTM showed a roughly flat profile (up to roughly 100 sec). Subsequently when the specimen was fully gripped, both sources showed an increasing trend indicating stress and strain build-up.

The corresponding crosshead travel is shown in Fig. 5.11.

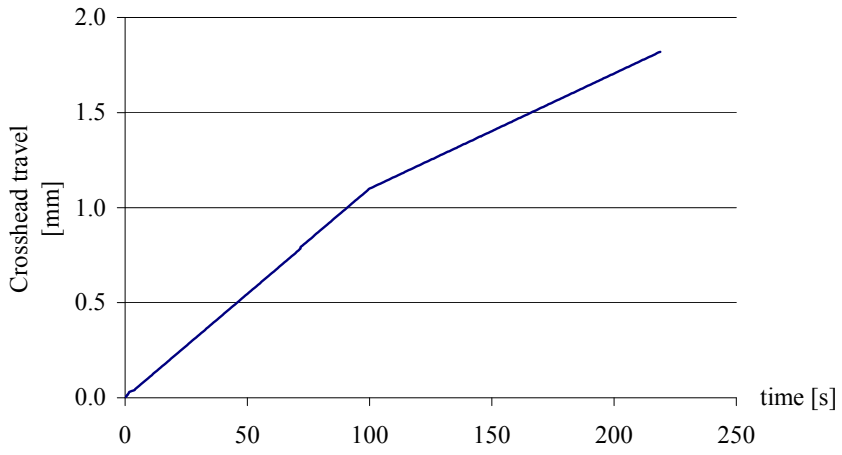

Fig. 5.11: crosshead travel

Specimen strains were calculated from UTM stress output using the elastic modulus. Therefore specimen strain could be estimated from UTM stress output.

5.5.4 Relating calibration to restraint in actual bonded overlays

In order to correlate restraint in laboratory specimens to restraint in bonded concrete overlays, calibration results were used. Restraint in actual overlays was found to be 60% of free shrinkage (Beushausen, 2006). For example the relevant parameters for 7 day, 0.45 w/c ratio specimens are:

ε_{FSS} =120 x 10^{-6}

E_t = 17 GPa

f_t = 2.4 MPa

Strain imposed (ε_r): $0.6 \cdot (120 \times 10^{-6}) = 72 \times 10^{-6}$

However strain application was stress-controlled. Therefore required stress was:

$$\sigma_{req} = E_t \varepsilon_r = 17GPa \cdot 72 \times 10^{-6} \quad [5.1]$$

$$= 1.2MPa$$

Where ε_{FSS} = free shrinkage strain

E_t = Elastic modulus in tension

f_t = tensile strength

ε_r = restraint strain

In this example, restraint equivalent to that observed in actual bonded concrete overlays was found to be 50% of the tensile strength. Imposed stress essentially corresponds to a stress-strength ratio of 50%. This value is well within the linear proportional range of concrete mortar, however it corresponds to a low initial stress. Overlay cracking often experienced in practice is as a result of tensile stresses equivalent to and above 100% of overlay tensile strength. In reality cracking may not be caused by restraint stresses of 50% of overlay tensile strength.

In order to investigate relaxation under extreme conditions, higher restraint is required for application in experiments. Furthermore higher restraint is more realistic in simulating behaviour of bonded concrete overlays under service conditions. As a result 80% stress-strength ratio was adopted. This is because concrete mortar may exhibit linear proportionality up to 80%-85% of its ultimate strength (Neville, 1981). Using stress-strain curves resultant imposed strain could be deduced.

5.5.5 Strain losses during tensile relaxation tests

As discussed in the previous section, bonded strain gauges were attached to relaxation specimens. A typical strain profile is shown in Fig. 5.12.

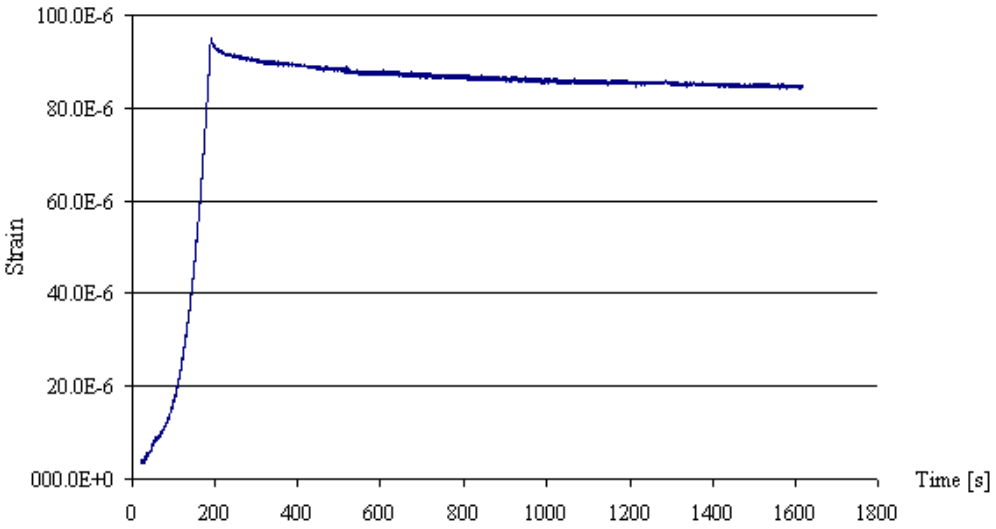

Fig. 5.12: Typical strain output from tensile relaxation test.

This output showed that there was approximately 10% loss in strain within the initial 30 minutes of the test. All specimens exhibited similar behaviour.

Jaeseung, Gregory and Sungho (2008) cited similar observations while conducting relaxation tests on asphalt. As was the case in this study, they had no accurate device for controlling strain. As a result, they also relied on displacement-controlled mode test. Jaeseung *et al* (2008) also found a strain profile as uneven as that observed in Fig. 5.12. Their conclusion was that it may have resulted from non-homogeneity of asphalt mixture during initial stages of testing. Hence a function was developed in order to accommodate non-homogeneity of the strain curve (Jaeseung *et al*, 2008).

In this study, 10% loss in strain develops over 30 minutes and relaxation develops largely during this time. Furthermore tensile strength gain and shrinkage gain are marginal. Therefore the influence of strain loss can be neglected. Loss in strain corresponds to a slight over-estimation of imposed strain and a slight over-estimation of relaxation.

5.6 Tensile relaxation results

5.6.1 General

In this section, stress relaxation results for specimens tested at specific ages are presented. All specimens were sealed. Specimens were sealed using paraffin wax. As mentioned in Chapter 4, sealed specimens represent bonded concrete overlays subjected to partial restraint. Sealing of specimens allows for restraint without additional strain due to drying (shrinkage). Hence, restraint was kept constant throughout the duration of the test. Results were recorded and analysed as discussed in the following sub-section.

5.6.2 General principle of relaxation analysis

Relaxation is the decrease in stress due to imposed strain. In this study, restraint was imposed by applying an initial stress and maintaining constant strain thereafter. Subsequently, the resultant stress decay was monitored. Imposed initial stress is denoted as σ_0. Resultant stress at a specific time is denoted as σ_t. Degree of relaxation was taken as the ratio between resultant stress (σ_t) and imposed stress (σ_0) at specific times. Fig. 5.13 shows a typical relaxation curve.

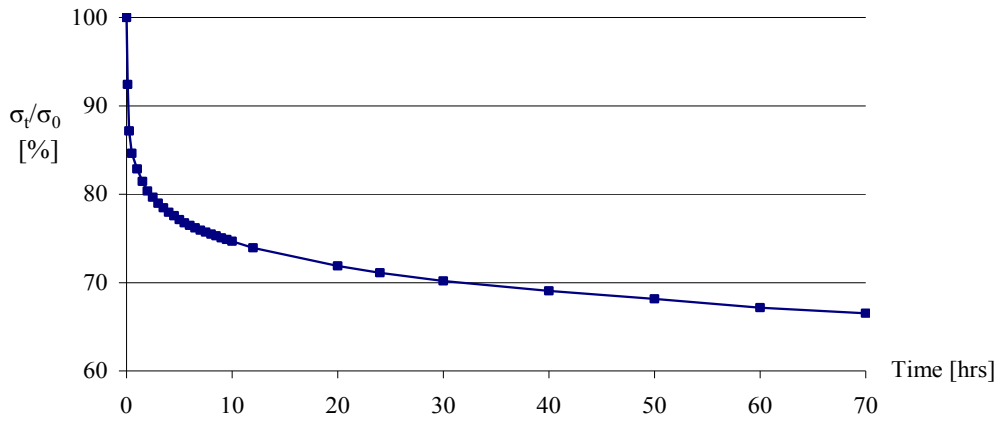

Fig. 5.13: Typical relaxation curve (72 hour test)

Generally tests were carried out for at least 72 hours. Hence relaxation after 72 hours was taken as the datum for comparing all results. For example in relative relaxation-time development tests the 72 hour relaxation is taken as 100%. Curve profiles are

analysed by calculating slope and ultimate relaxation values. Ultimate relaxation values are plotted graphically. Furthermore, relaxation curve profiles can be modelled analytically and empirically. Relaxation modelling is examined in Chapter 6.

5.6.3 Statistical evaluation of results

At least 4 specimens were tested for tensile relaxation per mix and per test age. Hence statistical evaluation of data was essential. Statistical analysis of results was done using Grubb's outlier test (Grubbs, 1979). This method was used to exclude outliers and give an indication of consistency in the measured data. Grubb's test is discussed in the following example.

Specimens of 0.45 w/c ratio were tested at 2 days. The typical scatter of the four relaxation curves is shown in Fig. 5.14.

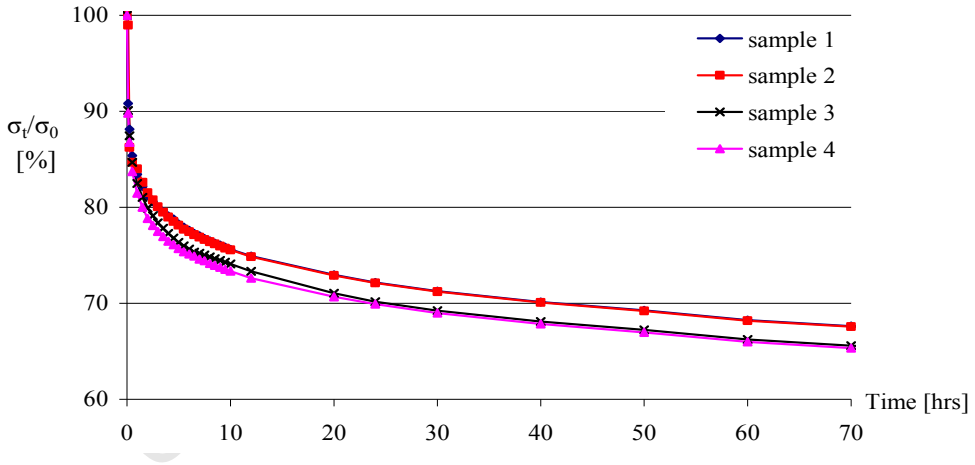

Fig. 5.14: Typical scatter for stress relaxation of 0.45 w/c samples at age of 2 days.

Results in Fig. 5.14 show a slight variation in stress relaxation margin. A small scatter was observed. Curves for sample 1 and sample 2 are superimposed whilst the curve for sample 3 and sample 4 also follow a similar profile. A comparatively constant variation of about 2% was observed. This variation was observed between sample 1 and 2 and sample 3 and 4 (between 10 hours and 72 hours).

5.6.3.1 Grubbs method

It is impossible to identify outliers from observing raw data such as that shown in Fig. 5.14. In such a case Grubbs method is applicable. This method is used to determine single-sided outliers when both population mean (μ) and population standard deviation (s) are unknown. It was developed by Grubbs (Grubbs, 1979) and is included in standard methods. The first step is to determine test values using equation [5.2] and [5.3].

$$T_u = \frac{X_n - \bar{x}}{\sigma} \quad \text{(for high-sided outliers)} \qquad [5.2]$$

$$T_l = \frac{\bar{x} - X_l}{\sigma} \quad \text{(for low-sided outliers)} \qquad [5.3]$$

Where: T_u, T_l = Upper and lower determinant.

X_n, X_l = data point on curve (suspected outlier).

$\bar{x}$ = sample mean.

Depending on the number of replicates and significance (or confidence) level, T_u or T_l are then compared against critical values. If T_u or T_l is greater than the critical value for the appropriate number of replicates at the appropriate significance level, the questionable data point is an outlier. Therefore it may be rejected. Critical values for various numbers of replicates at 1% and 5% significance levels are given in Table 5.1.

Table 5.1: Critical values for Grubb's outlier test
Source: Barnett, Lewis and Rothamsted (1994)

No. of observations	*Significance level*	
	1%	*5%*
3	1.15	1.15
4	1.49	1.46
5	1.75	1.67
6	1.94	1.82
7	2.10	1.94
8	2.22	2.03
9	2.32	2.11

The 5% significance level was selected. Using Table 5.1, no outliers were found and the data satisfied all critical values. The scatter is presented in Fig. 5.15.

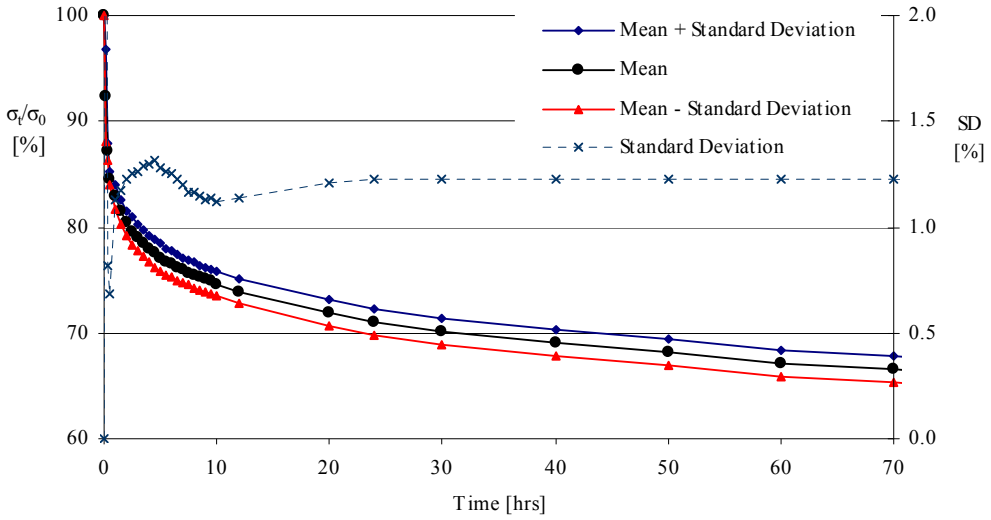

Fig. 5.15: Statistical characteristics of stress relaxation (2 days 0.45 w/c ratio)

The uppermost curve denotes the highest values (upper limit) obtained from experiments whilst the lower curve denotes lower limit. The area bounded by both curves is the data space of results obtained. The middle curve is the mean curve. From Fig. 5.14, variability is expressed more clearly than in Fig. 5.15.

A greater scatter was observed in 0.60 w/c ratio specimens tested at 2 days. Even so, no outliers were found. Statistical evaluation of results for 2 day 0.60 w/c ratio and repair mortar specimens are detailed in Appendix A.

5.6.4 Specific results of relaxation

Specific stress relaxation results include comparison of results for the same mix, i.e. repair mortar, 0.45 or 0.60 w/c ratio specimens. These are compared at different testing ages i.e. at 2 days and 7 days. The other set of results are for all specimens tested at the same age i.e. either at the age of 2 days or 7 days. Results are presented as relaxation curves profiles within a period of 72 hours. To account for time periods less than or greater than 72 hours, a detailed analysis of time development is also presented. Through this process, it was easy to identify the influence of main

parameters being investigated in this study. These are specimen w/c ratio and maturity.

It was discovered that the age of loading had a major influence on relaxation. This is because relaxation is dependent on material properties, for instance, the degree of hydration. Furthermore, material properties under investigation are time-dependant. The main findings and discussions are detailed in the sections that follow.

5.6.4.1 Influence of w/c ratio

The influence of w/c ratio was investigated by comparing relaxation patterns obtained from all mixes i.e. repair mortar, 0.45 and 0.60 w/c ratio specimens. These were considered at the same age. In order to verify the test results, Grubbs outlier test was used. Mean values are plotted as shown in Fig. 5.16.

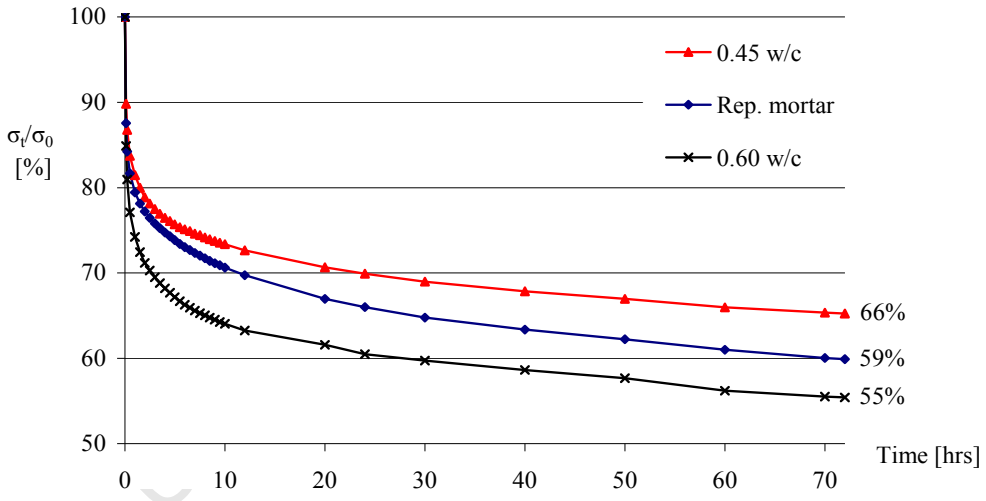

Fig. 5.16: Stress relaxation of repair mortar, 0.60 & 0.45 w/c samples at age 2 days.

0.60 w/c ratio specimens showed higher relaxation than 0.45 and repair mortar. After 72 hours 45% stress relaxation was observed in 0.60 w/c ratio specimens compared to 34% in 0.45. Relaxation in repair mortar was 41%. Between 12 and 72 hours the slope of 0.60 w/c ratio specimen was 14% per hour whilst that of the 0.45 was 12% per hour. The slope of repair mortar curve was 17% per hour. Higher slope indicates a higher relaxation potential whilst a lower slope indicates a diminishing relaxation. The margin of relaxation after 72 hours is shown clearly at the end of each curve in Fig. 5.16.

Fig. 5.17 shows results of relaxation at the age of 7 days.

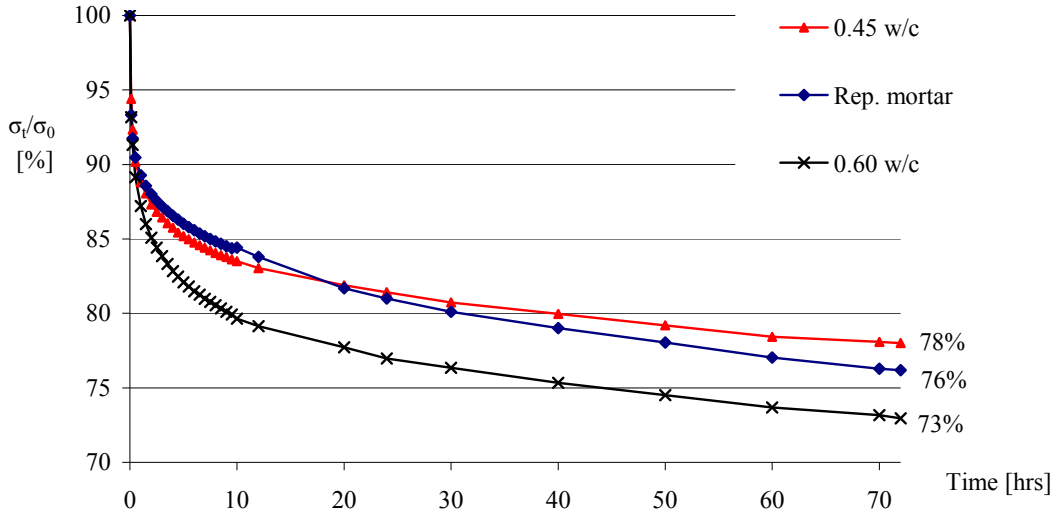

Fig. 5.17: Stress relaxation of repair mortar, 0.60 & 0.45 w/c samples at age 7 days.

In Fig. 5.17, the 0.60 w/c ratio showed more stress relaxation than repair mortar and 0.45 specimens at 7 days. This trend is similar to that observed in Fig. 5.16. However compared to the 0.45 and 0.60 w/c ratio curves which are similar, the repair mortar exhibits a different curve profile (Fig. 5.17). In this instance the repair mortar seems to have relatively less initial relaxation and higher sustained relaxation at later ages.

The slopes of repair mortar curve between 12 and 72 hours were 13% per hour. The slope of 0.45 and 0.60 w/c ratio specimens was 9% and 10% per hour respectively. 0.60 w/c mix specimens had approximately 27% stress relaxation at the end of 72 hours compared to 22% from 0.45. 24% relaxation was observed in the repair mortar after 72 hours.

In general, relaxation may reduce tensile overlay stress by approximately 33-45% (2 days) and 23-26% (7 days) in mixes tested. Beushausen (2005) reported 40-50% stress relaxation in actual bonded concrete overlays. Pigeon *et al* (2000) found relaxation in fully restrained specimens in the order of 67%. Morimoto & Koyanagi (1994) observed 20% relaxation after 96 hours. These findings show wide ranging differences in relaxation. Therefore it is noteworthy that a general comparison of relaxation values obtained using different concrete mixes and test equipments is problematic.

A summary of relaxation margins obtained above may be presented as shown in Fig. 5.18.

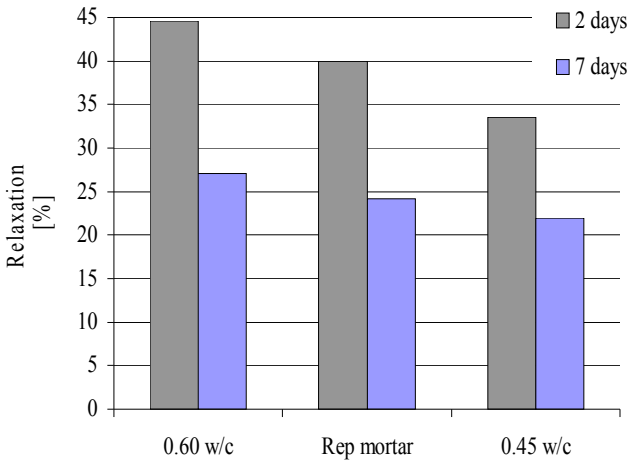

Fig. 5.18: 72 hour relaxation of repair mortar, 0.60 & 0.45 w/c samples (age 2 &7 days).

Considering normal concrete mixes, results above show a general dependency of relaxation on w/c (w/b) ratio or mix composition. Östergaard *et al* (2001) found that basic tensile creep of concrete with w/c ratios between 0.32 and 0.50 decreased with decreasing w/c ratio. Similar results for concrete with w/c ratios of 0.32 and 0.40 have also been reported by Bissonnette & Pigeon (1995). However, Carlswärd (2006) cited somewhat contradicting results. These were regarding influence of w/c ratio and also type and the content of cement. In his study, results did not indicate any particular difference in response when w/c ratio was varied from 0.4 to 0.6.

0.60 w/c ratio specimens generally showed 10% higher relaxation than 0.45 w/c ratio specimens after 72 hours. This may be attributed to the porous nature of 0.60 w/c ratio specimens. This facilitates water movement through pore spaces (Rusch *et al*, 1983). Subsequently redistribution of stresses occurs. As a result greater relaxation is achieved. Another factor may be the additional free movement of gel layers in higher (0.60) w/c ratio compared to lower (0.45 and repair mortar (w/b)) w/c ratio specimens (Wittmann, 1981).

The relationship between tensile strength, shrinkage and relaxation in all mixes is shown in Fig. 5.19. In Fig. 5.19, the highest value in each parameter is denoted as 100%.

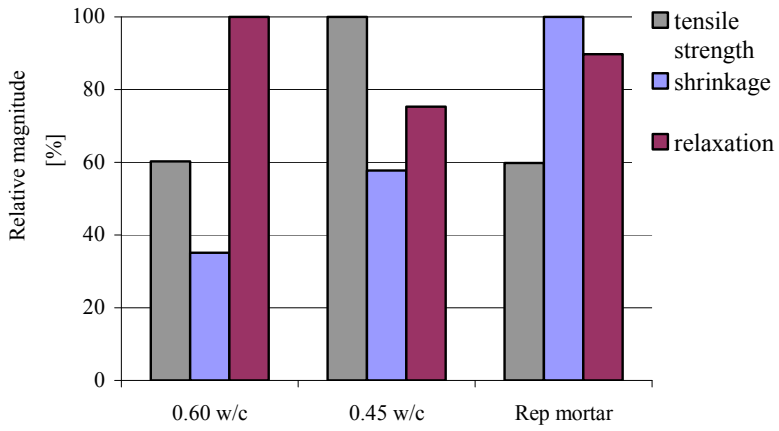

Fig. 5.19: Comparison of main factors between the 3 mixes.

Regardless of age, the respective specimens exhibited characteristics corresponding to that shown in Fig. 5.19. Although the tensile strength of 0.60 w/c ratio specimens is lower than that of 0.45 w/c ratio, 0.60 w/c ratio specimens had lower shrinkage and the higher relaxation. Therefore the combined influence of these properties in bonded concrete overlays more valuable as it leads to less stress and subsequently less possibility of cracking. Repair mortar specimens had the highest shrinkage hence high shrinkage induced stresses and the least tensile strength. However relaxation in repair mortar is lower than in 0.60 w/c ratio specimens. In bonded concrete overlays with this repair mortar, there is a greater possibility of cracking as tensile stresses may reach the magnitude of tensile strength.

It is difficult to draw conclusions on relaxation of repair mortar specimens. Information regarding constituents of the commercial repair mortar was not provided. It is noteworthy that Fig. 5.19 serves as a performance indicator for common repair and self-made overlay mortar mixes. From observations made above, fundamental characteristics affecting relaxation development in commercial repair mortar mix could not be identified.

Considering normal concrete mixes only, shrinkage and relaxation may be assumed to be influenced by porosity and permeability. These factors are related to the mix composition (cement content, cement paste and w/c ratio). The w/c ratio controls the tensile strength, elastic modulus and permeability of the cement paste (Alexander, 2001). Since stronger pastes are also stiffer, it is found that a decrease in the w/c ratio causes a decrease in tensile relaxation. Beushausen and Alexander (2006) showed that elastic modulus influences resistance to shrinkage. The resistance to shrinkage increases overlay stresses which in turn depend on relaxation.

5.6.4.2 Influence of age at loading

The influence of the age at loading was investigated by comparing relaxation results obtained from repair mortar, 0.45 and 0.60 w/c ratio specimens. For each mix, results were compared at different ages. Fig. 5.20 shows relaxation results of 0.45 w/c ratio specimens.

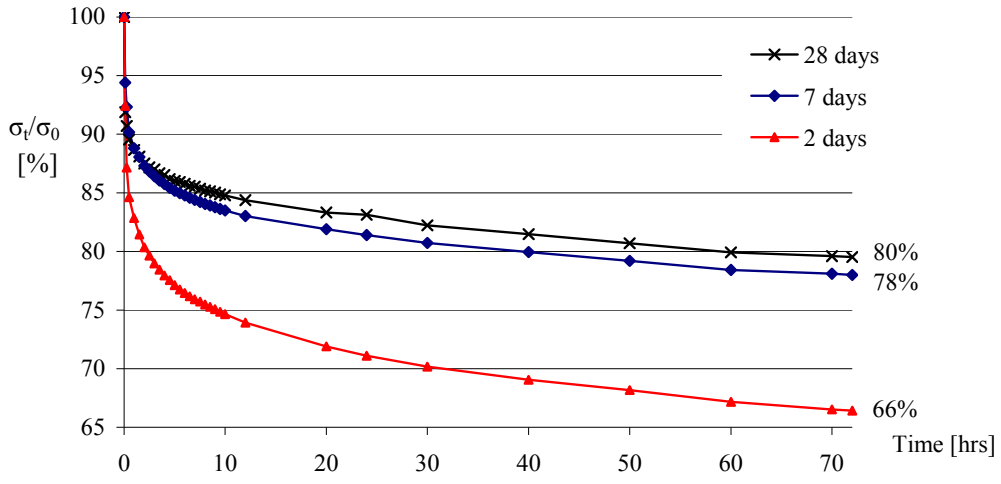

Fig. 5.20: Stress relaxation of 0.45 w/c samples at ages of 2, 7 & 28 days.

Fig. 5.20 shows stress relaxation curves for 0.45 w/c ratio specimens. Specimens were tested at 2, 7 and 28 days. After 72 hours, higher relaxation was observed in 2 day specimens compared to 7 and 28 day specimens. 34% relaxation was observed on specimens tested at 2 days compared to 22% and 20% at 7 and 28 days respectively.

The difference between 7 day and 28 day relaxation was low compared to the relaxation margin between 2 days and 7 days. The 72 hour magnitude of relaxation at different ages is shown at the edge of the curves (Fig. 5.20).

Relaxation of 0.60 w/c ratio specimens tested at 2, 7 and 28 days is shown in Fig. 5.21.

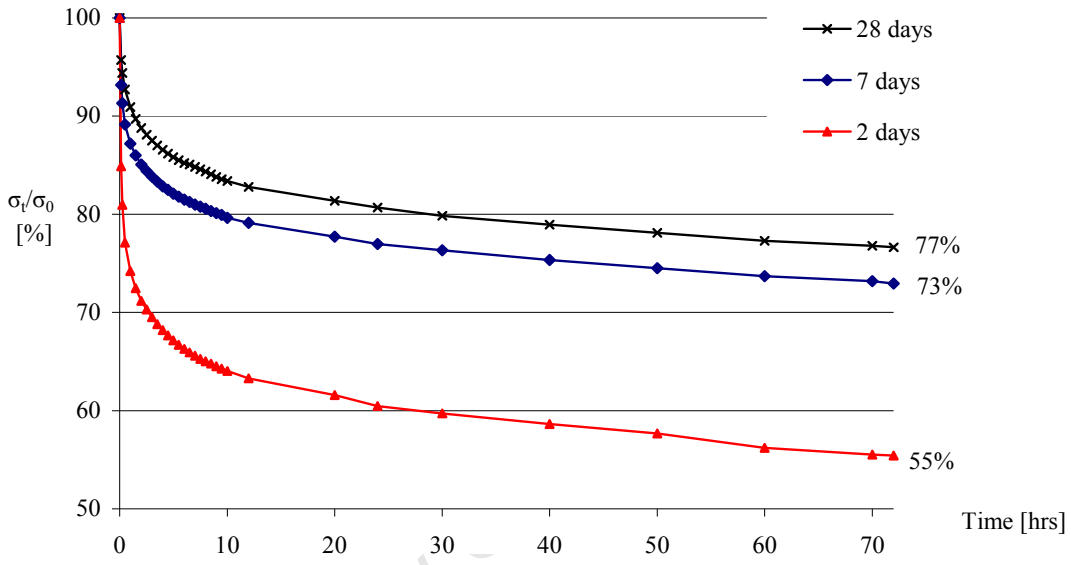

Fig. 5.21: Stress relaxation of 0.60 w/c samples at ages of 2, 7 & 28 days.

The magnitude of relaxation after 72 hours was 45%, 27% and 23% for 2 day, 7 day and 28 day specimens respectively. Between 12 and 72 hours, slope was 13%, 11% and 10% tested at 2 days, 7 days and 28 days respectively. Magnitude of relaxation for 0.60 w/c ratio specimens are shown clearly in Fig. 5.21.

Similar to 0.45 w/c ratio specimens, 0.60 showed higher relaxation at the age of 2 days. This agrees with observations from studies carried out by Gutsch & Rostásy (1994), Morimoto & Koyanagi (1994), Bissonnette & Pigeon (1995), Kordina *et al* (2000), and Beushausen & Alexander (2006). These studies all agree that there is greater relaxation during early ages than later ages. In this case early age refers to 2 days. Influence of age on repair mortar specimens is presented in Fig. 5.22.

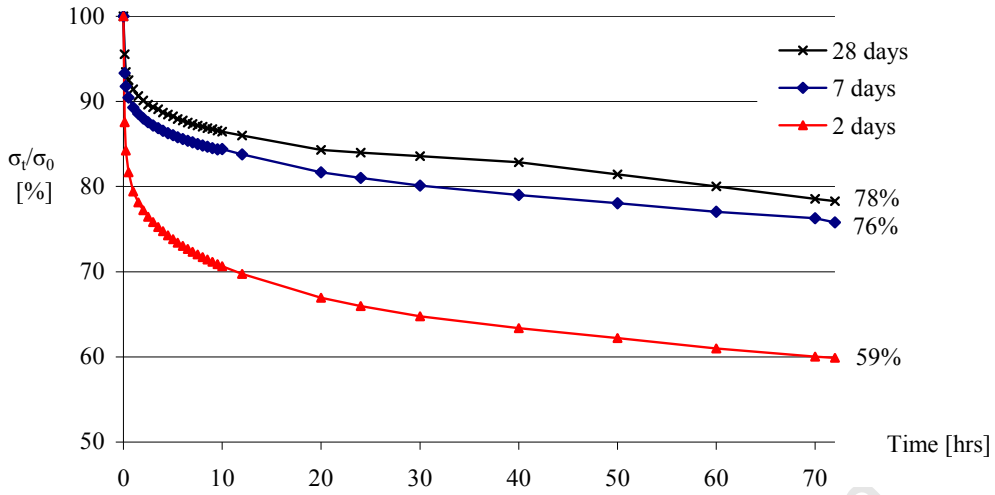

Fig. 5.22: Stress relaxation of repair mortar specimens at ages 2, 7 & 28 days.

Relaxation magnitude after 72 hours for repair mortar specimens is shown in Fig. 5.22. 41%, 24% and 22% relaxation was observed at 2, 7 and 28 days respectively.

The effect of age in all specimens was similar. Relaxation reduces with increasing age. This is because relaxation is dependant on the degree of hydration (Neville, 1981). Hydration is initially rapid but reduces gradually with time. In addition, the difference in relaxation is low at later ages (i.e. 7 days and 28 days) compared to earlier on (2 days and 7 days). At later ages concrete would be more mature and therefore less capable of undergoing significant relaxation (Rusch *et al*, 1983). Effect of age is summarised in Fig. 5.23.

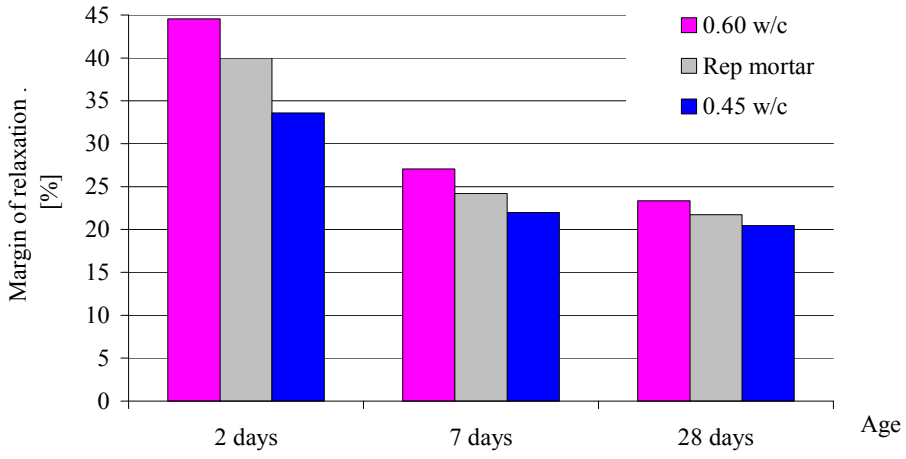

Fig. 5.23: Summary of effect of age in all mixes

The strong age dependency for early loading ages (in this case, 2 days) has been verified by several authors e.g. Carlswärd (2006). However most of these studies were in relation to concrete loaded in compression. Östergaard *et al* (2001) showed that a similar relation may be expected for a tensile creep/relaxation response. For instance, a rational difference in specific creep strain and rate was obtained when comparing the loading ages 0.67 days and 1 day (Carlswärd, 2006). This seems to agree with results obtained in this study as higher relaxation was achieved when the concrete was loaded at 2 days compared to loading at 7 days and 28 days.

In general, specimens tested at 2 days had higher rate of relaxation than specimens tested at 7 days and 28 days. A more detailed overview of development of relaxation with respect to time is discussed in the following section.

5.6.4.3 Time development of tensile relaxation

In this section, progression of relaxation at various stages in time is discussed and analysed. Unlike in previous sections, analysis is not only based on the 72 hour relaxation. Furthermore, time development analysis is divided into short-term and long-term phase. Short-term in this context refers to the time interval within the first 12 hours. Long term is any other period beyond 72 hours.

Mean relative relaxation curves were compared for all mix specimens. Comparisons were done mainly at ages of 2 days, 7 days and 28 days. This is due to differences in results obtained between 2 days, 7 days and 28 days.

A general relationship for relaxation development in all mix specimens is shown in Fig. 5.29. In this case relaxation values at 72 hours were used as a reference for evaluation. This is because all tests were carried out for 72 hours. Therefore 72 hour relaxation was taken as 100%.

Relative relaxation rates at ages of 2 days, 7 days and 28 days are shown in Fig. 5.24.

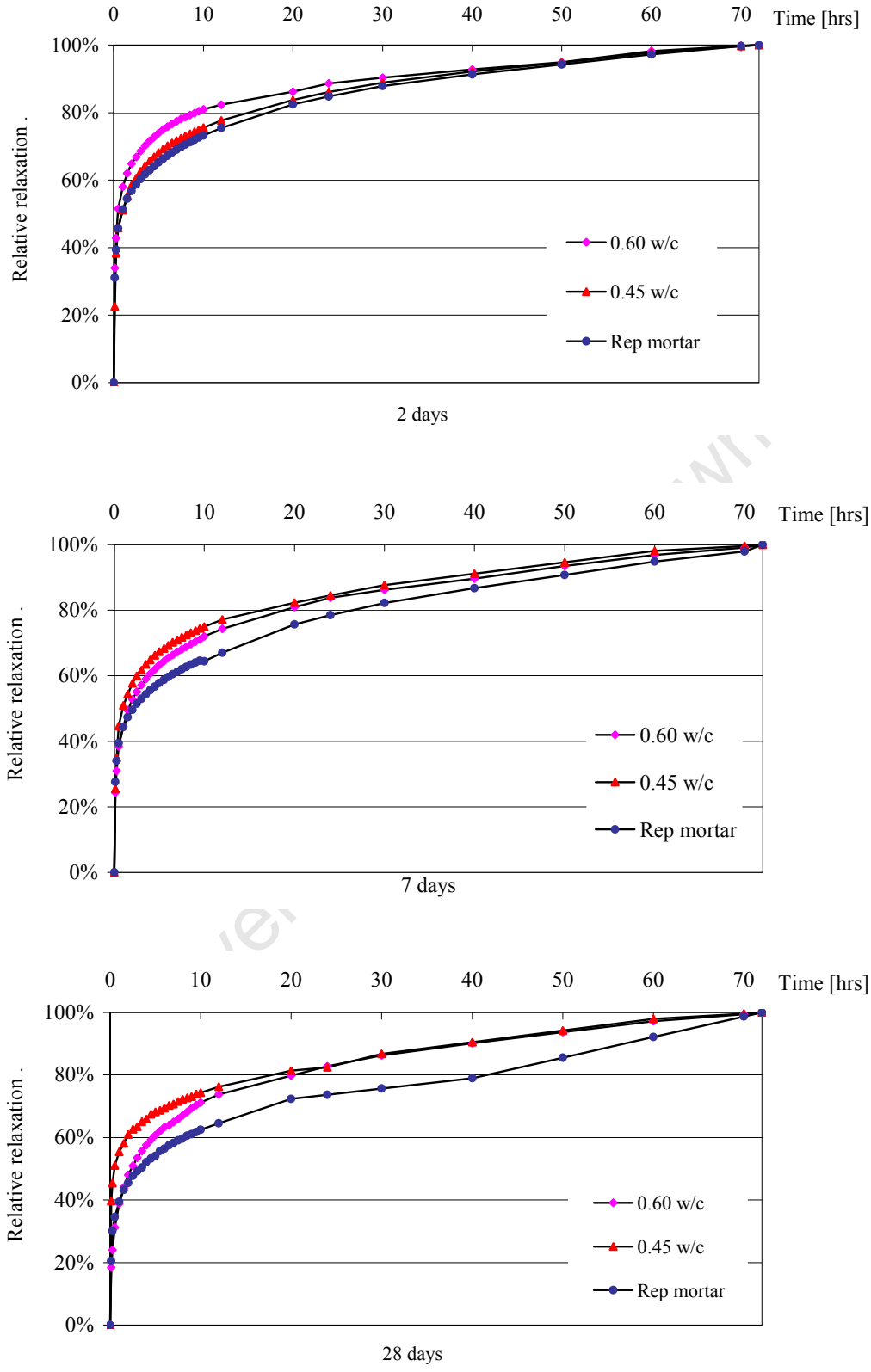

Fig. 5.24: Relative development of relaxation up to 72 hours (a) 2 days (b) 7 days (c) 28 days

Irrespective of the mix, relaxation curves in Fig. 5.24 (a) and Fig. 5.24 (b) are similar. However, some differences were identified. For example in Fig 5.24 (a), 0.60 w/c ratio specimens tested at 2 days underwent relaxation more rapidly than other specimens. Development of relaxation in both 0.45 w/c ratio and repair mortar specimens tested at 2 days followed a similar profile. However 0.45 w/c ratio specimens tested at 2 days showed slightly rapid relaxation compared to the repair mortar. 2 day repair mortar specimens showed a slightly less relaxation build-up.

At 7 days and 28 days, 0.45 w/c ratio specimens showed a higher relaxation build up compared to that observed at 2 days. The profiles of 0.45 and 0.60 w/c ratio curves are similar (Fig. 5.24b). In Fig. 5.24 (c), 0.45 w/c ratio tested at 28 days showed the highest relaxation rate. Repair mortar specimens had the lowest rate of relaxation. The profile for 0.60 w/c ratio was very different from the other two profiles. 0.60 w/c ratio specimens had a low initial relaxation rate (0-10hrs) and higher relaxation rate at later ages. The curve profiles of 0.45 and 0.60 w/c ratio specimens were superimposed from 24 hours to 72 hours (Fig. 5.24c).

5.6.4.3.1 Short-term relaxation rate

To illustrate overall relaxation development at early ages, 12 hour relaxation curves are shown (Fig. 5.25).

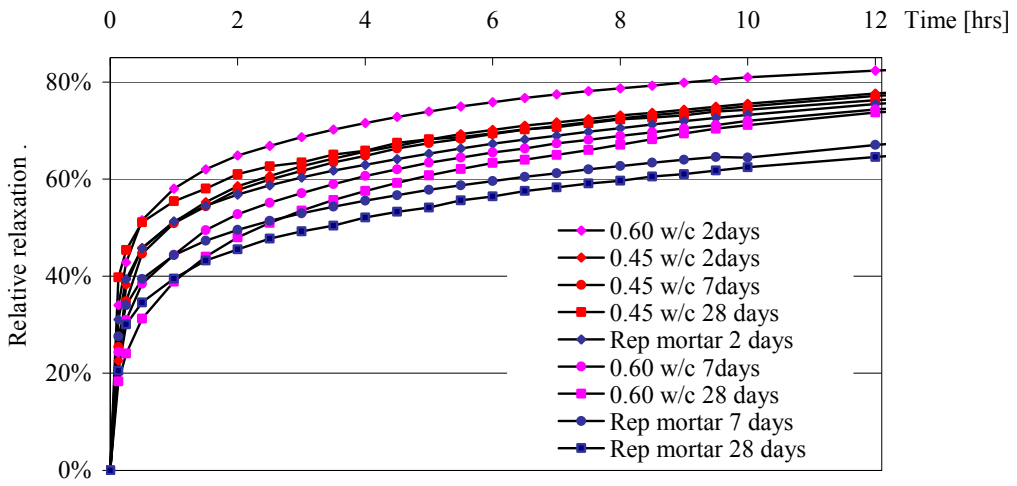

Fig. 5.25: Relative development of relaxation up to 12 hours

It should be noted that the legend in Fig. 5.25 is representative of the order in which the curves appear. Considering the first 12 hours, 82% relative relaxation was observed from 0.60 w/c ratio specimens tested at 2 days. 0.45 w/c ratio specimens tested at 2, 7 and 28 days showed 78%, 77% and 76% relative relaxation respectively. The relative relaxation in 0.45 w/c ratio specimens was very close. Repair mortar specimens tested at 2days showed 75% relative relaxation. 0.60 w/c ratio specimens tested at 7 days and 28 days both indicated 74% relative relaxation (after 12 hours). Finally repair mortar specimens tested at 7 days and 28 days showed 67% and 65% relative relaxation respectively. These figures are presented in Fig. 5.26.

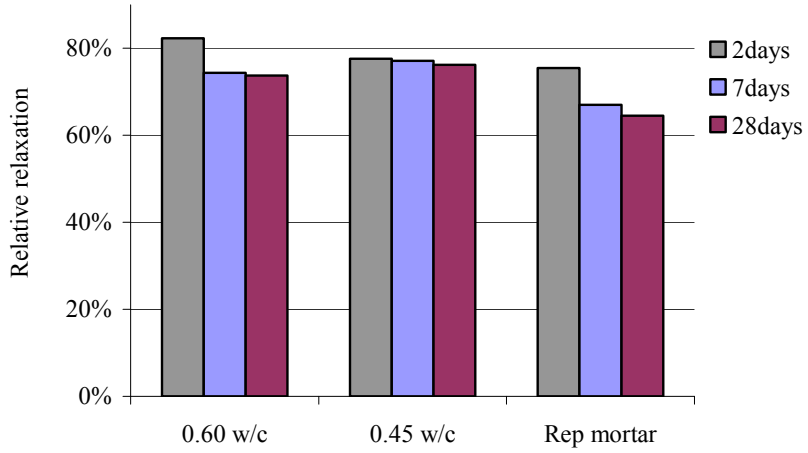

Fig. 5.26: Relative development of relaxation up to 12 hours

For each mix, relaxation was found to develop more rapidly in specimens tested at an earlier age. The overall relative relaxation rate for repair mortar specimens was the lowest. Considering normal concrete mixes tested at 2 days, the relaxation rate becomes less rapid with reducing w/c ratio. However at later ages the effect is the relaxation rate becomes less rapid with increasing w/c ratio. In general, Fig. 5.26 reveals a two-fold effect i.e. age and binder type.

For an in-depth rate of relaxation analysis, cumulative relative relaxation was for 2 days and 7 days was analysed at specific times. 2 hours, 12 hours, 24 hours, 48 hours and 72 hours were selected for analysis. These time intervals were chosen based on the change in slope of relaxation curves. Cumulative relaxation rates at specified times are shown in Fig. 5.27.

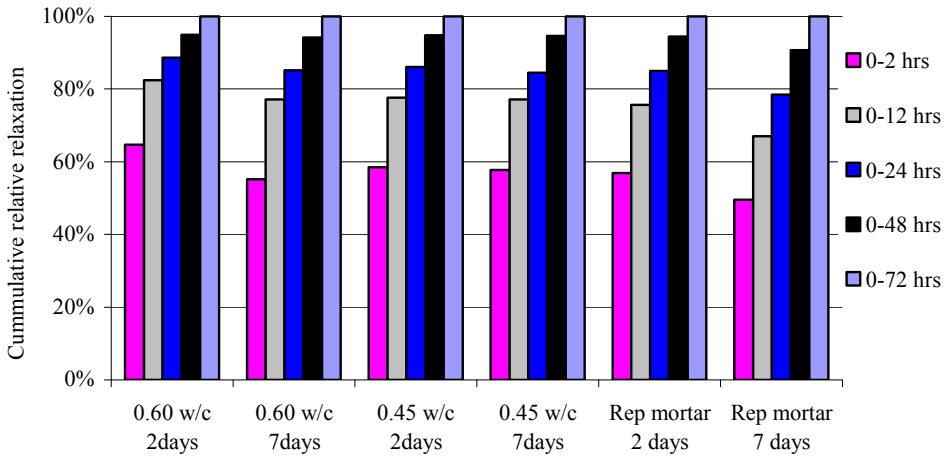

Fig. 5.27: Accumulated relative relaxation for all mixes at specific intervals

In order to find relative rate of development of relaxation, the magnitude of relaxation at 48-72 hours was used as a reference. Relaxation margins at other intervals were then compared to the reference (Fig. 5.28). This was done so as to calculate the contribution of each interval to the overall relaxation.

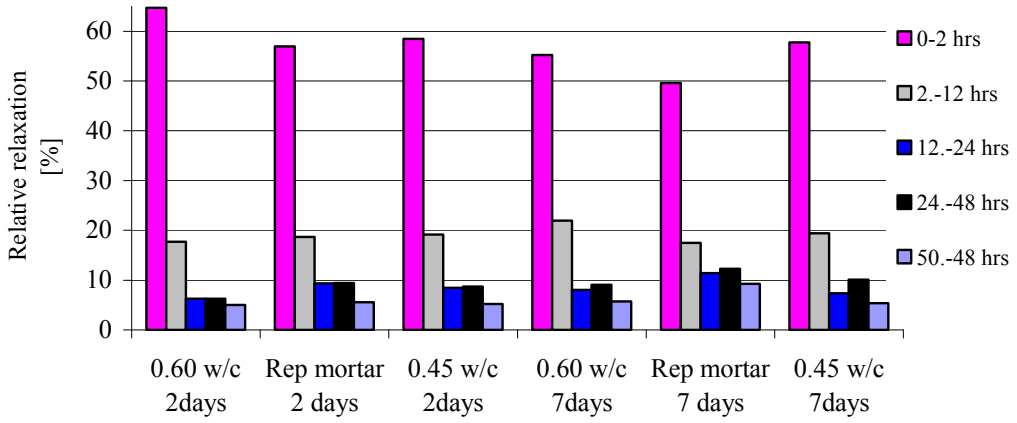

Fig. 5.28: Relative relaxation for all mixes during specific intervals

Fig. 5.28 shows a high ratio in relaxation within the initial 2 hours compared to other intervals. Within the first 2 hours a mean of 57% of 72 hour relaxation was observed. This led to the conclusion that a large amount of tensile stress relaxation takes place at early ages of loading. More studies such as Morimoto and Koyanagi (1994), Gutsch & Rostásy (1994), Kordina *et al* (2000) and Beushausen (2005) confirmed that tensile stress relaxation develops rapidly after loading. In particular, Morimoto and Koyanagi (1994) reported that it took only 2-3 hours to reach ultimate values of tensile

relaxation. This confirms that a significant amount of relaxation occurs during early hours.

The ratio of the initial 2 hour to 72 hour shrinkage and tensile strength was found to be roughly 3% and 4% respectively. The 2 hour rate of relaxation was found to be roughly 57% of 72 hour relaxation. Therefore in comparison to shrinkage and strength gain, the rate of relaxation was found to be significantly higher during early hours of loading i.e. between 0-2 hours. Therefore, in agreement with findings reported by Beushausen (2005), it may be assumed that tensile stress relaxation occurs instantaneously after loading. This is illustrated schematically in Fig. 5.29.

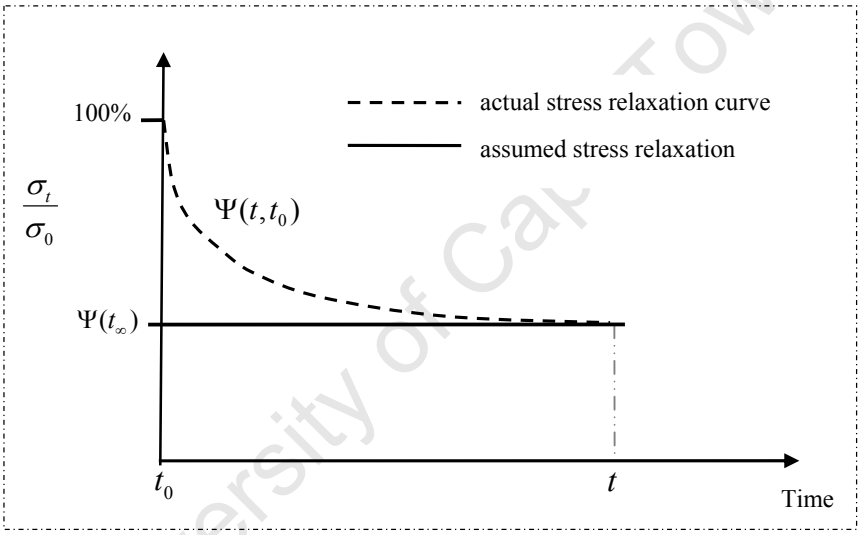

Fig. 5.29: Schematic of simplified approach for the consideration of overlay stress relaxation *(Beushausen, 2005)*

The relaxation function $\Psi(t, t_0)$ represents the curve profile. $\Psi(t, t_0)$ for tensile creep was introduced by Gutsch and Rostásy (1994) and Morimoto and Koyanagi (1994) (refer to Section 2.4.3). In general, information on stress relaxation functions in literature is scarce. Therefore results acquired in this study may prove valuable in estimating $\Psi(t, t_0)$.

Long-term time development is discussed in the following section.

5.6.4.3.2 Long term time development

Due to time constraints, few long-term relaxation tests were carried out compared to 72 hour relaxation tests. At least 3 specimens were tested per curve. The main purpose of long term tests was to determine relaxation curve profiles for periods beyond 72 hours. Long-term relaxation results may be used to confirm important observations from experimental research through modelling.

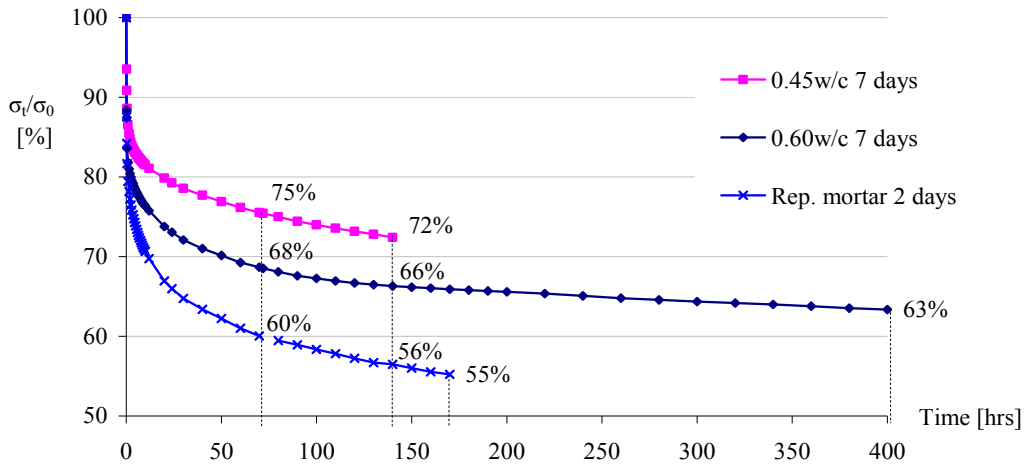

Fig. 5.30: Long-term relaxation curves for respective mix specimens

Fig. 5.30 shows 3 curve profiles of specimens tested for periods exceeding 72 hours. 7 day 0.45, 7 day 0.60 w/c ratio and 2 day repair mortar specimens were tested for 140, 170 and 400 hours respectively. Relaxation values at 72 hours, 140 hours, 170 hours and 400 hours are indicated in Fig. 5.30. It is interesting to note that all specimens showed continuing relaxation beyond 72 hours.

Since a few specimens were tested for long periods, it was necessary to model relaxation at later ages. In determining the amount of relaxation at later ages, empirical models were used. Empirical models can be used to capture a set of data and predict long-term relaxation (Atashi *et al*, 2007). The empirical model used was based on an algebraic equation represented by equation [5.4]. Equation [5.4] is an algebraic equation.

$$\Psi(t)=100-At^{(C)} \qquad [5.4]$$

Where: $\Psi(t)$ = relaxation function (%)

A, C = empirical constants

t = time (hrs)

Equation [5.4] is based on algebraic curves obtained in literature (Von Seggern, 1993). The constants termed 'A' and 'C' are determined from a trial and error method. In Fig. 5.31 'A' and 'C' correspond to 18.5 and 0.12 respectively.

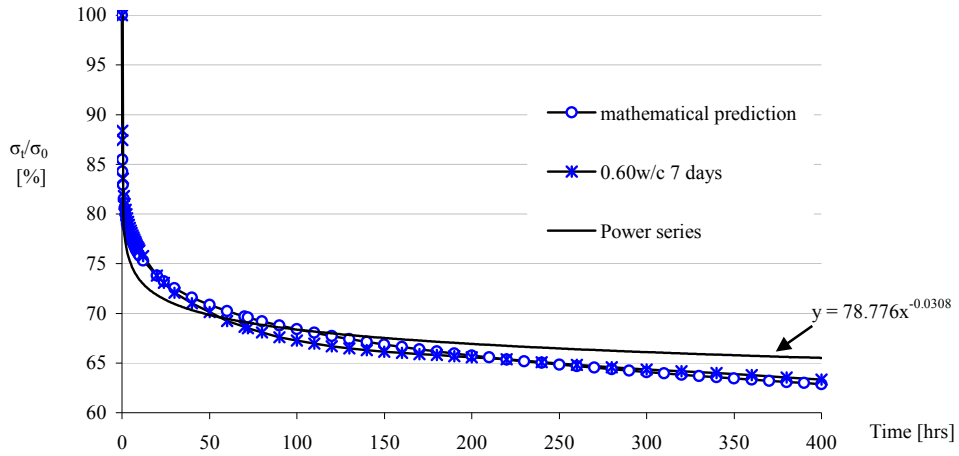

Fig. 5.31: Mean relaxation curves for respective mix specimens.

The stress does not necessarily tend to zero as time tends to infinity (Fig. 5.31). Although 0.60 w/c ratio curve seems slightly flat, minor relaxation can be observed. The power function does not show a good correlation with the data especially at later ages where it becomes flatter. The relaxation rate becomes less significant at later ages. This clearly shows that relaxation does not cease completely.

Modelling of relaxation curves is detailed in Chapter 6.

5.7 Summary and discussion

The importance of tensile stress relaxation in bonded overlays has long been recognised. However available information regarding relevant experimental campaigns is insufficient in literature. Furthermore actual relaxation values in bonded concrete overlay systems are rare. Therefore, results obtained in this study serve as an

important indication of relaxation characteristics in bonded concrete overlays. Included in this summary are relaxation characteristics of common overlay materials, including concrete repair mortars. In addition the rate of development of relaxation is discussed.

Magnitude of relaxation

The overall magnitude of relaxation is based on the total relaxation after 72 hrs (see Fig. 5.23). Relaxation values observed in this study are listed in order of magnitudes in Table 5.2.

Table 5.2: Magnitudes of relaxation for all specimens

Specimen	*Relaxation margin [%]*
0.60 w/c 2 days	45
Rep. mortar 2 days	41
0.45 w/c 2 days	34
0.60 w/c 7 days	27
Rep. mortar 7 days	24
0.60 w/c 28 days	23
0.45 w/c 7 days	22
Rep. mortar 28 days	22
0.45 w/c 28 days	20

As shown in Table 5.2, relaxation was found to be in the order of 20-45%. Beushausen and Alexander (2006) found relaxation in bonded concrete overlays in the range of 40-50%. This is in the order of magnitude as that reported in literature (Gutsch & Rostásy, 1994; Morimoto & Koyanagi, 1994 and Kordina *et al*, 2000). Pigeon *et al* (2000) measured relaxation in fully restrained specimens in the order of 67%. The relaxation margins reported in literature are slightly different. This may be due to the use different concrete mixes and test equipments.

Influence of w/c ratio

Regardless of age, the 0.60 w/c ratio specimens had the highest relaxation than repair mortar and 0.45 w/c ratio specimens. It was difficult to draw conclusions on relaxation of repair mortar specimens as information regarding constituents (w/b ratio) of the commercial repair mortar was not provided. Therefore, considering normal concrete mixes, relaxation may be influenced by the difference in pore

structure and paste characteristics of the mixes. For example 0.45 w/c ratio specimens have a denser pore structure than 0.60 which may result in higher strength. Since stronger pastes are also stiffer, it has been found that a decrease in the w/c ratio may cause a decrease in tensile relaxation (Alexander, 2001).

Influence of age at loading

Irrespective of w/c ratio, the age had a high influence on the magnitude of tensile relaxation. For example after 72 hours, specimens tested at 2 days had roughly 15% higher relaxation compared to specimens tested at 7 days. Similar observations were reported in other studies (Östergaard *et al*, 2001; Carlswärd, 2006). Fig. 5.32 shows the effect that the maturity has on both the tensile strength and relaxation of 0.45 w/c ratio.

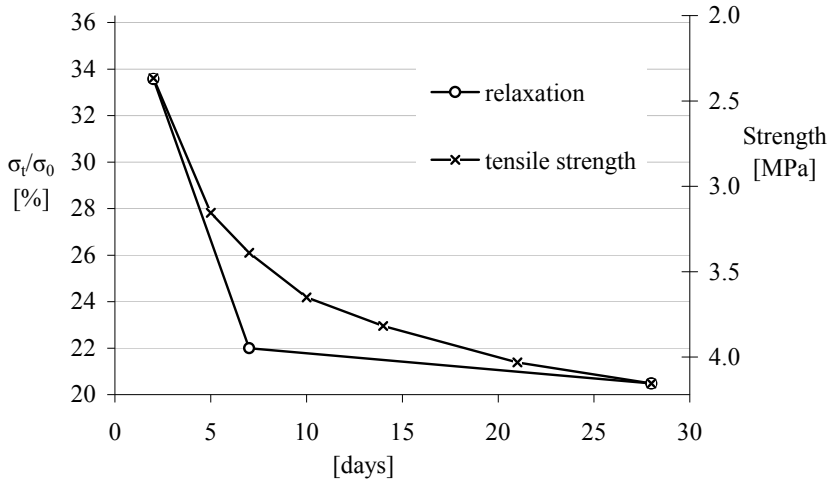

Fig. 5.32: Effect of maturity on tensile strength and relaxation

The typical relationship between maturity and tensile strength was identified through the time-strength graph (Fig. 5.3). The effect of maturity on relaxation was also investigated and the trend was roughly similar. As seen on Fig. 5.32, both curve profiles assume a similar profile. The curves in Fig. 5.32 are taken from tensile strength and relaxation data in 0.45 w/c ratio specimens.

Tests carried out at 28 days revealed minor differences in relaxation margin from 7 days onwards. Furthermore for any given mix, the rate of development of relaxation

was dependant on the age of loading. Relaxation was found to progress more rapidly in specimens tested at 2 days compared to those tested at 7 days.

Time development of relaxation

In general specimens tested at 2 days showed a more rapid time development of relaxation. 50% relaxation was achieved within 45 minutes in 2 day specimens. On the other hand, 7 day specimens achieved 50% relaxation after 80 minutes. The order of relaxation rates per mix is presented in Fig. 5.24. In all mixes, a mean of 57% of 72 hour relaxation was achieved within the first 2 hours of loading. In comparison to shrinkage and strength gain, the rate of relaxation was found to be significantly higher at early hours. Morimoto and Koyanagi (1994) found ultimate relaxation values to occur within 2-3 hours. Therefore compared to the rate of development of tensile strength and shrinkage, relaxation in bonded concrete overlays may be assumed to be instantaneous.

Long-term relaxation development showed that relaxation proceeds beyond 72 hours. However the rate of relaxation becomes lower with time. Therefore overlay relaxation achieved at later ages may be insignificant. Empirical modelling of relaxation based on relaxation curve profiles is discussed in detail in Chapter 6. The algebraic equation used is shown below.

$$\Psi(t)=100-At^{(C)} \qquad [5.4]$$

Where: $\Psi(t)$ = relaxation function (%)

A, C = empirical constants

t = time (hrs)

CHAPTER SIX: MODELLING OF RESULTS

6.1 Introduction

In the modelling of relaxation of bonded overlays, empirical and analytical models were applied. Analytical models were focussed on predicting the onset of cracking per mix proportion and age. Fundamental principles were identified through carrying out a parametric study. Owing to the complex nature of relaxation, a simplified approach was adopted. In order to apply the above-mentioned approach to bonded concrete overlays, reasonable assumptions and references to existing literature are made. The main assumptions made are:

- No shrinkage occurs during curing period.
- Tensile relaxation is instantaneous from the onset of loading.
- Restraint is equivalent to 60% of free shrinkage strain.

Based on aspects listed above, an analytical model for predicting failure (cracking) in bonded overlays is introduced. The results obtained are used to confirm important observations and to make recommendations pertaining to bonded concrete overlays. Furthermore, observations and recommendations made may be applied in practice to optimize design and application of bonded concrete overlays

Empirical models were used to determine relaxation curve profiles at specific intervals of time. Short term and long term durations were considered. An algebraic system of equations was used in the estimation of relaxation curve profiles. Consequently a universal empirical equation is formulated to account for the relaxation in all mixes tested.

Relevant information, procedure followed and ultimately modelling is presented in the following sections.

6.2 Empirical models for relaxation

Empirical models in the form of algebraic equations were derived for all curves. The algebraic equations developed were in the form of equation [5.4]. Description of all the parameters in equation [5.4] was done in Chapter 5.

$$\Psi(t) = 100 - At^{(C)} \qquad [5.4]$$

The empirical models accounted for short-term intervals i.e. 0-12 hrs and 0-72 hrs as well as for long-term intervals between 0-400 hrs.

A detailed discussion of the 0-12 hrs interval is dealt with in the following section.

6.2.1 Empirical models for 0-12 hrs relaxation

Fig 6.1 shows all the relaxation curves investigated within 0-12 hrs. All curves are shape and colour coded depending on the age of testing and mix. It is noteworthy that the legend is arranged in the order in which the curves appear.

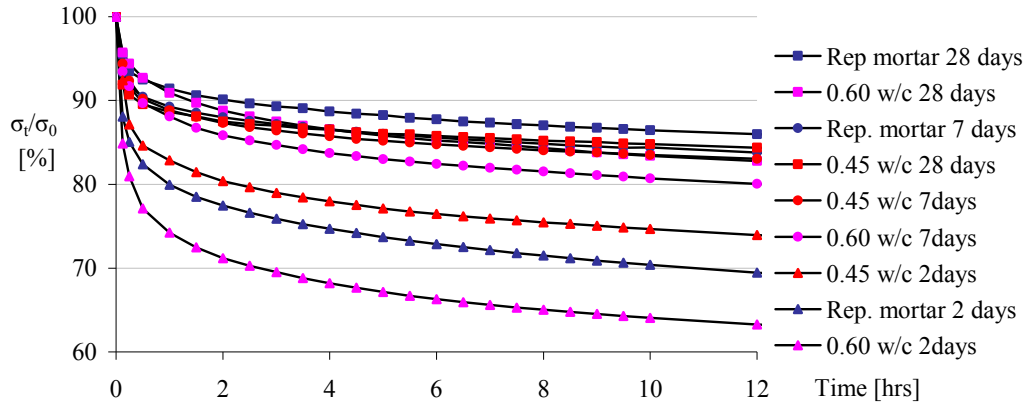

Fig. 6.1: Relaxation curves for 0-12 hours

As seen in Fig.6.1, there is a high similarity in relaxation of specimens tested at 7 and 28 days. In particular, 28 day 0.60, 28 day 0.45, 7 day 0.45 w/c ratio and 7 day repair mortar specimens all follow a similar profile. It is interesting to note that even though the 7 day 0.60 w/c ratio curve is similar to the above curves in the initial 1 hr it shows

more relaxation thereafter. The 28 day 0.60 w/c ratio curve also shows a similar change in profile within the first hour.

As a result of the similarity observed in Fig. 6.1, only six models were derived in the 0-12 hrs interval. This is because one of the equations could account for the four similar curve profiles. Fig. 6.2 shows the empirical equation for the four similar curves.

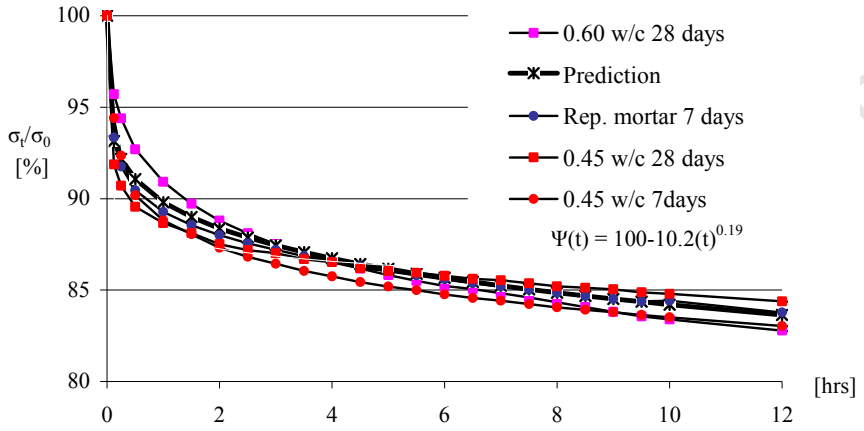

Fig. 6.2: Empirical model for four similar curves (0-12 hrs)

Even if the empirical curve does not exactly follow relaxation curve profiles, the estimation of relaxation within 0-12 hrs is fairly accurate. It follows the mean of the four curves. The empirical constants for respective curves are indicated in the equation shown in Fig. 6.2. The constants for the rest of the curves within the 0-12 hrs interval are shown in Table 6.1.

Table 6.1: Empirical constants for respective mixes (0-12 hrs)

Specimen	*Constant A*	*Constant B*
Rep. mortar 28 days	8.6	0.19
0.60 w/c 28 days	10.2	0.19
Rep. mortar 7 days	10.2	0.19
0.45 w/c 28 days	10.2	0.19
0.45 w/c 7 days	10.2	0.19
0.60 w/c 7 days	12.4	0.19
0.45 w/c 2 days	17.0	0.18
Rep. mortar 28 days	20.0	0.17
0.60 w/c 7 days	25.5	0.15

6.2.2 Empirical models for 0-72 hrs relaxation

Due to the difference in relaxation at later ages, empirical models derived for 0-12 hrs interval may not accurately estimate curve profiles during 0-72 hrs interval. To illustrate this, the example in Fig. 6.2 will be used. However, the time duration is extended to 72 hrs (Fig. 6.3).

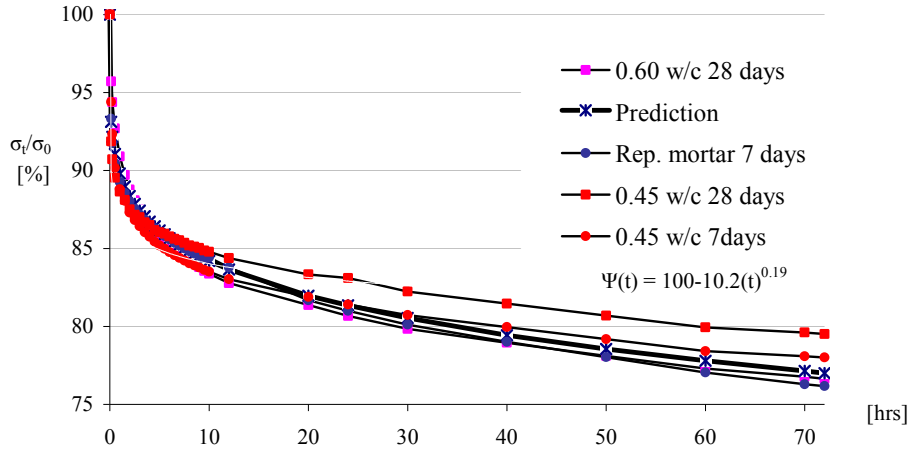

Fig. 6.3: Empirical model for four similar curves (0-72 hrs)

During 0-12 hrs interval, the empirical model is a good approximation for all curves. However from 12 hrs to 72 hrs, the model cannot accurately predict relaxation particularly in the 28 day 0.45 w/c ratio specimens. The constants for the rest of the curves within the 0-72 hrs interval are shown in Table 6.2.

Table 6.2: Empirical constants for respective mixes (0-72 hrs)

Specimen	*Constant A*	*Constant B*
Rep. mortar 28 days	8.6	0.21
0.60 w/c 28 days	10.2	0.19
Rep. mortar 7 days	10.2	0.19
0.45 w/c 28 days	10.5	0.16
0.45 w/c 7 days	10.2	0.19
0.60 w/c 7 days	12.4	0.18
0.45 w/c 2 days	17.0	0.16
Rep. mortar 2 days	20.0	0.17
0.60 w/c 2 days	27.0	0.12

Table 6.2 shows that the values of constant A increase and constant B decrease with increasing relaxation.

6.2.3 Empirical models of long-term relaxation (0-400 hrs)

Fig. 6.4 shows the empirical equations relating to long-term relaxation.

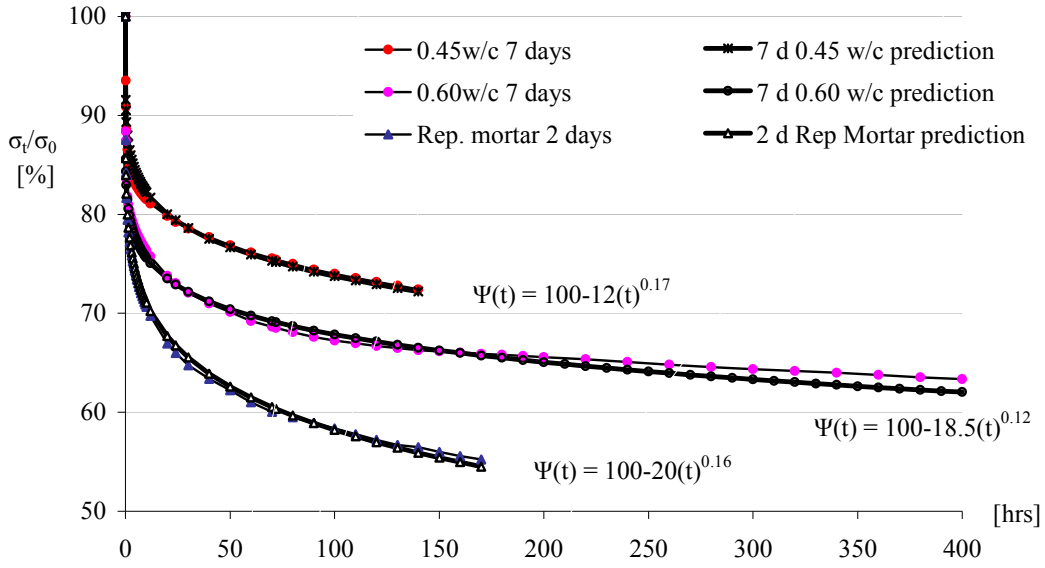

Fig. 6.4: Empirical model for four long-term relaxation (0-400 hrs)

In general, all the model curves in Fig. 6.4 show a good representation of data. However it is noteworthy that not all the data is sufficiently represented. For example, the model curve for 7 day 0.45 w/c ratio specimens shows a good relationship at later ages but it overestimates the data at early ages. Similarly the model curve for 0.60 w/c ratio specimens shows a good estimate at early ages and underestimates the data at later ages. The 2 day repair mortar curve is roughly similar to the original data however there are slight differences particularly at ages beyond 50 hours.

The above observations show that it is difficult to adequately represent data at later ages. This is because whilst the model is based on a mathematical equation, relaxation is dependant on parameters which cannot be represented purely mathematically.

6.2.4 Representation of all data

Fig. 6.5 and Fig. 6.6 show a representation of all the results in terms of empirical equations. In Fig. 6.5 data is classified in terms of age and mean values are calculated. The empirical model is fitted through the mean curves.

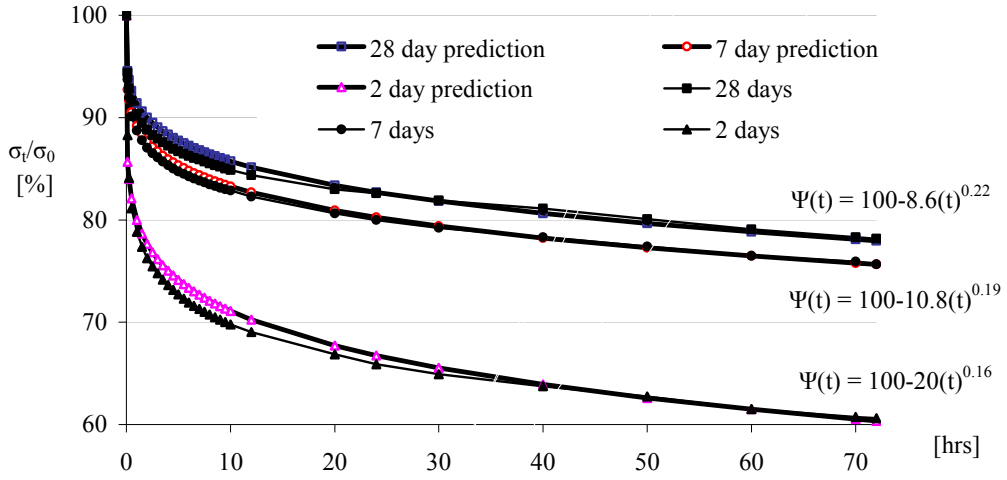

Fig. 6.5: Empirical equations for mean curves at 2, 7 and 28 days

As seen in Fig. 6.5, all curves seem to have a poor estimate of the early age data but the data at 72 hours is approximated more accurately. All the model curves overestimate the data at early ages. The standard deviations of the constants A and C are given in absolute values and in terms of percentages (Table 6.3).

Table 6.3: Standard deviations of empirical equations for mean curves

Age	*Standard deviation*		*Standard deviation [%]*	
	Constant A	*Constant B*	*Constant A*	*Constant B*
2 days	5.13	0.026	24	18
7 days	1.27	0.006	12	3
28 days	1.02	0.025	10	13

The model representing all the data measured in this study is presented in Fig. 6.6. The standard deviations for empirical constants A and C are 6.14 and 0.026 respectively. This corresponds to 44% and 15% standard deviations. The standard deviation shows how high the scatter in the data may be. Expectedly in this case the model curve has a high standard deviation as the scatter of input data is large.

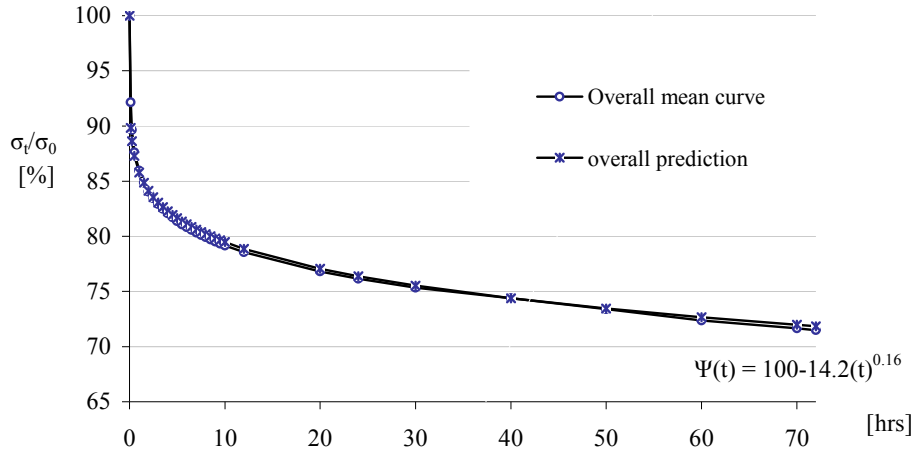

Fig. 6.6: Empirical equation for mean overall curve

Analytical modelling is discussed in the following sections.

6.3 Main experimental results for analytical modelling

As part of a comprehensive investigation of relaxation in bonded concrete overlays, various mixes were produced and tested. Tests and measurements were carried out on free shrinkage strain, elastic modulus, tensile strength, tensile stress and tensile relaxation. These experiments were discussed in Chapter 5.

6.3.1 Tensile relaxation

2 and 7 day results for relaxation curves of all mixes are presented in Fig. 6.7.

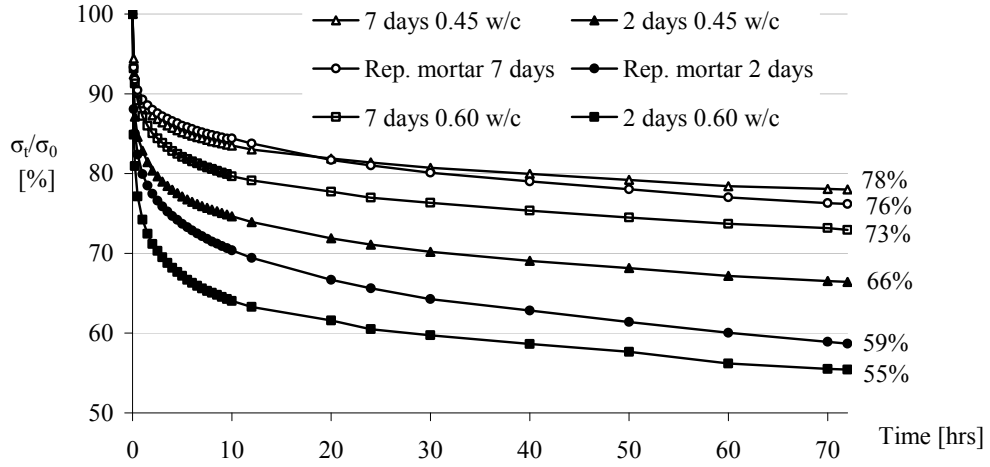

Fig. 6.7: Mean relaxation curves for respective mix specimens (2 days and 7 days)

Corresponding margins of relaxation after 72 hours are presented as shown in Fig. 6.8. It should be noted that Fig. 6.7 and Fig. 6.8 is a repeat from the previous chapter.

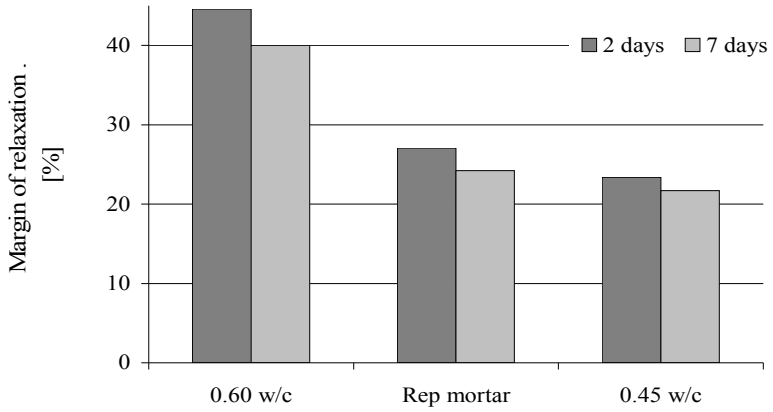

Fig. 6.8: Mean relaxation margins for respective mix specimens (2 days and 7 days)

Ultimate relaxation values, defined as relaxation at 72 hours after loading, are used in modelling (Section 6.5).

6.3.2 Tensile strength

Tensile strength tests were carried out at intervals of 2, 5, 7, 10, 14, 21 and 28 days. Tensile strength is required to determine the onset of cracking. For a complete summary of tensile strength results, readers are referred to Section 5.2.

6.3.3 Elastic modulus

The modulus of elasticity is a significant parameter in modelling. Through a parametric study Beushausen and Alexander (2006) showed that elastic modulus influences resistance to shrinkage cracking. An increase in elastic modulus increases overlay stresses which in turn depend on relaxation. The elastic modulus and tensile strength both increase with maturity and are also dependant on mix proportion/composition. This parameter is required for calculation of direct stresses caused by restraint (Section 6.3.5). Elastic modulus values of the concrete mixes investigated are covered in detail in Section 5.3.

6.3.4 Free shrinkage strain and restraint

Free shrinkage strain was measured starting from after completion of curing. Studies by Beushausen (2005) showed a direct relationship between restraint in bonded concrete overlays and free shrinkage. It was found that restraint was equivalent to 60% of free shrinkage strain. This relationship is discussed later in the approach to be covered. Detailed results of free shrinkage and restraint are shown in Section 5.4.

6.3.5 Tensile stress

Cracking in concrete occurs when tensile stresses exceed tensile strength. This may be represented by Fig. 6.9.

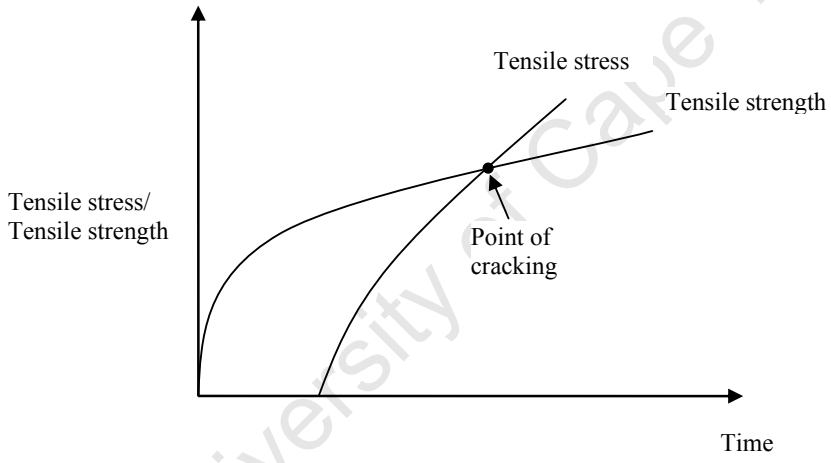

Fig. 6.9: Schematic showing likelihood of cracking.

Direct tensile stresses may be calculated using equation [6.1].

$$\sigma(t) = 0.6\ \varepsilon_{FSS}(t)\ E(t)\ \Psi(t_\infty) \qquad [6.1]$$

Where $\sigma(t)$ = direct tensile stress at given time

$0.6\ \varepsilon_{FSS}(t)$ = restraint corresponding to 60% free shrinkage

$E(t)$ = time dependant modulus of elasticity

$\Psi(t_\infty)$ = magnitude of relaxation

In order to apply the above-mentioned parameters in the model, a number of assumptions were made. A review of assumptions is presented in the following section.

6.4 Assumptions regarding main parameters

As emphasised earlier in this study, there is insufficient detail regarding investigations carried out on tensile relaxation. Hence only a few models have been developed. The few that exist are complex and rely on numerous input parameters, some of them being rather difficult to asses (Charron, Marchand, Bissonnette, Pigeon & Gerard, 2003). Therefore fundamental aspects were considered in the model presented in this study. Assumptions governing the main parameters are discussed in this section.

6.4.1 No shrinkage occurs during curing

To facilitate calculation of stresses resulting from restraint, shrinkage is assumed to occur only from the period after curing. This may be represented in Fig. 6.10.

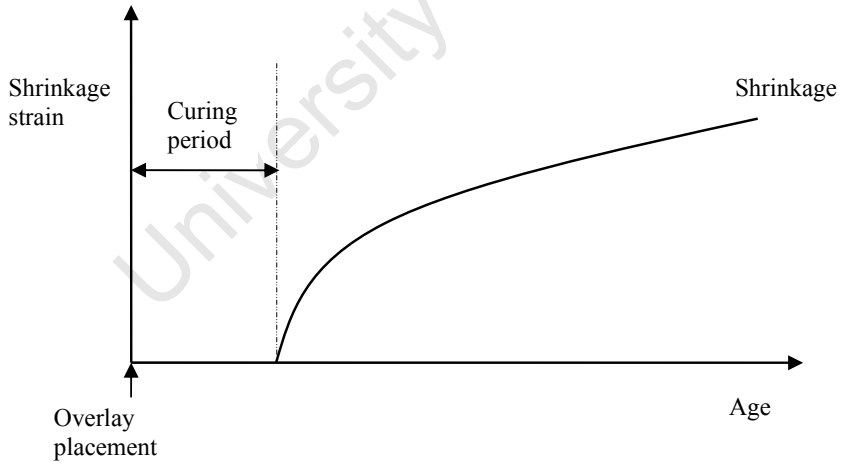

Fig. 6.10: Schematic showing commencement of shrinkage.

During curing, shrinkage may occur due to autogenous and plastic shrinkage. Alexander (2001) states that shrinkage during curing is noteworthy particularly in concrete with a low w/c ratio (i.e. <0.40), which is not appreciable for the majority of

bonded concrete overlays used in practice. A more sophisticated approach however, should consider autogenous shrinkage effects.

6.4.2 Tensile relaxation is instantaneous

Beushausen (2005) carried out strain measurements on cracked concrete overlays. Subsequent results led to the conclusion that a large amount of tensile stress relaxation takes place at early ages of loading. This was also confirmed in other literature (Morimoto and Koyanagi, 1994; Gutsch & Rostásy, 1994; and Kordina *et al*, 2000). These authors found tensile stress relaxation to develop rapidly after loading (compare Section 2.4.3). Relaxation results obtained in this study confirmed the findings above (compare Section 5.6.4.3).

Stress relaxation develops at a much faster rate than stresses resulting from ongoing overlay shrinkage. Therefore, in order to facilitate analytical modelling of overlay and substrate stresses, it appears appropriate to account for overlay stress relaxation in a simple manner. For the analysis of stresses it is assumed that tensile stress relaxation occurs instantaneously after loading (Fig. 6.11) (Beushausen (2005).

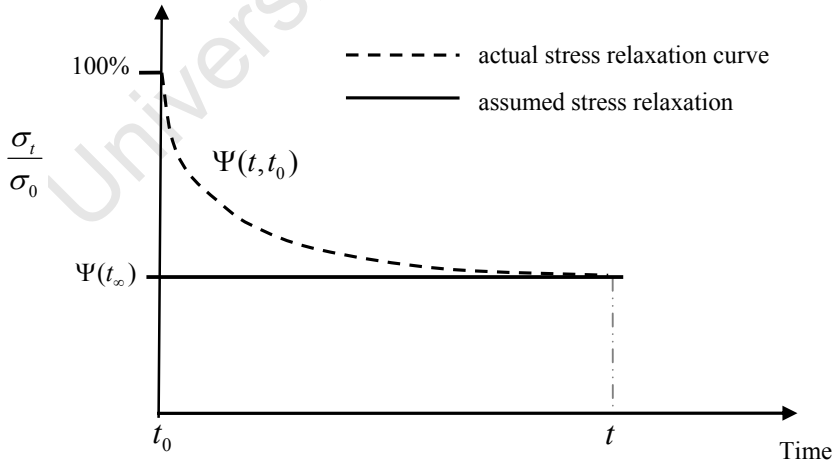

Fig. 6.11: Schematic of simplified approach for the consideration of overlay stress relaxation

From Fig. 6.11 the relaxation function may be taken as a constant value. In this case 72 hour relaxation is applied in modelling.

6.4.3 Restraint is proportional to free shrinkage strain

Research by Beushausen (2006), showed restraint in bonded concrete overlays to be 60% of overlay free shrinkage. In this study, this proportion was found to correspond to a low initial stress. Therefore, in order to investigate relaxation under extreme conditions, higher restraint was used in experiments. 80% stress-strength ratio was then applied.

To facilitate modelling, restraint is taken as 60% of free shrinkage.

6.5 Analytical modelling Approach

6.5.1 General

The analytical modelling is based on the development of relevant material properties from the period after curing is discontinued. Fig. 6.12 shows a schematic of model presentation.

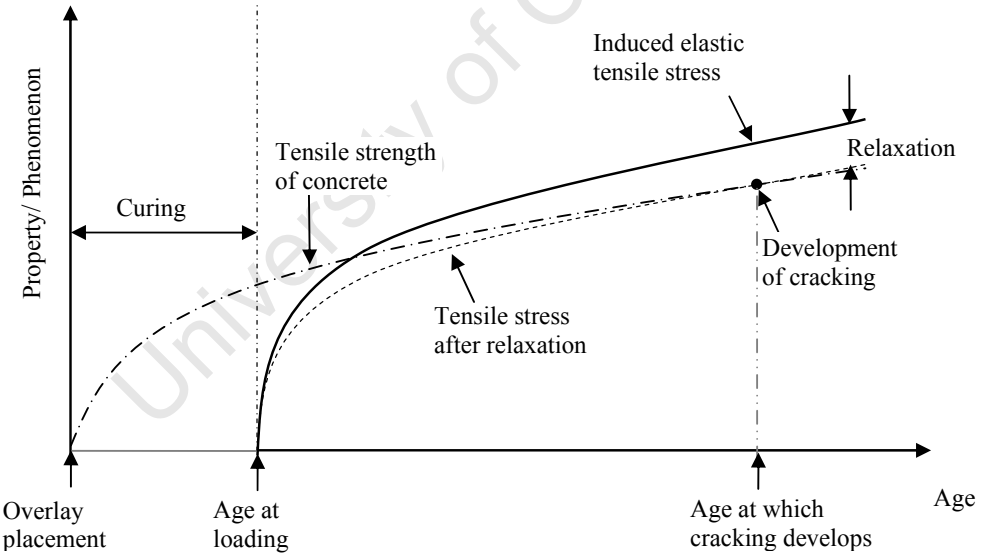

Fig. 6.12: Schematic of simplified approach for modelling overlay stress relaxation

Specimens were cured for 2 days and 7 days. For that reason the model shows time development of main parameters starting from age 2 or 7 days. The above approach may be used to predict the likelihood of cracking. If cracking is likely, then it may be used for calculating the age at which cracking initiates. Based on results from this

model, optimal curing periods are recommended. Furthermore, the performance of all mixes in practice is revealed.

The following section compares performance of selected mixes.

6.5.2 Application of model

In this section, the performance of repair mortar, 0.45 and 0.60 w/c ratio mixes is investigated using the above-mentioned method. Mean values of tensile strength and elastic modulus are used. In addition, tensile relaxation margins are calculated from time-dependant empirical equations (discussed in Chapter 5). It is noteworthy that the values given below are purely theoretical and hence serve as an estimate of the performance of bonded concrete overlays in practice.

6.5.2.1 2 day 0.45 w/c ratio

Table 6.4 shows material properties of 0.45 w/c ratio specimens cured for 2 days.

Table 6.4: Material properties for 2 day 0.45 w/c ratio specimens

Period [days]	*Change in free shrinkage strain* ε_{FSS} *[10^{-6}]*	*Mean elastic modulus [GPa]*	*Mean tensile strength [MPa]*	*Tensile relaxation [%]*	*Elastic tensile stress [MPa]*	*Induced tensile stress after relaxation [MPa]*
2 - 5	120	20.0	3.52	34.0	1.35	0.95
5 - 7	70	23.0	3.73	28.0	3.57	1.79
7 - 14	180	24.3	3.86	22.0	6.82	3.94
14-28	180	25.6	3.95	20.0	10.67	6.36

A plot of data presented in Table 6.4 is shown in Fig. 6.13.

It may be noted that Fig. 6.3 starts from the age of 2 days. This is the age up to which specimens were cured and subsequently loaded. In addition, shrinkage and particularly, shrinkage induced stresses are assumed to start at 2 days. This format applies from Fig. 6.13 up to Fig. 6.19.

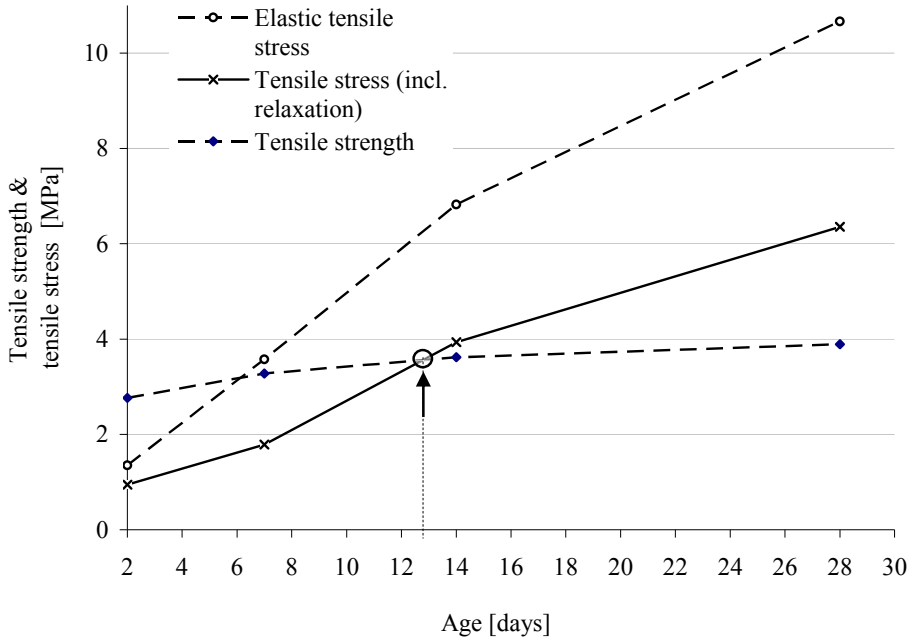

Fig. 6.13: 2 day 0.45 w/c ratio. Overlay strength and stress development
(Arrow indicates the potential age at crack initiation)

According to Fig. 6.13, 0.45 w/c ratio specimens cured for 2 days are likely to crack at age 13 days. This corresponds to 11 days after curing. This is because the rate of increase in shrinkage is higher than the rate of gain in tensile strength. An increase in shrinkage causes a build-up of shrinkage induced stresses. Relaxation is insufficient to relieve stresses. The elastic modulus of concrete also causes an increase in shrinkage induced stresses. This leads to cracking.

6.5.2.2 7 day 0.45 w/c ratio

Table 6.5 shows the material properties of 0.45 w/c ratio specimens cured for 7 days.

Table 6.5: Material properties for 7 day 0.45 w/c ratio specimens

Period [days]	*Change in free shrinkage strain* ε_{FSS} *[10^{-6}]*	*Mean elastic modulus [GPa]*	*Mean tensile strength [MPa]*	*Tensile relaxation [%]*	*Elastic tensile stress [MPa]*	*Induced tensile stress after relaxation [MPa]*
7 - 10	120	24.0	3.52	22.0	1.47	1.35
10 - 14	125	24.8	3.73	21.5	4.54	2.85
14 - 21	160	25.4	3.86	20.5	8.28	4.86
21 - 28	100	25.9	3.95	20.0	11.77	6.20

A plot of data presented in Table 6.5 is shown in Fig. 6.14.

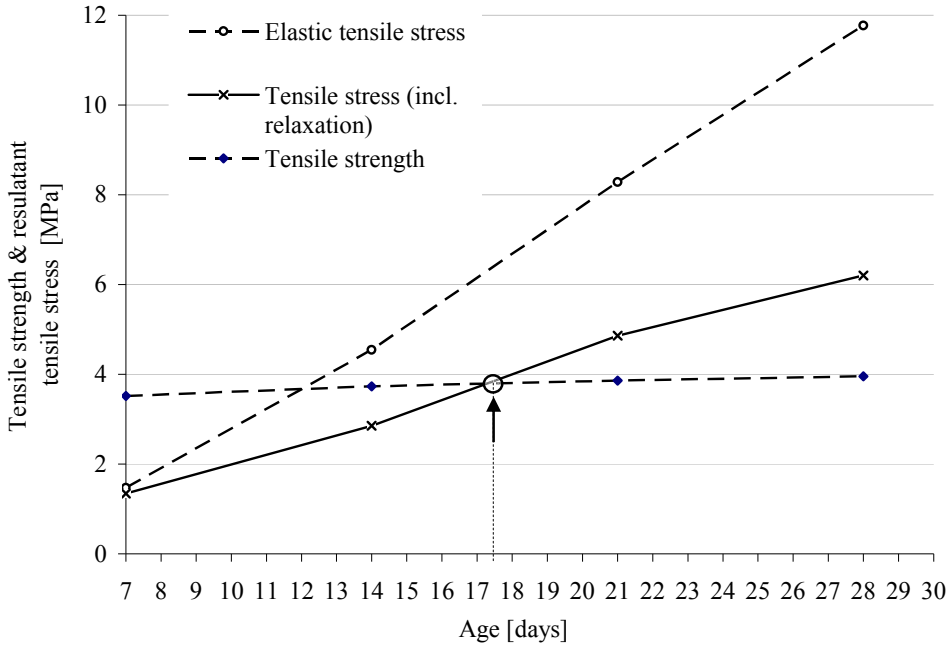

Fig. 6.14: 7 day 0.45 w/c ratio. Overlay strength and stress development
(Arrow indicates the potential age at crack initiation)

Although relaxation is lower in 0.45 w/c ratio specimens cured for 7 days, likelihood of cracking is predicted to occur roughly 10 days after curing. This corresponds to overlay age of 17 days. The elastic modulus of concrete increases with an increase in the duration of curing. Subsequently, shrinkage induced stresses are likely to be higher. Overlay strength also increases with duration of curing. As a result, onset of cracking is delayed.

6.5.2.3 2 day 0.60 w/c ratio

Table 6.6 shows the material properties of 0.60 w/c ratio specimens cured for 2 days.

Table 6.6: Material properties for 2 day 0.60 w/c ratio specimens

Period [days]	*Change in free shrinkage strain* ε_{FSS} *[10^{-6}]*	*Mean elastic modulus [GPa]*	*Mean tensile strength [MPa]*	*Tensile relaxation [%]*	*Elastic tensile stress [MPa]*	*Induced tensile stress after relaxation [MPa]*
2 - 5	92	13.7	2.00	45.0	0.76	0.41
5 - 7	53	17.2	2.68	36.0	2.05	0.87
7 - 14	155	19.3	3.11	27.0	4.31	2.29
14-28	120	21.3	3.48	23.0	7.73	3.71

Fig. 6.15 represents data shown in Table 6.6.

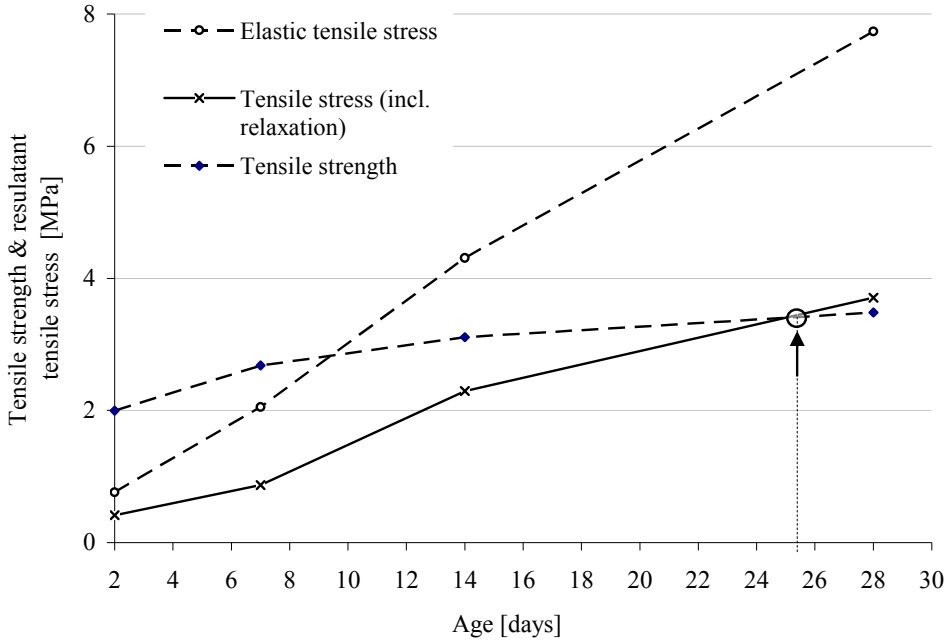

Fig. 6.15: 2 day 0.60 w/c ratio. Overlay strength and stress development
(Arrow indicates the potential age at crack initiation)

Compared to 0.45 w/c ratio specimens, relaxation is higher. Tensile strength, elastic modulus, shrinkage and shrinkage induced stresses are lower in 0.60 w/c ratio specimens. As a result, cracking in 0.60 w/c ratio specimens cured for 2 days is likely to occur at 25 days. The main influence is the high magnitude of relaxation in 0.60 w/c ratio specimens cured for 2 days.

6.5.2.4 7 day 0.60 w/c ratio

Table 6.7 shows the material properties of 0.60 w/c ratio specimens cured for 7 days.

Table 6.7: Material properties for 7 day 0.60 w/c ratio specimens

Period [days]	*Change in free shrinkage strain* ε_{FSS} *[10^{-6}]*	*Mean elastic modulus [GPa]*	*Mean tensile strength [MPa]*	*Tensile relaxation [%]*	*Elastic tensile stress [MPa]*	*Induced tensile stress after relaxation [MPa]*
7 - 10	92	18.8	3.00	27.0	0.91	0.76
10 - 14	98	20.1	3.27	25.6	2.85	1.69
14 - 21	124	21.0	3.43	24.3	5.31	2.94
21 - 28	67	21.7	3.57	23.0	7.55	3.72

A plot of data presented in Table 6.7 is shown in Fig. 6.16.

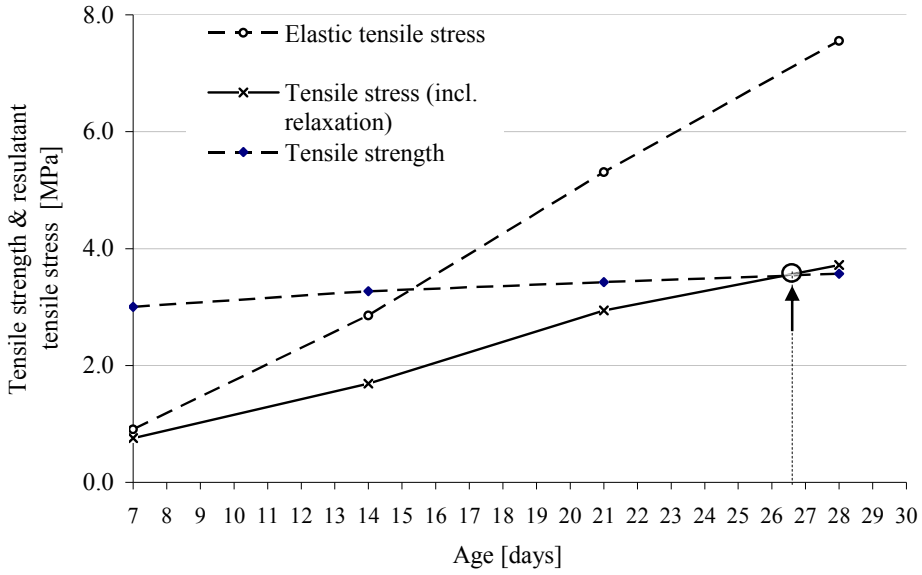

Fig. 6.16: 7 day 0.60 w/c ratio. Overlay stress and strength development
Arrow indicates the potential age at crack initiation.

The potential cracking age is 26 days for 0.60 w/c ratio specimens cured for and tested after 7 days. This constitutes a delay in cracking of 19 days. Compared to 2 day 0.60 w/c ratio specimens, 7 day specimens may exhibit lower relaxation but more delayed onset of cracking. Cracking occurs due to high elastic modulus, shrinkage and shrinkage induced stress.

6.5.2.5 Repair mortar cured for 2 day

Table 6.8 shows the material properties of repair mortar specimens cured for 2 days.

Table 6.8: Material properties for 2 day repair mortar specimens

Period [days]	*Change in free shrinkage strain* ε_{FSS} *[10^{-6}]*	*Mean elastic modulus [GPa]*	*Mean tensile strength [MPa]*	*Tensile relaxation [%]*	*Elastic tensile stress [MPa]*	*Induced tensile stress after relaxation [MPa]*
2 - 5	300	7.6	1.65	41.0	1.29	0.80
5 - 7	140	9.0	1.99	24.0	3.34	1.52
7 - 14	235	10.2	2.32	23.0	5.76	2.83
14-28	215	11.5	2.61	22.0	9.11	4.36

Data shown in Table 6.8 is presented in Fig. 6.17.

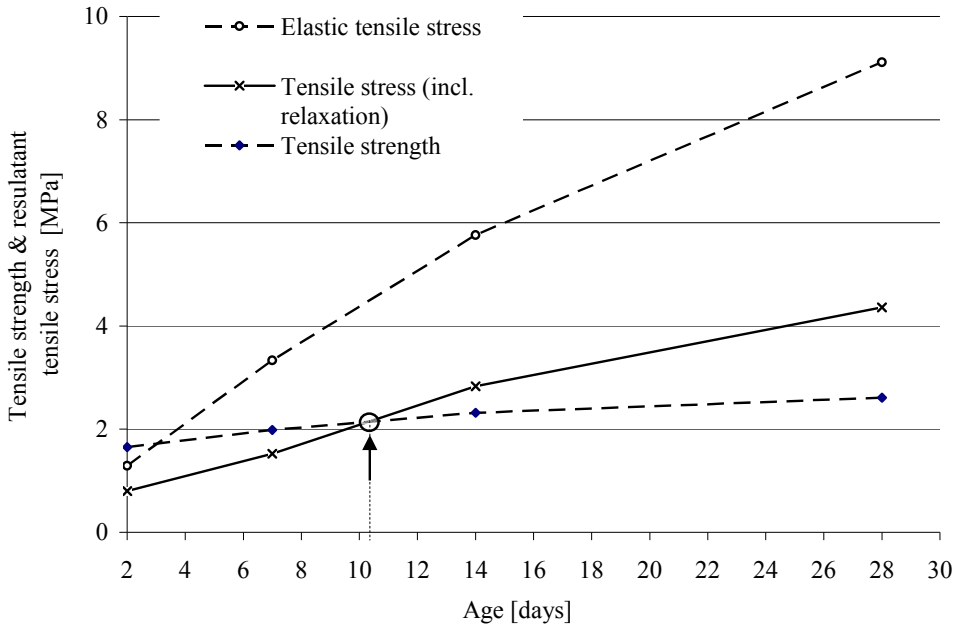

Fig. 6.17: 2 day repair mortar. Overlay strength and stress development
(Arrow indicates the potential age at crack initiation)

Crack development in repair mortar specimens cured for 2 days may occur roughly at 10 days. This corresponds to 8 days after curing. Compared to the predicted cracking in 2 day 0.45 w/c ratio specimens, cracking occurs earlier in repair mortar. Although tensile relaxation, shrinkage and hence shrinkage induced stresses are high, this may be attributed to lower tensile strength in the repair mortar.

6.5.2.6 Repair mortar cured for 7 day

Table 6.9 shows the material properties of repair mortar specimens cured for 7 days.

Table 6.9: Material properties for 7 day repair mortar specimens

Period [days]	*Change in free shrinkage strain* ε_{FSS} *[10^{-6}]*	*Mean elastic modulus [GPa]*	*Mean tensile strength [MPa]*	*Tensile relaxation [%]*	*Elastic tensile stress [MPa]*	*Induced tensile stress after relaxation [MPa]*
7 - 10	300	9.8	2.22	24.0	1.53	1.33
10 - 14	230	10.6	2.42	23.4	4.45	2.57
14 - 21	190	11.3	2.56	22.7	7.06	3.72
21 - 28	110	11.8	2.66	22.0	9.12	4.49

A plot of data presented in Table 6.9 is shown in Fig. 6.18.

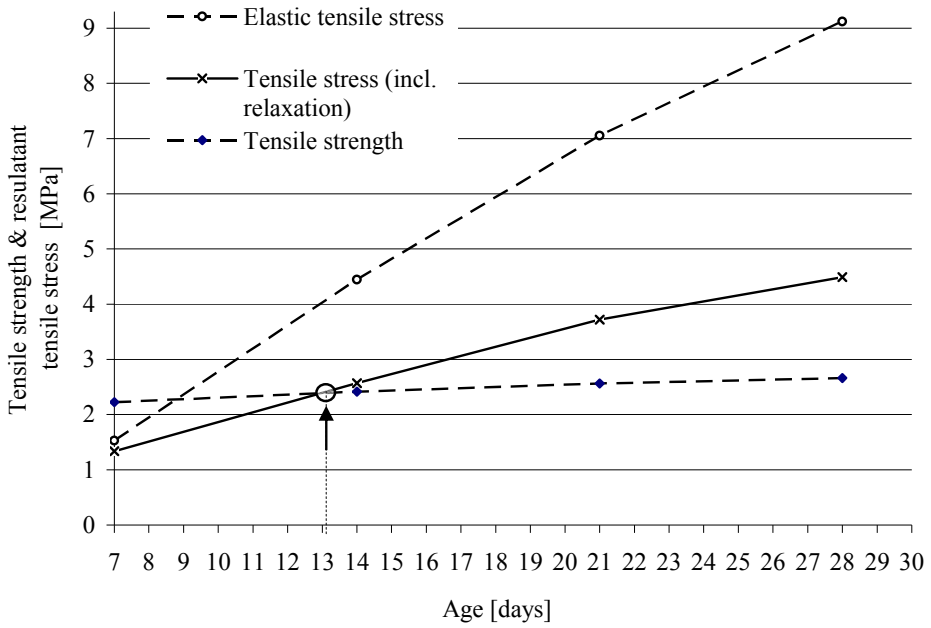

Fig. 6.18: Repair mortar. Overlay strength and stress development
Arrow indicates the probable age at crack initiation.

From Fig. 6.17 and Fig. 6.18, repair mortar specimens cured for 7 days may crack at 13 days whilst those cured for 2 days crack at the age of 10 days. Although relaxation is greater at 2 days, the tensile strength is lower than that in specimens cured for 7 days. In addition the rate of shrinkage gain is higher at 2 days compared to that at 7 days. The high rate of shrinkage increases shrinkage induced stresses. This may cause cracking to occur earlier.

6.5 Summary and recommendations

Using a simple analytical model, the onset of cracking in bonded concrete overlays can be estimated. The model is based on main parameters affecting relaxation. Duration of curing may be recommended and the associated period of cracking after curing calculated. However the abovementioned model is not a defined approximation of actual bonded concrete overlay behaviour. For example, bonded concrete overlays made from common commercial repair mortars other than that used in this study, may not exhibit distinctly similar cracking behaviour. Nonetheless, the development of main parameters can be identified and used in modelling.

Analytical modelling findings are summarised in Table 6.10.

Table 6.10: Summary of anticipated age and time to cracking

Specimen	*Curing period [days]*	*Anticipated age at cracking [days]*	*Anticipated cracking time after curing. [days]*
0.45 w/c ratio	2	13	11
	7	17	10
0.60 w/c ratio	2	25	23
	7	26	19
Repair mortar	2	10	8
	7	13	6

In general, curing overlays for long periods may be recommended. There is less risk of early cracking due to significant gain in tensile strength during the curing period. Apart from the greater strength achieved in specimens cured for longer periods, the margin of shrinkage is less than that observed from early age specimens. As a result, shrinkage induced tensile stresses are reduced leading to prolonged period before cracking ensues.

It is interesting to note that the anticipated time to cracking after curing is lower in specimens cured for 7 days compared to those cured for 2 days. This may be attributed to the high margin of relaxation at early age.

Another interesting observation in Table 6.10 is that the difference in the anticipated age of cracking in relation to the curing durations, particularly between 0.60 w/c ratio and repair mortar specimens is small. This leads to the conclusion that long curing may be somewhat "overrated" and does not necessarily result in better performance in these concretes.

CHAPTER SEVEN: SUMMARY, CONCLUSIONS AND RECOMMENDATIONS

7.1 Introduction

A significant amount of concrete structures in South Africa are either approaching the end of their service life whilst others need regular repair and maintenance. Bonded concrete overlays remain the main tool used in lining, retrofitting and rehabilitating deteriorated concrete structures. Bonded overlay and substrate act as a composite system.

Differential shrinkage is often the main problem affecting performance of bonded overlays. Differential shrinkage may be caused by thermal and hygral changes. As a result, tensile stresses are set up in the overlay whilst the top section of the substrate is subjected to compression. Tensile overlay stresses may lead to cracking and or debonding.

Cracking and debonding may be prevented if shrinkage-induced stresses are reduced to levels below that of overlay tensile strength. Tensile relaxation may counteract effects of shrinkage restraint and considerably reduce restraint stresses. Tensile relaxation has been shown to reduce shrinkage-induced stresses, in some cases preventing cracking and debonding (Beushausen & Alexander, 2006).

Although a handful of studies have been carried out in this field (Bissonette & Pigeon, 1995; 1999; Beushausen & Alexander, 2006; Ghali & Favre, 1994; Gutsch & Rostásy, 1994; Morimoto & Koyanagi, 1994; and Kordina *et al*, 2000), there is still little experimental evidence regarding tensile relaxation. Furthermore no set guidelines for optimizing design and application of overlays exist. Investigations carried out have proven insufficient in determining overlay relaxation capacity.

The investigation covered in this study serves as an important contribution towards characterizing relaxation in representative overlay materials. In addition, effects of w/c ratio, mix composition and age at loading were detailed. The aforementioned

parameters were selected based on common overlay properties and in consensus with previous studies.

7.2 Summary of main conclusions

In general tensile relaxation was found to be w/c ratio, mix composition and maturity sensitive.

7.2.1 Magnitude of relaxation

Relaxation was found to be in the order of 20% to 45% in the mixes tested. A number of literatures have reported relaxation values ranging from 40-67% (Gutsch & Rostásy, 1994; Morimoto & Koyanagi, 1994; Pigeon *et al*, 2000; Kordina *et al*, 2000 and Beushausen & Alexander, 2006). These findings may not be entirely similar owing to different test set up and test conditions. The other parameter is the difference in mixes investigated.

7.2.2 Influence of w/c ratio and mix composition

At a given age of testing, relaxation appears to be w/c ratio-sensitive. 0.60 w/c ratio specimens generally showed 10% higher relaxation after 72 hours compared to their 0.45 w/c ratio counterparts. Relaxation in repair mortar was greater than in 0.45 w/c ratio specimens. This may be attributed to the pore structure which may determine the strength and stiffness of the mix. Generally in low w/c ratio concretes, strength and elastic modulus are usually higher than in higher w/c ratio mixes. Therefore there is a tendency to resist mechanisms which promote relaxation.

7.2.3 Influence of age at loading

Irrespective of w/c ratio, concrete age had a high influence on tensile relaxation. Specimens tested at 2 days had 15% more relaxation than those tested at 7 days. Relaxation was found to reduce with increasing age. This is because relaxation is dependant on the degree of hydration (Neville, 1981). The degree of hydration is

initially rapid but reduces gradually with time. In addition, the difference in relaxation is low at later ages (i.e. 7 days and 28 days) compared to earlier on (2 days and 7 days). At later ages concrete would be more mature and therefore less capable of undergoing significant relaxation (Rusch *et al*, 1983). Hence minor differences were observed in relaxation between specimens tested at 28 days and 7 days.

7.2.4 Time development of relaxation

Generally, relaxation was found to progress more rapidly in specimens tested at 2 days compared to those tested at 7 days. In comparison to shrinkage and tensile strength gain, overall rate of relaxation was found to be significantly higher during early hours (2 hours). Therefore, compared to the rate of development of tensile strength and shrinkage, relaxation in bonded concrete overlays may be assumed to be instantaneous. Long-term relaxation was also investigated and it was found that relaxation does not diminish totally as it continues to occur, however at a lower rate at later ages. Time development was also dependant on both the type of mix and age investigated. For example, 0.60 w/c ratio specimens tested at 2 days had a more rapid development of relaxation than 0.45 w/c ratio specimens tested at the same age. However the converse was true at 7 days and 28 days.

7.2.5 Modelling approach and results

In order to simplify analytical modelling, the following main assumptions were applied:

- No shrinkage occurs during curing period.
- Tensile relaxation is instantaneous from the onset of loading (Beushausen, 2005).
- Restraint is equivalent to 60% of free shrinkage strain (Beushausen, 2005).

The analytical model showed that curing overlays for long periods may be recommended. For overlays with higher 0.60 w/c ratio and repair mortar, curing seemed to have a minor influence delaying the onset of cracking. This lead to the

conclusion that long curing may be somewhat "overrated" and may not necessarily result in better performance for certain concretes.

Empirical models were developed based on an algebraic equations relating to relaxation time development. These were time related and empirical constants were determined using a trial and error method. As such they may not be applicable for bonded concrete overlays used in practice. Therefore a more sophisticated approach should be considered.

7.3 Recommendations

This research identified effects of some main aspects affecting bonded concrete overlay relaxation. However more characteristics still need to be given exposure. For a deeper understanding of tensile relaxation of bonded concrete overlays, the following aspects should be considered:

- The practicality of laboratory developed models in actual overlays of similar mix compositions should be assessed. The model in this research was derived from experiments performed on small specimens under controlled conditions and as such does not account for realistic factors e.g. formation of cracks induced by temperature gradients.

- Research should be done to find the effect of other mix components such as aggregates and also other common repair mortars. Although mortar specimens were investigated, there is still a need to investigate typical concrete mixes commonly used in bonded concrete overlays.

- Only sealed specimens simulating bonded concrete overlays undergoing partial restraint were investigated in this research. The behaviour of unsealed specimens also needs to be established. Unsealed specimens represent overlays subjected to 100% restraint. This may not be a practical case. However, relaxation under incremental loads may need to be addressed.

- Finally more tests should be done to find influence of other parameters such as strain and stress imposed (restraint). In order to simplify the analysis in this study, these were kept constant.

APPENDICES

Appendix A: Statistical evaluation of stress relaxation

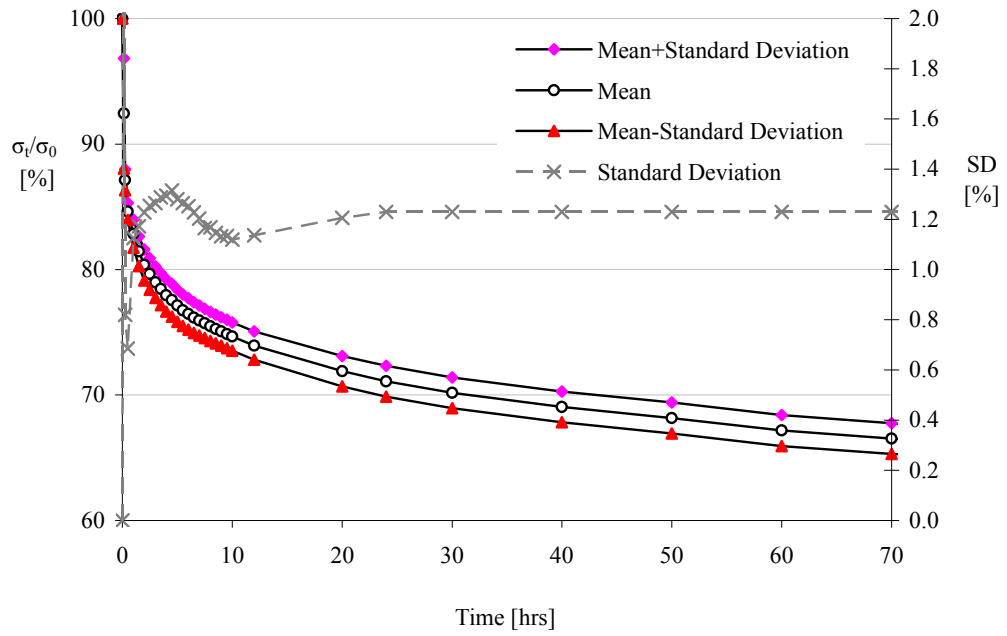

A1: Statistical evaluation of stress relaxation (2 days 0.45 w/c ratio).

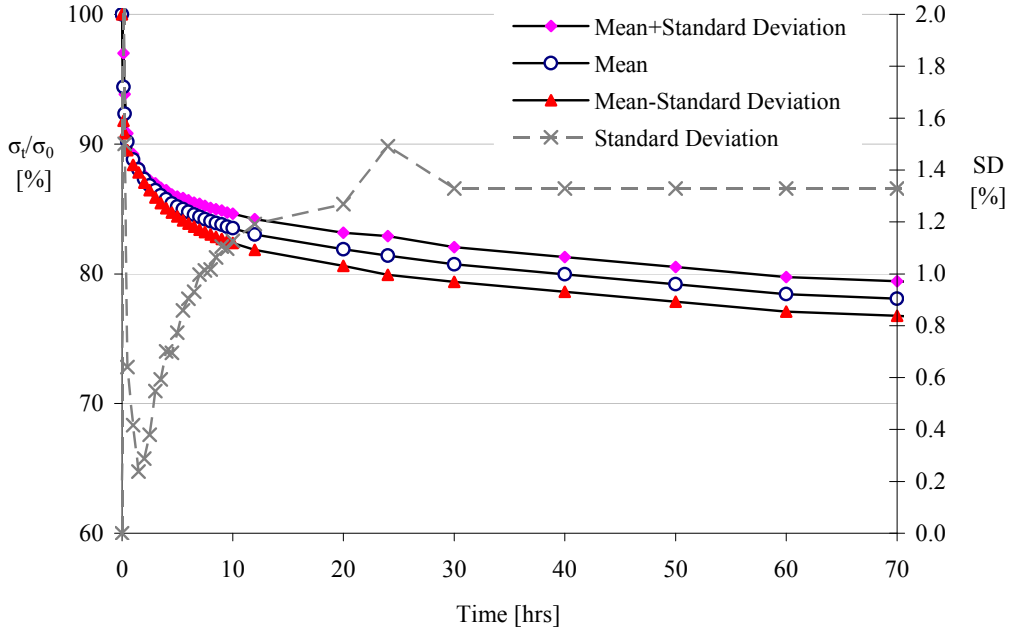

A2: Statistical evaluation of stress relaxation (7 days 0.45 w/c ratio).

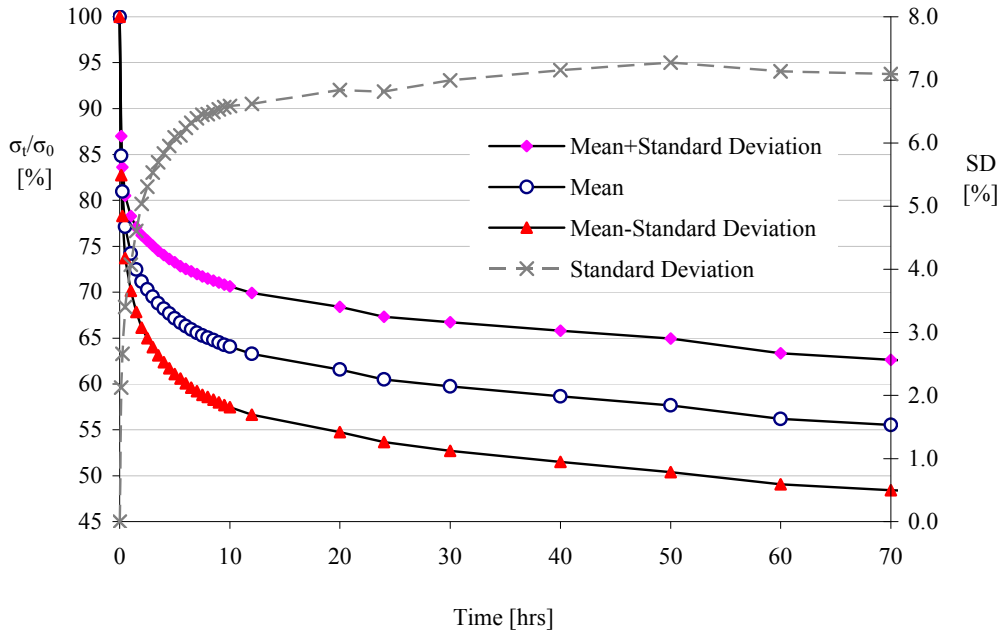

A3: Statistical evaluation of stress relaxation (2 days 0.60 w/c ratio).

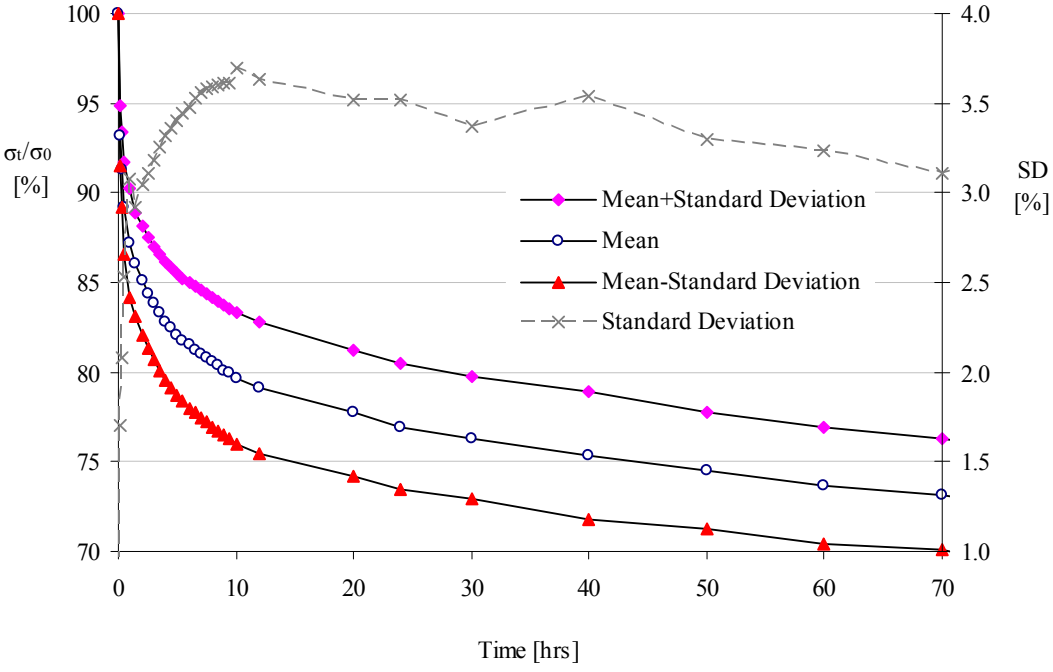

A4: Statistical evaluation of stress relaxation (7 days 0.60 w/c ratio).

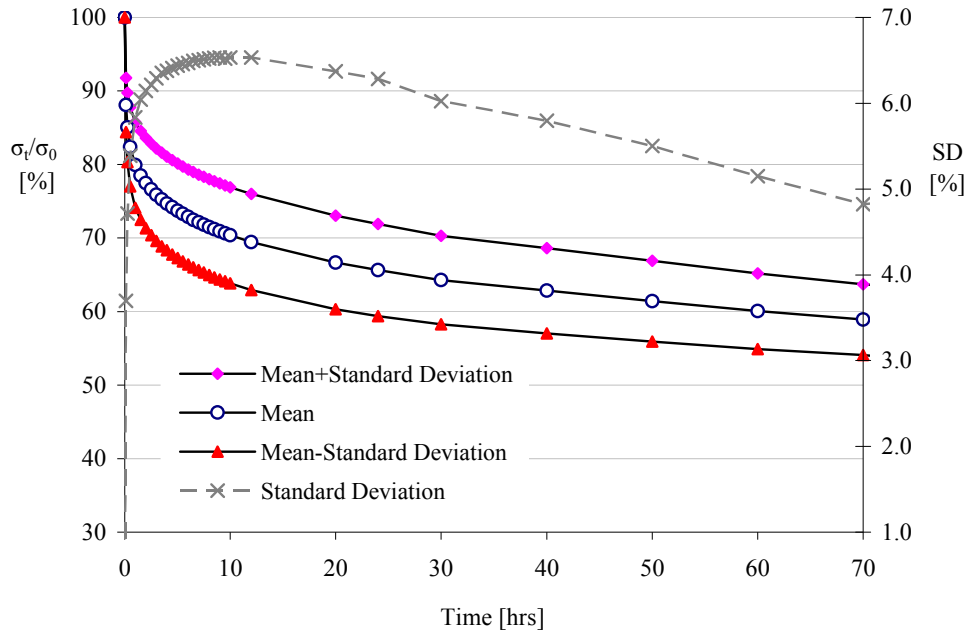

A5: Statistical evaluation of stress relaxation (2 days Repair mortar).

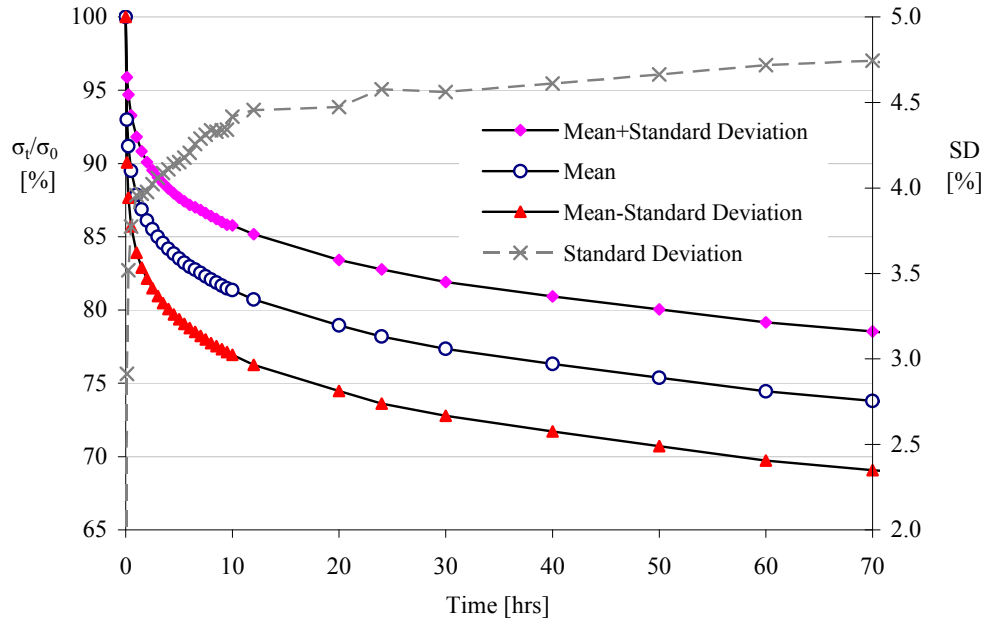

A6: Statistical evaluation of stress relaxation (7 days Repair mortar).

REFERENCES

Allen, R. T. L. and Edwards, S. C. Editors, (1987), *The Repair of Concrete Structures*, Glasgow & London: Blackie

Alexander, M.G. (2001), Deformation and volume change of hardened concrete, *Fulton's Concrete Technology*, 8th ed. 2001, Midrand, South Africa

American Concrete Institute (ACI) (1999), ACI 318 (1999). *Building Code Requirements for Structural Concrete (ACI 318-99) and Commentary (ACI 318R-99)*, Farmington Hills, Michigan, USA, 1999

Asad, M., M. H. Baluch and A. H. Al-Ghadib, (1997). Drying shrinkage stresses in concrete patch repair systems, *Magazine of Concrete Research*, 1997, 49, No. 181 Dec., pp283-293

Atashi M., M. Lachemi and M.R. Kianoush (2007). Numerical modelling of the behaviour of overlaid slab panels for reinforced concrete bridge decks, *Engineering Structures*, vol 29, 2, February, pp 271-281 ***citing*** ACI Committee 546 (2002). *Guide for repair of concrete bridge superstructures (ACI 546.1).* Farmington Hills (MI), American Concrete Institute; 2002.p. 8

Banthia N. and R. Gupta (2006). Influence of polypropylene fibre geometry on plastic shrinkage cracking in concrete, *Cement and Concrete Research* 36: 1263–1267

Barnett, V., Lewis, T. and Rothamsted, V., (1994), *Outliers in Statistical Data*, Wiley series in Probability and mathematical statistics, applied probability and statistics, John Wiley & Sons ***citing*** Grubbs, (1979)

Beushausen, H. D. (2005): Performance of bonded concrete overlays subjected to differential shrinkage, *Doctoral Thesis*, University of Cape Town, 2005

Beushausen, H. D. & M. G. Alexander (2006): Failure mechanisms and tensile relaxation of bonded concrete overlays subjected to differential shrinkage, *Cement and Concrete Research*, 36, pp1908-1914

Bissonette, B., and Pigeon, M. (1995), Tensile creep at early ages of ordinary, silica fume and fibre reinforced concretes, *Cement and Concrete Research*, Vol.25, No.5, 1995

Brooks J.J., and Neville, A. M., (1997) A Comparison of Creep, Elasticity and Strength of Concrete in Tension and in Compression *Magazine of Concrete Research*. V29, No. 100, pp131-141 ***cited by*** Rusch, H, Jungwirth, D and Hilsdorf H, K. (1983): *Creep and Shrinkage; Their effect on the Behaviour of Concrete Structures*, New York, USA

Carlswärd, J (2006): Shrinkage cracking of steel fibre reinforced self compacting concrete overlays; Test methods and theoretical modelling. *Unpublished Doctoral Thesis*, Luleå University of Technology, 2005:02, January 2005, Luleå, Sweden

Charron, J.-P., J. Marchand, B. Bissonnette, M. Pigeon, and B. Gerard, (2003): Modelling Concepts, Early Age Cracking in Cementitious Systems: *Report of RILEM Technical Committee 181-EAS, Early Age Shrinkage Induced Stresses and Cracking in Cementitious Systems*, By Arnon Bentur, Early Age Shrinkage Induced Stresses and Cracking in Cementitious Systems RILEM Technical Committee 181-EAS, Published by RILEM Publications, 2003

Comité Euro-International du Béton & Federation Internationale de la Precontrainte, (1993),*CEB-FIP Model Code 1990*, Thomas Telford Services Ltd, London, 1993

Concrete and Cement Institute, 2003, *Cementitious Materials for Concrete: Standards, Selection and properties* Midrand, South Africa

Cook, D. J., (1972), Some aspects of The Mechanism f Tensile Creep in Concrete, *ACI Journal, Proceedings* V. 69, No. 10, pp 645-649 ***cited by*** Rusch, H, Jungwirth, D and Hilsdorf H, K. (1983): *Creep and Shrinkage; Their effect on the Behaviour of Concrete Structures*, New York, USA

Delatte N. J, Fowler D.W, McCullough B.F, and Grater S.F (1998). Investigating performance of bonded concrete overlays. *Journal of Performance of Constructed Facilities*, 12(2), pp62–70

Emberson, N.K. and Mays, G.C. (1990), Significance of property mismatch in the patch repair of structural concrete. Part 1: Properties of repair systems, *Magazine of Concrete Research*, 1990, 42, No. 152, Sept., pp.147-160

Emmanuel, B.O.A., K. Lev, and T.G. Leslie, (1998), Mechanistic-based model for predicting reflective cracking in asphalt concrete-overlaid pavements, *Transport. Res. Rec*. 1629 234–241 ***cited by*** Jun Z., and, Victor C. L., (2002), Monotonic and fatigue performance in bending of fibre-reinforced engineered cementitious composite in overlay system, *Cement and Concrete Research* 32 p 415-423

Emmons, H., Vaysburd, A. M., and. MacDonald J. E (1995), Durability of concrete repairs: Current problems and future prospects, *Technical Report REMR-SP-172-9*, US Army Corps of Engineers, April 1995, pp 156-169

Eurocode 2 (1991). *Design of Concrete Structures, Part 1: General Rules and Rules for Buildings*. European Prestandard, ENV 1992-1: 1991E, European Committee for Standardization, rue de Stassart 36, B-1050 Brussels, Belgium ***cited by*** Ghali, A., and Favre, R. (1994), *Concrete structures – Stresses and deformations*, second edition, published by E & FN Spon, London, 1994

Fiebrich, M. (1994), Grundlagen der Adhäsionskunde, *Deutscher Ausschuss für Stahlbeton*, Heft 334, Beuth Verlag, Berlin 1994, pp. 75-90 ***cited by*** Beushausen, H D (2005): Performance of bonded concrete overlays subjected to differential shrinkage, *Doctoral Thesis*, University of Cape Town, 2005

Ghali, A., and Favre, R. (1994), *Concrete structures – Stresses and deformations*, second edition, published by E & FN Spon, London, 1994

Granju, J.L. (1996), Thin bonded overlays –About the role of fibre reinforcement on the limitation of their debonding, *Advanced cement based materials*, 1996

Gutsch, A., and Rostásy, F.S. (1994), Young concrete under high tensile stresses – creep relaxation and cracking, *Proceedings: RILEM Symposium Thermal Cracking in Concrete at early ages*, edited by R. Springenschmidt, Chapman & Hall, London 1994, pp.95–102 ***citing*** Bretenbucher, R. (1989), Zwangspanungen und RiBbildung infologe Hydratationswarme *Doctoral Thesis, TU Munchen*, Emborg, M. (1989), Thermal stresses in concrete structures at early ages, *Doctoral Thesis,* Lulea University of Technology, Sweden

Grzybowski M, Shah S. P (1990). Shrinkage cracking of fibre reinforced concrete, *ACI Mat J* pp.138–48

Indrajit R., Julio F. D. & Shiwei L., (2005), Interface evaluations of overlay-concrete bi-layer composites by a direct shear test method, *Cement & Concrete Composites* 339–347

Jaeseung K, Gregory A. S, and Sungho K. (2008). Determination of Accurate Creep Compliance and Relaxation Modulus at a Single Temperature for Viscoelastic Solids, *Journal Of Materials In Civil Engineering © ASCE* / February 2008, pp147-156

Jun Z., and Victor C. L., (2002), Monotonic and fatigue performance in bending of fibre-reinforced engineered cementitious composite in overlay system, *Cement and Concrete Research* 32 p 415-423

Kim S. M and P. K. Nelson (2004). Experimental and numerical analyses of PCC overlays on PCC slabs-on-grade subjected to climatic loading, *International Journal of Solids and Structures* 41 785–800

Kordina, K., Schubert, L., and Troitzsch, U. (2000), *Kriechen von Beton unter Zugbeanspruchung* (Creep of concrete subjected to tensile stress), *Deutscher usschiss für Stahlbeton*, Heft 498, Beuth Verlag, Berlin, Germany, 2000 ***cited by*** Beushausen, H. D. & M. G. Alexander (2006): Failure mechanisms and tensile relaxation of bonded concrete overlays subjected to differential shrinkage, *Cement and Concrete Research*, 36, pp1908-1914

Laube, M (1990), Werkstoffmodell zur Berechnung von Temperaturspannungen in massigen Betnbauteilen im jungen Alter, *Doctoral Thesis,* TU Braunschweig

Lecture Notes CIV5002Z, (2007)., Structural Concrete Properties & Practice CIV5002Z, University of Cape Town, 2007

Letsch, R. H. (1991), Shrinkage and temperature stresses in PC and PCC due to hindered deformation, *International Symposium on Concrete Polymer Composites*, Bo chum, Germany, 1991, Conference proceedings, pp.53-62

Matsushitaa F., Y. Aonob, and S. Shibata (2004). Calcium silicate structure and carbonation shrinkage of a tobermorite-based material, *Cement and Concrete Research*, 34:1251–1257

Meftah S.A., R. Yeghnem, A. Tounsi, and Adda bedia. E.A. (2006), Seismic behaviour of RC coupled shear walls repaired with CFRP laminates having variable fibres spacing *Construction and Building Materials*, (2007)

Morgan D. R., (1996).Compatibility of concrete repair materials and systems, *Construction and Building Materials,* 10(1):57–67

Morimoto H. & Koyanagi, W., (1994). Estimation of stress relaxation in concrete at early ages, *Proceedings of the RILEM International Symposium on Thermal cracking in early ages*, Munich, 10-12 October 1994, edited by R. Springenschmidt, Chapman & Hall, London 1995, pp.111 - 116

Mumenya, S. W. (2007). Evaluation of mechanical properties of textile concrete subjected to different environmental exposure, *Doctoral Thesis*, University of Cape Town, 2007

Neville, A.M (1981), *Properties of Concrete*, 3rd Edition, Pittman, p. 388

OSCO Gunite & Mudjacking Ltd*,* (2007). Available on *http://www.mudjacking.com* [11.12.2007]

Pigeon, M. and Saucier, F. (1992), Durability of repaired concrete structures, *Proceedings, International Symposium on Advances in Concrete Technology*, Athens, 11-12 May, October 1992

Pigeon, M. and Bissonette, B. (1999), Bonded concrete repairs - Tensile creep and cracking potential, *Concrete International*, November 1999, pp.31-35

Pigeon M., G. Toma, A. Delagrave, B. Bissonnette, J. Marchand, J.C. Prince, (2000), Equipment for the analysis of the behaviour of concrete under restrained shrinkage at early ages, *Magazine of Concrete Research*, 52 (4):297–302

Rusch, H, Jungwirth, D and Hilsdorf H, K. (1983): *Creep and Shrinkage; Their effect on the Behaviour of Concrete Structures*, New York, USA

Sauman, Z. (1971). *Cement and Concrete Research,* 1,p. 645

Schrader, E, K (1992): *Mistakes, Misconceptions and Controversial Issues concerning concrete and concrete Repairs*; Part 2 of 3 Part Series

Sika® Product Manual 2008

Sivakumar A. and M. Santhanam (2007).A quantitative study on the plastic shrinkage cracking in high strength hybrid fibre reinforced concrete, *Cement and Concrete Composites*, August 2007, 29(7): 575-581

South African National Standards. (1994), *SANS method 863:1994*

Stander., H, (2007):, Interfacial bond properties of ECC overlay systems, *Masters Thesis*, University of Stellenbosch, 2007

Tao, Z & Weizu, Q. (2005), Tensile creep due to restraining stresses in high-strength concrete at early ages. *Cement and Concrete Research,* November 2005, 36, pp 584-591

Vaysburd, A.M., and McDonald, J.E. (1999), An Evaluation of Equipment and Procedures for Tensile Bond Testing of Concrete Repairs. *Technical Report REMR-CS-61*, US Army Corps of Engineers, Waterways Experiment Station, Vicksburg, Mississippi USA

Vaysburd, A.M., Emmons, P.H., McDonald, J.E., Poston, R.W. and Kesner, K.E. (2000), Selecting durable repair materials: performance criteria – field studies, *Concrete International*, December 2000, pp.39-45

Von Seggern, D., H., (1993), *CRC standard curves and surfaces*. Boca Raton, CRC Press, 1993, p. 388

Wittmann, F., (1974). Bestimung physikalischer Eigenschaften des Zementeinsin Heft 232 *Deutscher Ausschub fur Stahlbeton* ***cited by*** Gutsch, A., and Rostásy, F.S. (1994), Young concrete under high tensile stresses – creep relaxation and cracking, *Proceedings: RILEM Symposium Thermal Cracking in Concrete at early ages*, edited by R. Springenschmidt, Chapman & Hall, London 1994, pp.95 - 102

Wittmann, F. H, Editor (1981)., *Fundamental research on creep and shrinkage of concrete* Martinus Nirjjhoff, The Hague pp 3-11 ***citing*** Powers T. C. (1968) *Material structure*, 1, p.487

Wittmann, F. H, Editor (1981)., *Fundamental research on creep and shrinkage of concrete* Martinus Nirjjhoff, The Hague pp 3-11 ***citing*** Feldman, R. F, and Sereda P. J. (1968) *Material structure*, 1, p.509

Zhutovsky S., K. Kovler and A. Bentur, (2004). Influence of cement paste matrix properties on the autogenous curing of high-performance concrete, *Cement and Concrete Composites*, July 2004, 26(5):499-507

Östergaard, L., Lange, D.A., Altoubat, S.A. and Stang, H. (2001) Tensile basic creep of early-age concrete under constant load, Cement & Concrete Research, Vol. 31, pp. 1895-1899